Technische Universität München

Wissenschaftszentrum Weihenstephan für Ernährung, Landnutzung und Umwelt

Lehrstuhl für Phytopathologie

Functions of the RAC/ROP GTPase HvRACB in the early plant immune response and in transcriptional reprogramming of barley

Vera Maria Schnepf

Vollständiger Abdruck der von der Fakultät Wissenschaftszentrum Weihenstephan für Ernährung, Landnutzung und Umwelt der Technischen Universität München zur Erlangung des akademischen Grades eines

Doktors der Naturwissenschaften (Dr. rer. nat.)

genehmigten Dissertation.

Vorsitzender:	Prof. Dr. Erwin Grill
Prüfer der	1. Prof. Dr. Ralph Hückelhoven
Dissertation:	2. Priv. –Doz. Dr. Erika Isono

Die Dissertation wurde am 16.06.2016 bei der Technischen Universität München eingereicht und durch die Fakultät Wissenschaftszentrum Weihenstephan für Ernährung, Landnutzung und Umwelt am 29.09.2016 angenommen.

Für meine Eltern Jutta & Jürgen

1. CONTENT

2. LIST OF FIGURES

3. LIST OF TABLES

4. ABBREVIATIONS

%	percent
°C	degree Celsius
AP	alkaline phosphatase
A. thaliana	*Arabidopsis thaliana*
BAK	BRI-1-associated kinase
Bgh	*Blumeria graminis* f. sp. *hordei*
bp	base pairs
BSA	bovine serum albumin
CA	constitutive active
cDNA	complementary deoxyribonucleic acid
CFP	cyan fluorescing protein
COP	copine
cRNA	complementary ribonucleic acid
DNA	deoxyribonucleic acid
dNTP	deoxyribonucleotide triphosphate
dH_2O	distilled water
dpi	days post inoculation
DTT	dithiothreitol
DUF	domain of unknown function
EDTA	ethylene diamine tetraacetic acid
EtBr	ethidium bromide
ETI	effector-triggered immunity
EtOH	ethanol
ETS	effector-triggered susceptibilty
EV	empty vector
FDR	false discovery rate
flg22	flagellin; 22 AA sequence of N-terminus known for defence activation
FLS2	flagellin-sensitive 2
fw	forward
gDNA	genomic DNA

GFP	green fluorescent protein
HCl	hydrochloric acid
hpi	hours post infection
HR	hypersensitive response
HRP	horseradish peroxidase
Hv	*Hordeum vulgare*
JIP	jasmonate-induced protein
LB	lysogeny broth; Luria Bertani
LD	Leaf disc
LOG2	logarithm to the base 2
LRR	leucine-rich repeat
M	molar
mA	milliampere
MAPK	mitogen-activated protein kinase
mg	milligram
$MgCl_2$	magnesium chloride
min	minute
ml	milliliter
mm	millimeter
mM	millimolar
MW	molecular weight
NaOAc	sodium acetate
NaCl	sodium chloride
NADPH	nicotinamide adenine dinucleotide phosphate hydrogen
NaF	sodium fluoride
Na_2MoO_4	sodium molybdate
ng	nanogram
NIK	NSP-interacting kinase
NO	nitric oxide
NOS	nitric oxide synthase
NSP	nuclear shuttle protein
o/n	over night
Os	*Oryza sativa*
PAMP	pathogen-associated molecular patterns
PCR	polymerase chain reaction
PR	pathogenesis-related
PRR	pattern-recognition receptor
PTI	pattern-triggered immunity
qPCR	quantitative polymerase chain reaction
RAC	rat Sarcoma-related C3 botulinum toxin substrate

RLK	receptor-like kinase
RLP	receptor-like protein
RNA	ribonucleic acid
ROI	region of interest
ROP	Rho-like GTPases of plants
ROS	reactive oxygen species
Rpm	rounds per minute
RT	room temperature/ reverse-transcriptase
Rv	reverse
Sec	second
SAR	systemic acquired resistance
SDS	sodium dodecyl sulfate
SERK	somatic embryogenesis receptor kinase
SF	susceptibility factor
Taq	polymerase named after *Thermus aquaticus*
Tris	TRIS amino methane
TIGS	transient-induced gene silencing
WAK	wall-associated kinase
WGA-TMR	Wheat germ agglutinin-tetramethylrhodamine
WT	wildtype
µl	microliter
Zm	*Zea mays*

5. PUBLICATIONS

Parts of this thesis have already been published in:

Scheler B, **Schnepf V**, Galgenmueller C, Ranf S, Hueckelhoven R. 2016. Barley disease susceptibility factor RACB acts in epidermal cell polarity and nucleus positioning. *Journal of Experimental Botany,* **67**, 3263-3275.

6. SUMMARY

Plant disease susceptibility factors are recently recognized as instrument for a better understanding of plant-microbe interactions and as targets for breeding for disease resistance of crop plants. The barley RAC/ROP small monomeric GTPase RACB acts as susceptibility factor in the interaction of barley (*Hordeum vulgare*) with the biotrophic ascomycete *Blumeria graminis* f. sp. *hordei (Bgh*). Investigations on the role of RACB in basal immunity and on transcriptional reprogramming of barley in the powdery mildew interaction should elucidate new components of *RACB*-mediated signalling and help explaining susceptibility to *Bgh*.

For *Poaceae* little information is available for the early plant immune response. However, it was recently shown that RAC/ROP proteins are involved in pattern-triggered immunity (PTI) in rice. Molecular structures of potential pathogens (pathogen-associated molecular patterns, PAMPs) are recognized via plant surface sensors to activate downstream signalling with first responses such as reactive oxygen species (ROS) production, activation of mitogen-activated protein kinases (MAPKs) and defence gene expression. However, no influence of RACB abundance and RACB activity status was observed on these early PTI responses. Noteworthy, barley MAPK homologs influenced fungal success in establishing feeding structures in epidermal cells, as shown by transient knock-down of MAPKs by RNA interference (RNAi). Therefore, barley MAPKs appear to fulfil similar functions as their most related homologs in *Arabidopsis thaliana,* suggesting a functional conservation.

In order to reveal potential functions of *RACB* on gene expression, a microarray-based study was performed to follow transcriptome changes in course of *Bgh* infection. Therefore, wildtype (WT) and *RACB* up- or down-regulated transgenic lines (over-expressing a constitutively activated (CA) *RACB* version or expressing a RNAi construct of *RACB*, respectively) were employed for transcriptome analysis. This revealed numerous pathways to be regulated including stress, signalling, hormone homeostasis and protein synthesis. Receptor-like kinase families were strongly de-regulated in the transgenic lines. Many of the *CA RACB*-regulated genes were also expressed under influence of the fungus, suggesting that virulent *Bgh* might co-opt *RACB* for reprogramming host gene expression. Six candidate genes were analysed in transient RNAi experiments because they showed interesting changes in their expression in response to *RACB* and *Bgh* at both analysed points in time. Three of them caused reduced susceptibility to fungal penetration upon transient down-regulation *via* RNAi, of which one, a leucine-rich repeat-containing protein (LRR-P; Harvest Assembly 35_15510), was characterized in more detail. The findings suggest LRR-P as a new susceptibility factor that genetically interacts with *RACB*. LRR-P might constitute a potential ligand or co-receptor of an unknown receptor kinase that could function upstream of *RACB* and be involved in a feed-forward regulation of *RACB* signalling. Taken together, the data obtained in this study propose a new function of *RACB* in transcriptional reprogramming of barley supporting susceptibility to *Bgh*.

7. ZUSAMMENFASSUNG

Faktoren, die die Anfälligkeit der Pflanze gegenüber Krankheitserregern erhöhen, werden als Suszeptibilitätsfaktoren bezeichnet. Diese werden eingehend untersucht, um die Interaktion zwischen Pflanze und Mikroorganismen besser zu verstehen. Mit diesem Verständnis können neue biotechnologische und züchtungsrelevante Ansätze entwickelt werden, um krankheitsresistentere Nutzpflanzen zu generieren. In der Interaktion von Gerste (*Hordeum vulgare*) mit dem biotrophen Echten Mehltaupilz *Blumeria graminis* f. sp. *hordei (Bgh*) (Asycomycet) agiert die kleine monomere Gersten-GTPase RACB als solch ein Suszeptibilitätsfaktor. Untersuchungen zur Rolle von *RACB* in der basalen Immunität und der transkriptionellen Umprogrammierung von Gerste im Zuge ihrer Interaktion mit Mehltau sollen neue Komponenten aufdecken, die in der *RACB*-abhängigen Pathogen-Antwort agieren und dadurch die Anfälligkeit von Gerste gegenüber *Bgh* erklären könnten.

Es gibt bisher nur wenige Untersuchungen zur frühen Immunantwort in *Triticeen*. Für Reis konnte jedoch gezeigt werden, dass RAC/ROP-Proteine in die pathogen-assoziierte Immunantwort (PTI) involviert sind. Diese in PTI erkannten Strukturen werden von potentiellen Pathogenen abgesondert (und deshalb auch als pathogen-assoziierte molekulare Strukturen, PAMPs, bezeichnet) und durch pflanzliche Oberflächensensoren erkannt. Infolge dieser Erkennung werden Signalkaskasden aktiviert, welche frühe Immunantworten wie die Produktion von reaktiven Sauerstoffspezies (reactive oxygen species, ROS), die Aktivierung von Mitogen-aktivierten Proteinkinasen (MAPK) oder die Expression von Abwehrgenen einschließen. Hier zeigen Untersuchungen zur frühen Immunantwort in Gerste, dass ROS-Produktion und die Aktivierung von MAPK beteiligt sind, aber nicht durch die Aktivität und die Menge an RACB beeinflusst werden. Gersten-MAP Kinasen beeinflussen den Penetrationserfolg pathogener Pilze maßgeblich: Unter transient regulierten Bedingungen (MAP Kinasen-"*Knockdown*") durch RNA-Interferenz wurden in epidermalen Zellen pilzliche Strukturen nachgewiesen. Somit scheinen Gersten MAP Kinasen ähnliche Funktionen zu erfüllen wie ihre Homologen aus *Arabidopsis thaliana*. Diese Ergebnisse sprechen daher für eine funktionelle interspezifische Konservierung von MAP Kinasen in PTI von mono- und dikotylen Pflanzen.

Um den Einfluss von *RACB* auf die Genexpression zu charakterisieren, wurden 44k Mikroarrays verwendet, um das Gerstentranskriptom vor und nach Infektion mit *Bgh* abzubilden. Dazu wurden Wildtyp-Pflanzen und transgene Linien mit veränderter *RACB*-Menge analysiert (konstitutiv aktiviertes *RACB* in überexprimierenden (*CA RACB*) Linien sowie *RACB RNAi* Konstrukt-transkribierende Linien mit reduzierter *RACB*-Expression). Die entsprechenden Transkriptomanalysen zeigten, dass verschiedenste Stoffwechselwege assoziiert mit Stressantworten, Signaltransduktion, Hormonhaushalt, Proteinsynthese und vielen mehr moduliert wurden. Rezeptorkinasen waren in den transgenen Linien deutlich dereguliert. Viele der in *CA RACB*-Linien beeinflussten Gene waren zusätzlich auch *Bgh*-abhängig, was darauf hindeutet, dass *Bgh* die Genexpression im Zusammenspiel mit *RACB* umprogrammiert. In transienten RNAi-Experimenten wurden sechs Kandidatengene genauer analysiert, die sowohl unter veränderten *RACB*-Spiegeln, als auch bei *Bgh*-Befall zu zwei Analysenzeitpunkten ein interessantes Expressionsprofil aufwiesen. Drei dieser Gene erhöhten die

Anfälligkeit gegenüber dem Mehltaupilz. Eines davon, das viele Leucin-reiche Wiederholungen enhält (leucin-rich repeat protein LRR-P, Harvest Assembly 35_15510), wurde funktionell charakterisiert. Die erhaltenen Daten legen nahe, dass LRR-P ein neuer Suszeptibilitätsfaktor ist, der genetisch mit *RACB* interagiert. LRR-P könnte dabei als potentieller Ligand oder als Ko-Rezeptor einer bisher unbekannten Rezeptorkinase in der *RACB*-Signalkaskade fungieren. Es wäre denkbar, dass *LRR-P* vorgeschaltet vor *RACB* agiert und daher an einer vorwärts-orientierten Regulation von *RACB* beteiligt ist. Zusammenfassend deuten die Daten auf neue Funktionen von *RACB* in der transkriptionellen Umprogrammierung von Gerste im Zuge ihrer Anfälligkeit gegenüber *Bgh* hin.

8. INTRODUCTION

8.1 PLANT IMMUNITY.

In regard of a steadily increasing human population it is essential to secure food production, particularly under conditions of a changing environment. Along with climate changes and man-borne environmental pressures, plants are frequently struggling with invading pathogens. As they do not possess specific immune cells, plants have evolved strategies to combat pathogen invasion by mounting cellular responses to ensure survival. Such events which regulate these responses during infection are for example the synthesis of proteins or hormone homeostasis. Their activation and regulation rely on intracellular signalling, which has to be tightly controlled to ensure successful defence reaction cascades and interactions between different pathogen-activated pathways. In spite of the fact that different layers of immunity act against fungi, oomycetes, viruses, nematodes and bacteria, these pathogens can overcome plant defence by means of various response mechanisms, targeting distinct host components (Jones and Dangl, 2006; Lapin and Van den Ackerveken, 2013).

The plant`s immune system comprises two main layers of defence (Fig. 1), in which cells recognize and respond to external signals directly at the infection sites (Jones and Dangl, 2006). These external signals are known as pathogen-, microbe-, or damage-associated molecular patterns (PAMPs, MAMPs, DAMPs) which are recognized via plant pattern recognition receptors (PRRs). PAMPs can be oomycetes-derived or fungi-derived glucans (e.g. chitin) (Felix *et al.*, 1999; Newman *et al.*, 2013) but also bacteria-derived proteins (e.g. flagellin) or lipopolysaccharides (LPS). This first layer of defence is called PAMP-triggered immunity (PTI) (Boller and Felix, 2009) inducing basal resistance; it restricts pathogen invasion and development. In turn, successful pathogens secret effector molecules that interfere with PTI, which leads to effector-triggered susceptibility (ETS). In a subsequent step, such virulence effectors are recognized via intracellular immune receptors, resulting in effector-triggered immunity (ETI) counteracting pathogen invasion on a second level (Jones and Dangl, 2006; Macho and Zipfel, 2014) (Fig. 1).

In the following sections the PTI components relevant for this work will be explained in more detail.

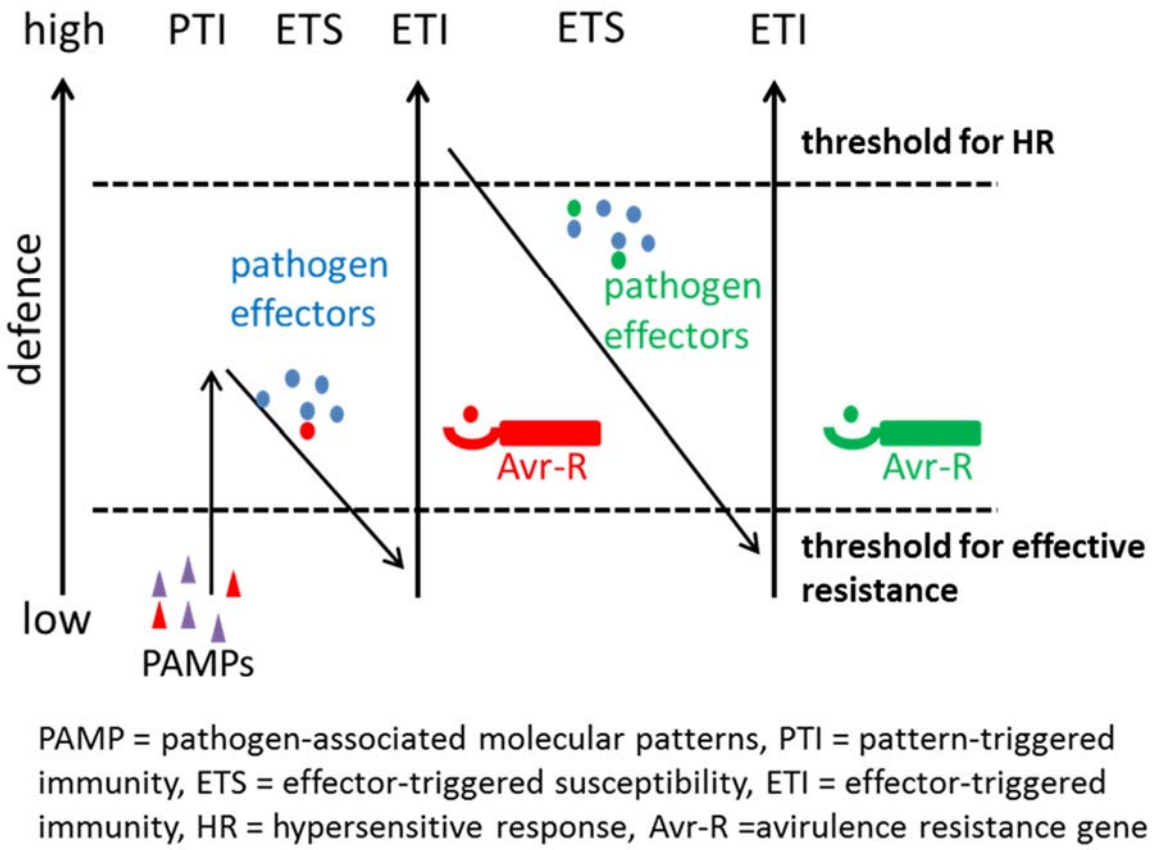

Fig.1: **The plant`s immune system combats pathogens in several steps.** During pattern-triggered immunity (PTI) pathogen-associated molecular patterns (PAMPs) are recognized via plant receptors leading to basal resistance. In a second step, the pathogen itself secrets effectors combating PTI. The plant in turn recognizes these effectors leading to effector-triggered immunity (ETI). Modified from Jones and Dangl (2006).

8.1.1 PATTERN-RECOGNITION RECEPTORS (PRR).

Proteins recognizing molecules characteristic of certain pathogens belong to the class of pattern-recognition receptors (PRRs). PRRs consist of receptor-like kinases (RLKs) and receptor-like proteins (RLPs). RLKs have an ectodomain responsible for ligand binding, a transmembrane domain and an intracellular (e.g. serine/threonine) kinase domain enabling signal transduction (Macho and Zipfel, 2014). Their ectodomains can have different structural motifs such as leucine-rich repeats (LRR), lysin motifs (LysM), lectin motifs, malectin-like domains, S-domains or epidermal growth factor (EGF)-like domains (Kessler *et al.*, 2015; Macho and Zipfel, 2014; Vaid *et al.*, 2013; Zipfel, 2014). Malectin-like domains are predicted to bind carbohydrate moieties and are suggested to monitor cell wall perturbations (Kessler *et al.*, 2015; Lindner *et al.*, 2012). S-domains consist of three modules: B-Lectin, S-Locus glycoprotein and PAN apple and are predicted to have key roles in protein-protein interaction (Chen *et al.*, 2013). EGF-like domains are extra-cytoplasmic and contain lots of disulphide bonds (He *et al.*, 1996).

LRR-RLKs present the largest group of RLKs and can be sub-divided into several classes according to their respective LRR organisation (Dievart and Clark, 2004). For *Arabidopsis thaliana* 216 LRR-RLKs (Dievart and Clark, 2004), and for *Oryza sativa* 292 members are known (Hu *et al.*, 2015; Shiu *et al.*, 2004), whereas for barley the knowledge is sparse. One or more LRRs form a pocket for binding of ligands (Gish and Clark, 2011; Kolade *et al.*, 2006) and each LRR consists of 20-30 amino acid residues. In general, one main category of LRR-RLKs functions is the regulation of plant development and growth (Hu *et al.*, 2015; Shiu *et al.*, 2004). The *Arabidopsis thaliana* LRR-RLKs ERECTA, CLAVATA, BRI1 and BAK1 are involved in organ shaping (Torii *et al.*, 1996), cell elongation (Duan *et al.*, 2010; Guo *et al.*, 2009), meristem maintenance (Clark *et al.*, 1997) and somatic embryogenesis (Li and Chory, 1997). The LRR subclass II in *Arabidopsis thaliana* is known to be involved in both defence and development, and contains proteins in three different classes (Hecht *et al.*, 2001). All of them are characterized by less than 10 LRRs and can be classified into antiviral defence proteins such as nuclear shuttle protein-interacting kinases (NSP-interacting kinases, NIKs) with 5 LRR domains (Santos *et al.*, 2010) involved in viral detection, developmental and defence proteins such as the somatic embryogenesis receptor-like kinases (SERKs) carrying 5 LRRs with functions in both plant development and pathogen control (Albrecht *et al.*, 2008), and functionally unassigned proteins. The five members of the arabidopsis SERKs contribute mainly to hormone responses and immunity. The most prominent SERK protein described so far is AtSERK3. AtSERK3 was identified as BRASSINOSTEROID INSENSITIVE (BRI1)-ASSOCIATED KINASE1 (AtBAK1), regulating not only the brassinosteroid hormone pathway, but also the building up of a receptor-complex with flagellin sensitive2 (FLS2) protein initiating defence (Chinchilla *et al.*, 2007; Li *et al.*, 2002; Nam and Li, 2002; Roux *et al.*, 2011; Sun *et al.*, 2013). Furthermore, it contributes to the yet unravelled Ve1-mediated resistance of tomato to *Verticillium dahlia* (Fradin *et al.*, 2009). Recently, most of the respective studies have been done by use of *Arabidopsis thaliana.* Little information for SERK proteins in monocotoyledons is available (Pandey and Chaudhary, 2014; Park *et al.*, 2011; Singla *et al.*, 2009). From the two known rice OsSERK proteins, OsSERK2 was shown to regulate plant growth via the brassinosteroid pathway and to directly interact with rice immune receptors (Chen *et al.*, 2014). In contrast, OsSERK1 seems to be exclusively involved in developmental processes (Zuo *et al.*, 2014). AtNIK proteins were shown to enhance susceptibility to geminivirus infection (Fontes *et al.*, 2004; Mariano *et al.*, 2004), AtBAK1/AtSERK3 to initiate defence after bacterial flagellin perception together with FLS2 (Sun *et al.*, 2013). The OsSERK2-XA21/XA26 receptor complex is involved in resistance to *Xanthomonas oryzae* pv. *oryzae (Xoo)* (Song *et al.*, 1995; Sun *et al.*, 2004). Other LRR-motif containing RLKs such as PANGLOSS1 and PANGLOSS2 of *Zea mays* are necessary for asymmetric cell division (Cartwright *et al.*, 2009), and the pollen tube receptor kinases of tomato (LePRK1 and LePRK2) regulate pollen tube growth (Gui *et al.*, 2014; Muschietti *et al.*, 1998). Besides the well-known LRR-RLKs, there are RLKs with other extracellular domains involved during plant innate immunity, e.g. the arabidopsis elongation factor Tu (EF-Tu) receptor (AtEFR) which recognizes this bacterial translation factor (Zipfel *et al.*, 2006), the tomato PBS1 and Pto all of which contribute to resistance against bacterial pathogens (Martin *et al.*, 1993; Swiderski and Innes, 2001; Zhou *et al.*, 1995), SR160 recognizing systemin, a wounding-induced polypeptide released from

affected tissues (Scheer and Ryan, 2002)., or the LysM-RLK CERK1 from arabidopsis and rice which is necessary for chitin recognition (Kaku *et al.*, 2006; Miya *et al.*, 2007).

RLKs often work in receptor complexes consisting of either more than one RLK (e.g. AtBAK1 and AtBRI1), or in combination with RLKs with non-functional kinase domains (ZmPAN1 and ZmPAN2), or, alternatively, with receptor-like proteins (RLPs). RLPs are likely deduced from receptor-like kinases but lacking the kinase domain, which is replaced by a cytoplasmic tail; they often function as soluble apoplastic ligands or co-receptors to activate downstream signalling (Kruijt *et al.*, 2005; Liebrand *et al.*, 2013). Several RLPs have biological function (Lannoo and Van Damme, 2014) as for example in defence. The well-studied tomato LRR-RLP LeEIX1/EIX2 perceives the cell wall-derived ethylene-inducing xylanase (Eix) from *Trichoderma* (Ron and Avni, 2004), Ve1 induces resistance towards *Verticillium* strains (de Jonge *et al.*, 2012; Fradin *et al.*, 2009), or Cf2, Cf4, or Cf9 mediate resistance to *Cladosporium fulvum* (Cf) carrying the avirulence genes Avr2, Avr4, or Avr9, respectively. Cf proteins can act in a complex with the RLK Suppressor Of BIR1-1/Evershed (SOBIR1/EVR) of *Arabidopsis thaliana* and the tomato ortholog important for immunity (Liebrand *et al.*, 2013). Arabidopsis RLPs have a crucial role in defence. They are very redundant and can have parallel roles in immunity and development (Zhang *et al.*, 2013). AtRLP52 contributes to basal resistance to the powdery mildew fungus *Erysiphe cichoracearum* (Ramonell *et al.*, 2005) and AtRLP30 is involved in resistance to the gram-negative bacterium *Pseudomonas syringae* pv. *phaseolicola.* The characterized RLPs involved in developmental processes include for example the arabidopsis TOO MANY MOUTHS (TMM, AtRLP17) (Shpak *et al.*, 2005). TMM forms a complex with the LRR-RLK ERECTA to trigger stomatal differentiation (Lee *et al.*, 2012). CLAVATA2 (CLV2, AtRLP10) builds a complex with the LRR-RLK CLAVATA1 (Ogawa *et al.*, 2008; Waites and Simon, 2000) fostering meristem development (Kayes and Clark, 1998). Moreover, CLV2 was shown to be important for nematode parasitism (Replogle *et al.*, 2013).

8.1.2 CELLULAR PTI RESPONSES

After recognition of the pathogen, several cellular responses were found to be crucial for the plant`s defence system. These responses can be divided into early and late events. Events up to 30 minutes after pathogen recognition are classified as early PTI responses and comprises influx of Ca^{2+} ions which probably act as second messenger (Ranf *et al.*, 2011), oxidative burst recordable via H_2O_2-dependent luminescence of luminol, MAPK activation and subsequent WRKY transcription factor activation. Late events which are detectable later than half an hour after pathogen recognition can last from hours to days and are for example deposition of callose, seedling growth inhibition or late responsive genes such as pathogenesis-related genes; they usually depend on *de novo* protein biosynthesis (Boller and Felix, 2009; Chisholm *et al.*, 2006; Lozano-Duran *et al.*, 2014; Smith and Heese, 2014).

The very early events such as ion influx leading to membrane depolarization are important for transducing the pathogen`s signal into the plant cell. As second messenger, the Ca^{2+}-influx serves as signal to open other membrane channels triggering downstream-processes. However, not only Ca^{2+} functions as second messenger, there are also nitric oxide (NO) and reactive oxygen species (ROS) promoting the danger signal released by the incoming pathogen. When prolonged and strong, these messengers cause hypersensitive response (HR) associated cell death during incompatible interactions

(Scheler *et al.*, 2013; Torres, 2010; Yoshioka *et al.*, 2011). No direct homolog of the animal nitric oxide synthase (NOS) is known for plants, but a NOS-like activity exists which is probably the major source for plant NO (Bellin *et al.*, 2013). ROS are at least partially produced by Respiratory Burst Oxidase Homologs (RBOHs), the NADPH oxidases. These plasma membrane proteins produce superoxide anions which are directly converted to H_2O_2 and can directly enter the cytosol for triggering intracellular responses. Beside its signalling and antimicrobial effects, H_2O_2 is needed for cross linking of cell wall glycoproteins and lignin-like substances at the site of interaction. Both polymer networks are needed for basal resistance as they lead to strengthening the host cell wall against degradation by the pathogen (Hueckelhoven, 2007; Kawano *et al.*, 2014). It was reported that ROS production is regulated by RAC/ROP GTPase signalling as described for animals (Bokoch and Diebold, 2002; Jones *et al.*, 2007; Wong *et al.*, 2007). Mitogen-activated protein kinase (MAPK) signalling is best analysed for *Arabidopsis thaliana* and *Oryza sativa* and several findings show that MAPKs are involved in both plant immunity and plant development (Pedley and Martin, 2005; Pitzschke *et al.*, 2009). Plant MAPKs are related to the mammalian extracellular signal-regulated kinase (ERK) subfamily and carry the typical TXY motif where X corresponds to any amino acid. Mainly a TEY (Thr-Glu-Tyr) or the plant-unique TDY (Thr-Asp-Tyr) phosphorylation motif can be found in plant MAPKs. MAPK activation is achieved in a three-step model from MAP kinase kinase kinase (MAPKKK) phosphorylating MAP kinase kinase (MAPKK), and subsequently phosphorylating MAPK activating then other cellular components such as for example WRKY transcription factors. The exact number of MAPK in the different species is mostly not known. For arabidopsis around 20 MAPKs are known which is a similar number to the MAPK repertoire of rice (Meng and Zhang, 2013). The complexity of MAPKs involved in stress and hormone responses and developmental processes throughout the different species is described in several publications. This is best unravelled for AtMPK3 and AtMPK6 which are involved in several signalling pathways (Gudesblat *et al.*, 2007; Ichimura *et al.*, 2002; Singh and Jwa, 2013; Wang *et al.*, 2008). The total number of characterized MAPKs is low; AtMPK3, AtMPK6, AtMPK4 and AtMPK11 are involved in growth and in response to abiotic and biotic stress. The bacterial PAMPs flg22 and elf18 trigger early MAPK activation of AtMPK3, AtMPK6, AtMPK4 and AtMPK11 by activation of the receptor complex BAK1 with FLS2 or EFR, respectively (Bethke *et al.*, 2012; Bethke *et al.*, 2009; Felix *et al.*, 1999; Gomez-Gomez and Boller, 2000; Ranf *et al.*, 2011; Zipfel *et al.*, 2006). AtMPK3 and AtMPK6 act as positive regulators in defence (Bethke *et al.*, 2009; Pitzschke *et al.*, 2009) whereas AtMPK4 is a negative regulator. *Atmpk4* mutants are more resistant to certain pathogens (Petersen *et al.*, 2000). *Atmpk3* mutants exhibit increased susceptibility to the fungal pathogen *B. cinerea* whereas *Atmpk6* mutants did not show this phenotype (Galletti *et al.*, 2011). AtMPK3 and AtMPK6 are also involved in stomata development or ethylene biosynthesis (Gudesblat *et al.*, 2007; Sheikh *et al.*, 2013) and other developmental processes such as root hair formation (Lopez-Bucio *et al.*, 2014; Walia *et al.*, 2009; Wang *et al.*, 2008). For rice, the nomenclature differs strongly and only OsMPK3, OsMPK4 and OsMPK6 were found to be involved in stress responses (nomenclature after (Singh and Jwa, 2013)). OsMPK3 and OsMPK6 can be integrated in the signalling cascade of chitin-mediated immunity in rice triggered by the OsCEBIP/OsCERK1-OsRAC-GEF1-OsRAC1 module (Akamatsu *et al.*, 2013; Kawano and Shimamoto, 2013; Kim *et al.*, 2012). This is also the only example for a RAC/ROP protein to be involved

in PTI. The only barley MAPK which was characterized up to now is HvMPK4 which corresponds to the OsMPK4. If knocked-down, transgenic *HvMPK4*-mutant plants were more resistant to the fungal pathogen *Magnaporthe grisea* (Abass and Morris, 2013). Downstream of MAPKs, numerous genes contributing to defence reactions against the corresponding type of pathogen get activated. This involves for example WRKY transcription factors, which are key regulators of plant defence (Eulgem and Somssich, 2007), but also up-regulation of pathogenesis-related (PR) proteins (Goehre *et al.*, 2012; Wu *et al.*, 2014). PR proteins are induced after pathogen attack and can be used as control genes for monitoring the molecular infection status (Schultheiss *et al.*, 2003; van Loon *et al.*, 1994). WRKY transcription factors (WRKYs) can be found in multifunctional signalling cascades in abiotic (Mare *et al.*, 2004; Ramamoorthy *et al.*, 2008; Zhang *et al.*, 2009) and biotic stresses (Eckey *et al.*, 2004; Peng *et al.*, 2008; Shen *et al.*, 2007), but also in developmental processes (Zhang *et al.*, 2011). They have several functions and can act positively or negatively in plant immunity.

Evidence for a MAPK-stimulated WRKY transcription factor activation was shown for AtWRKY22 and AtWRKY29 acting downstream of AtMPK3/AtMPK6 (Asai *et al.*, 2002) and for AtWRKY25 and AtWRKY33 acting downstream of AtMPK4 (Andreasson *et al.*, 2005; Qiu *et al.*, 2008b). HvWRKY1 and HvWRKY2 are for example negative regulators of resistance to *Bgh* in barley (Eckey *et al.*, 2004; Shen *et al.*, 2007).

8.1.3 Susceptibility factors

Susceptibility to fungal diseases is little understood, but Pavan (2010) summarized the principles of how a pathogen can overcome the host`s defence system. Secreted pathogen effectors overcome the first layer of defence (Boller and He, 2009) and thereby induce susceptibility. They can also directly interact with the transcriptome of a host to modify appropriate signaling components to enhance susceptibility (Motion *et al.*, 2015; Nottensteiner, 2015). Though the underlying processes of host reprogramming are not evaluated clearly, so called susceptibility factors (SFs) seem to play a key role in the host-pathogen interaction (Vogel *et al.*, 2002). SFs are identified when their loss of function results in a reduced disease. In spite the fact that after infection the plant`s immune system is activated, host-derived SFs support the pathogen. This counter intuitive response can be considered as failure of the host where immune response-independent processes additionally support the invasion of the pathogen (Dobon *et al.*, 2015). Either they are addressed as part of the pathogens virulence strategy or as supplier of essential nutrients for the pathogen. Susceptibility factors were identified for several host-pathogen interactions in rice (Cernadas *et al.*, 2014; Xu *et al.*, 2013), arabidopsis (Hewezi and Baum, 2013; Lorang *et al.*, 2012; Yang *et al.*, 2014), cotton (Wang *et al.*, 2014b) or maize (van der Linde *et al.*, 2012).

For the barley powdery mildew interaction several SFs have been characterized in the last decade. The loss-of-function mutation-induced recessive alleles of the Mildew resistance locus o (*Mlo*) gene lead to resistance to *Bgh* (Acevedo-Garcia *et al.*, 2014). This negative regulatory role lead to down-regulating leaf cell death and defence functions (Bueschges *et al.*, 1997), for example. Beside the wildtype MLO protein, other negative regulators of barley immunity are described such as the transcription factor WRKY2 induces resistance when down-regulated (Eckey *et al.*, 2004; Shen *et al.*,

2007), the cell death regulator BAX-inhibitor 1 (BI-1) decreases susceptibility when silenced (Eichmann *et al.*, 2010) and the RAC/ROP GTPase RACB supports fungal entry (Schultheiss *et al.*, 2002). It is rarely known whether and how these SFs influence the barley transcriptome. Up to now, investigations covering the understanding of the whole SF cascade activated by *Bgh* transcriptomic approaches were carried out with *mlo5*-mutant genotypes fully resistant to *Bgh* (Zierold *et al.*, 2005).

8.2 THE BARLEY POWDERY MILDEW PATHOSYSTEM

Barley (*Hordeum vulgare*) is a major cereal belonging to the family *Poaceae*. It is one of the most important crops – besides wheat, maize and rice - worldwide (FAOSTAT 2007; Food and Agriculture Organisation of the United Nations) and is mainly used for animal feed and the production of malt. As being highly stress-resistant, barley is a useful model plant which is highly adaptable to stressful conditions such as cold, drought and salts and thereby well suited for cultivation (Schulte *et al.*, 2009).

One of the most prominent barley pathogens is *Blumeria graminis forma specialis (f.sp.) hordei* (*Bgh*) (Ascomycetes – Erysiphales - Blumeriae), which is an obligate biotrophic ectoparasite infecting host-specifically barley (Glawe, 2008).

In the life cycle of *Bgh* wind-dispersed asexual conidia land on the barley leaf surface. Here, a first short primary germ tube is formed 0.5 – 1 h after leaf contact close to the contact site (Kunoh *et al.*, 1979). Functionally the primary germ tube is linked to water uptake and host surface feature perception (Green *et al.*, 2002). Subsequently a secondary infectious germ tube follows within eight to 10 hours after infection. At the tip of this germ tube the appressorium is built from which a penetration peg is formed before 15 hours post infection (hpi). Cutinases and cell wall degrading enzymes support penetration of the cuticle and the cell wall of the host epidermis cell (Francis *et al.*, 1996; Zhao *et al.*, 2013b). A haustorium which is a special feeding structure is established in a newly formed periplasmatic space up to 20 hpi. This complex consists of an inner haustorial cytoplasm surrounded by the haustorial plasma membrane, the haustorial cell wall, the extrahaustorial matrix and extrahaustorial membrane which is in continuum with the host plasma membrane (Gil and Gay, 1977). The haustorium remains within the intact epidermal cell while fungal hyphae grow epiphytically to invade neighbour cells (Eichmann and Hueckelhoven, 2008).

8.2.1 PTI IN THE BARLEY – POWDERY MILDEW SYSTEM

PTI as a first layer of defence includes several strategies of the plant to combat invading pathogens. For the barley powdery mildew system different approaches were started in the last decade to analyse these early responses. H_2O_2 can be aligned to crosslinking of cell-wall compositions during papillae formation (Hueckelhoven *et al.*, 1999; Wei *et al.*, 1998) and accumulates in cell wall appositions or small vesicle-like bodies or granules next to the penetration site (An *et al.*, 2006; Trujillo *et al.*, 2004). Those small vesicle-like bodies or granules contain H_2O_2 suggested to be secreted by a proposed discharge of chemical compounds for combating pathogens (Hafez *et al.*, 2014). Much research is ongoing in terms of defence-related genes involved in polyubiquitination, MAPK and WRKY signalling during PTI (Caldo *et al.*, 2004; Dong *et al.*, 2006; Eckey *et al.*, 2004; Ishihama and Yoshioka, 2012; Meng

and Wise, 2012). For barley two MAPKs MPK1 and MPK2 increased during *Bgh* germination (Zhang and Gurr, 2001). Further, MPK activity was evidenced to be only in fungal development structures such as appressoria (Kinane and Oliver, 2003; Zhang and Gurr, 2001). No data are available for arranging MAPK into a barley immunity cascade up to now. What is known is that several WRKY transcription factors are identified to have crucial roles within the combat against pathogens (Table S6). Those transcription factors are regulated by MAPKs in other species such as rice or arabidopsis (Akamatsu *et al.*, 2013; Chi *et al.*, 2013).

8.3 RAC/ROP SIGNALLING IN PLANT IMMUNITY

Rho of plants (ROPs), also known as RACs, are Rho-related small GTPases that regulate many processes like cell morphology, hormone responses, cytoskeleton organisation, production of reactive oxygen species (ROS), cell polarity and gene expression (Berken, 2006; Nibau *et al.*, 2006; Yang, 2002). They act as molecular switches existing in two states: an inactive cytosolic GDP-bound form and an activated GTP-membrane bound form. The GTP-bound form is activated via guanine nucleotide exchange factors (GEFs) whereas GTPase activating proteins (GAPs) hydrolyze the bound GTP leading again to the inactive GDP-bound form. RAC/ROP proteins can be divided into two groups: type I and type II (Winge *et al.*, 2000). Type I RAC/ROPs terminate with a canonical CaaX (a, aliphatic amino acid) motif (CSIL). The final lysine supports geranylgeranylation (Caldelari *et al.*, 2001) and CaaX processing proteins such as type I RAC/ROPs get attached to the membrane after prenylation in the cytoplasm (Sorek *et al.*, 2011; Sorek *et al.*, 2007). Those proteins have a high affinity for further processing at the endoplasmic reticulum (ER) (Bracha-Drori *et al.*, 2008). Type II RAC/ROPs contain a GC-CG box sequence motif and get anchored to the plasma membrane by palmitoylation (Lavy *et al.*, 2002; Lavy and Yalovsky, 2006). RAC/ROP proteins move more and more in the focus for several signalling mechanisms within physiological processes, abiotic stresses (Miyawaki and Yang, 2014; Qin and Dong, 2015) but also biotic stress to several pathogens (Doermann *et al.*, 2014; Feher and Lajko, 2015; Liu W, 2014). What the exact regulatory elements of RAC/ROP GTPases are, is currently under investigation (Akamatsu *et al.*, 2013; Kawano *et al.*, 2014; Kawano and Shimamoto, 2013; Pandey *et al.*, 2015).

Six ROPs are encoded in barley, seven in rice, nine in maize and 11 in arabidopsis (Berken, 2006; Christensen *et al.*, 2003). Arabidopsis ROPs are analyzed extensively and diverse functions were identified such as hormone responses (AtROP10, AtROP11) (Craddock *et al.*, 2012), root hair development and promoting cortical microtubule arrangements (AtROP4, AtROP6) (Molendijk *et al.*, 2004), cell polarity (AtROP2) (Yang and Fu, 2007) and pollen tube growth (AtROP1, AtROP3, AtROP5) (Gu *et al.*, 2004). AtROP2, AtROP4 and AtROP6 are also involved in microtubule and/or actin dynamics (Chen *et al.*, 2012; Craddock *et al.*, 2012). The rice ROP RAC1, for example, was identified as positive regulator of disease resistance by functioning in a complex with MAPK6 (Lieberherr *et al.*, 2005). It also interacts with NADPH oxidase in modulating ROS production (Kawasaki *et al.*, 2006; Wong *et al.*, 2007). OsRACB, also known as OsRAC6 (Chen *et al.*, 2010b; Miki *et al.*, 2005), OsRAC4 and OsRAC5 are other RAC/ROP proteins of rice which contribute to immunity. They were shown to regulate blast resistance

negatively (Chen *et al.*, 2010b; Jung *et al.*, 2006). For OsRAC3 and OsRAC7 no defence-related connection was evaluated up to now (Chen *et al.*, 2010b; Kawano *et al.*, 2014).

For some maize RAC/ROP proteins a function in developmental processes was observed. Type I ZmROPs 2, 4 and 9 (Christensen *et al.*, 2003) are involved in the pollen growth. ZmROP2 possible guides the signaling to the pollen tube in the male gametophyte (Arthur *et al.*, 2003). As ZmROP9 is differing in only one amino acid compared to ZmROP2, both were shown to have a key role during polarization in cell division and growth (Humphries *et al.*, 2011). Additionally, for the correct localization of the ROPs the catalytically inactive RLKs, PANGLOSS1 and PANGLOSS2, are needed. Both are required for the interaction with ROP during cell division (Cartwright *et al.*, 2009; Facette and Smith, 2012; Humphries *et al.*, 2011). Recently, the SCAR/WAVE complex activating the actin-nucleating ARP2/3 compelx was identified driving ZmPAN1 and ZmPAN2 polarization prior to cell division (Facette *et al.*, 2015). Thereby an interaction between RLKs and ROPs is important for cell polarity formation.

8.4 RACB SIGNALLING IN BARLEY SUSCEPTIBILITY TO POWDERY MILDEW.

In barley six different ROP GTPases are known: HvRACB, HvRACD, HvRAC1, HvRAC3, HvROP4, HvROP6 (Schultheiss *et al.*, 2003), all of them harbouring highly conserved functional domains such as the GTP/GDP-binding domain, the GTP domain and the effector loop which is essential for interactions with regulatory proteins. ROP proteins can be divided into type I or type II proteins dependent on the length of their C-terminal sequence. The C-terminal region is hyper-variable and contains signals targeting the ROP proteins to the plasma membrane. This region is not similar between all barley ROP; type I RACB and RACD possess a shorter C-terminal sequence in comparison to the other barley ROPs.

All RAC/ROPs enhance susceptibility to *Bgh* when constitutively activated (Pathuri *et al.*, 2009; Schultheiss *et al.*, 2003) - except RACD which is the closest homolog to RACB (Schultheiss *et al.*, 2003). RACB is the best characterized RAC/ROP in barley: it leads not only to enhanced haustoria formation (Opalski *et al.*, 2005) but also interacts with the protein RIC171 *in planta* during pathogen attack (Schultheiss *et al.*, 2008) and with the RACB-counteracting protein kinase RBK1 and partners interacting in a possible complex such as SKP1-like protein (Huesmann *et al.*, 2012; Reiner *et al.*, 2015). Barley RAC/ROPs and MILDEW LOCUS O (MLO) are host proteins linked to cytoskeleton remodeling and cell polarity (Opalski *et al.*, 2005), which are somehow addressed by the fungus to invade epidermal cells (Bueschges *et al.*, 1997; Schulze-Lefert, 2004). Recently, a microtubule-associated GTPase activating protein (MAGAP1) was identified as an antagonist of RACB (Hoefle *et al.*, 2011). MAGAP1 colocalizes with microtubules and is recruited by activated RACB reducing susceptibility to *Bgh*.

In 2002, it was first described that barley RACB supports the fungal penetration process of *Bgh* (Schultheiss *et al.*, 2002), and barley plants stably expressing constitutively active (*CA*) *RACB* as well as plants with RNAi-mediated knock-down of *RACB* were generated (Hoefle *et al.*, 2011; Schultheiss *et al.*, 2005). Stable transgenic barley lines over-expressing constitutively active *RACB* (*CA RACB)* showed super-susceptibility to *Bgh,* whereas barley lines stably down-knocking *RACB* by RNAi exhibited

reduced susceptibility compared to wt plants (Hoefle *et al.*, 2011; Pathuri *et al.*, 2008; Schultheiss *et al.*, 2005). Those plant lines raise the possibility for analyzing functions of RACB during pathogen attack in a closer way.

8.5 TRANSCRIPTOMICS

Transcriptomics is referred to global gene expression studies. They encompass genome-wide analyses of transcript species, and their abundance under specific circumstances or in specific cells. By comparing different transcriptomes, one can identify differentially expressed genes in response to diverse stimuli. For this purpose, microarray studies are a powerful tool to analyse the complexity of the transcriptome, in order to support and expand the knowledge of the interaction between a pathogen and a host plant (Tan *et al.*, 2009; Wang *et al.*, 2009). Expression levels of thousands of genes can be measured in relation to different treatments in a single experiment. In principle, microarrays can be designed as cDNA or as oligonucleotide arrays. In the case of a cDNA array, double-stranded DNA is deposited onto a chip substrate using robotic pins (Stoughton, 2005); in the case of an oligonucleotide array, shorter sequences of around 20-60 nucleotides are synthesized and spotted in an ordered manner directly on an array chip patterned by e.g. photolithography (Lodha and Basak, 2012). Samples are prepared as cRNA or cDNA, depending on the available array. For Agilent arrays equipped with DNA oligonucleotide probes, cRNA samples are prepared. Basically RNA is extracted from un- (mock-) and differently treated material, which is converted into cDNA using reverse transcriptase, and further converted to cRNA with T7 RNA polymerase to produce cRNA. Concomitantly, cRNA is labelled with a fluorescent dye, usually one of the cyanine dyes Cy3 or Cy5. Subsequently, the labelled cRNA probes are hybridized onto the array probes for an extended period of time. Target RNA fragments will bind to array DNA if complementary. Residual RNA fragments are washed off, and spots can be analysed for their relative fluorescence intensity (indicating hybridization if high) with a laser scanner.

In the last decade, microarray technology was the method of choice for transcriptional profiling during infection processes, even if other methods such as RNA sequencing have been increasingly used. In recent years a number of transcriptome studies were performed with the focus on fungal diseases. *Magnaporthe oryzae, Blumeria graminis* f.sp. *hordei* and *Ustilago maydis* and their effects on their hosts rice, barley and maize were started to be analysed, focussing especially on developmental processes of the fungi (Tan *et al.*, 2009) by help of the microarrays. Wise (2007) collected examples of microarray analyses in host-pathogen interactions. The aim of those studies was mostly to understand responses with respect to compatibility or resistance. Through the identification of pathways, significantly regulated genes involved in immunity were identified. Those genes were then subsequently tested for their function in pathogen interactions (Bischof *et al.*, 2011).

Several barley microarray studies were conducted with different approaches. In regard to developmental processes, barley endosperm development was shown to be possibly regulated by methylation processes, mainly in the first pre-storage phase (Radchuk *et al.*, 2005). Druka *et al.* (2006) provide a whole expression set specifically determined for certain tissues, and correlated expression

patterns throughout all analysed tissues. With the long-term goal to improve nutritional quality, the barley grain was monitored for its amino acid profile. With that knowledge it could be possible to breed selectively for specific alleles. With an improved amino acid profile of the barley storage proteins, the utility of this crop as animal feed might be increased (Hansen *et al.*, 2009). Senescence is important for efficient nutrient supply during seed maturation. It was shown that NAC (NAM, ATAF1/2 and CUC2) genes belonging to a whole transcription factor family are important for the completion of the plant`s life cycle. These genes were found up-regulated during senescence and thereby supposed to have regulatory effects (Christiansen and Gregersen, 2014; Hollmann *et al.*, 2014). In regard to biotic stress situations, Bischof *et al.* (2011) list several studies performed with different barley genotypes, in combination with several biotrophic, hemibiotrophic or nectrotrophic fungi such as *Bgh*, *Blumeria graminis* f.sp. *tritici* (*Bgt*), *Puccinia hordei*, *Puccinia tritici*, *Fusarium graminearum*, *Puccinia striiformis* f.sp. *tritici*, *Puccinia triticina*, *Magnaporthe oryza.* Amongst others, these studies identified genes which might be involved in PTI (e.g. MAP kinases) or ETS (WRKY transcription factors) (Eckey *et al.*, 2004), but also compared gene expression of the epidermis with the other parts of the barley leaf (Bruggmann *et al.*, 2005). Other studies describe genes involved in resistance or compatibility to a certain pathogen. Molitor *et al.* (2011) found defence-related genes after *Bgh*-challenge of mycorrhiza-colonized roots at different time points. As those genes code for antifungal proteins, this is important to explain the reduced haustoria establishment in *Bgh*-infected leaves. It could also be shown that the hormone family brassinosteroids enhances resistance to *Fusarium* diseases in barley (Ali *et al.*, 2013). Microarray data showed that several pathways such as hormonal signalling or pathogenesis-related genes get activated when epibrassinolide was applied. Analysis of the whole barley transcriptome to defend its powdery mildew fungus *Bgh* dependent on the susceptibility factor RACB was not performed yet. Douchkov *et al.* (2014) performed an initial investigation of around 3 % of the barley transcriptome by a transient-induced gene silencing approach for their role during powdery mildew infection. Elucidation of those kinds of genes that are addressed by RACB during *Bgh*-challenge should explain susceptibility of barley to *Bgh* in more detail.

8.6 OBJECTIVES

The small monomeric GTPase RACB is a susceptibility factor in the interaction of barley with the biotrophic powdery mildew fungus *Blumeria graminis* f. sp. *hordei (Bgh)* (Hueckelhoven, 2005; Schultheiss *et al.*, 2002). Physiologically, RACB is needed for maintaining cell polarity and is negatively controlled during infection with *Bgh* by the microtubule-associated GTPase activating protein (MAGAP1) and ROP binding kinase (RBK1) that controls protein abundance of RACB (Hoefle *et al.*, 2011; Huesmann *et al.*, 2012; Reiner *et al.*, 2015). It is also known that RACB interacts with several downstream-acting proteins such as RIC171 (Schultheiss *et al.*, 2008). The role of *RACB* in PTI of basal defense and pathogen-modulated gene expression is not well understood.

In PTI, PAMPs get recognized by plant surface sensors triggering the external signals to first plant responses such as ROS production, the activation of MAPKs and defence gene expression. Recently it was found that rice RAC/ROP proteins are implicated in PTI of rice whereas for barley little information is available. Hence, I investigated ROS accumulation and MAPK activation in *RACB*-transgenic barley plants. Additionally, barley MAPK homologs were analysed for their impact on fungal establishment in barley epidermal cells.

To address *RACB*-modulated changes in gene expression, a transcriptome analysis employing 44k microarrays was conducted, comparing wild-type plants with plants over-expressing constitutively active *RACB*, or with plants with downregulated *RACB* by RNAi-mediated silencing (*CA RACB* and *RACB RNAi*). Two time points were chosen to cover the infection process in an early and in a later stage of fungal establishment. To delimit pathways important during the infection process, I conducted pathway analyses with regard on *RACB*- and *Bgh*-driven expression patterns.

A focus was to shed light on those genes modulated by both *RACB* and *Bgh* at the two time points. Six selected genes were analysed in transient RNAi experiments for their putative functions during infection. Three of them caused reduced susceptibility to fungal penetration upon their downregulation by transient RNAi. One of them, a leucine-rich repeat containing protein (LRR-P; Harvest Assembly 35_15510), was characterized in more detail.

This work intended to describe PTI in barley and its possible regulation by *RACB*. Furthermore, a transcriptional analysis was used to identify new genes that are possibly involved in *RACB*-mediated host reprogramming during powdery mildew infection.

9. MATERIALS AND METHODS

9.1 METHODS FOR PLANT ANALYSIS

9.1.1 Plant material and growth conditions.

For all experiments the barley (*Hordeum vulgare*) cultivar Golden Promise and transgenic *RACB* plants (in the Golden Promise background) CA RACB (line: 17/1-11) and RACB RNAi (line: 16/2-4B) were used (Hoefle *et al.*, 2011; Schultheiss *et al.*, 2005). Kernels were surface-sterilized in 20 ml sterilization solution (4% (w/v) NaOCl, 0.01% (w/v) Tween20) for 1.5 h on a horizontal shaker. After washing with MilliQ-H_2O for 30 min husks were carefully removed without hurting the embryo. Uncoated seeds were pre-germinated on wet filter paper for 2 days in the dark before sown on soil (Typ ED73, Einheitserde- und Humuswerke, Gebr. Patzer GmbH & Co KG, Sinntal-Jossa, Germany). Plants were grown in a growth chamber (Conviron, Winnipeg, Canada) at 18 °C with relative humidity of 65% and a photoperiod of 16 h with 150 µmol m^{-2} s^{-1} light intensity. Both transgenic genotypes do not produce homozygous offspring. Offspring of transgenic T3 donor plants was genotyped according to previous studies (Hoefle *et al.*, 2011; Schultheiss *et al.*, 2005) to separate transgenic offspring carrying the T-DNA from azygous offspring that lost the T-DNA due to segregation. The powdery mildew fungus *Blumeria graminis* (DC) Speer f. sp. *hordei* (*Bgh*) EM. Marchal was maintained on the cultivar Golden Promise under the same conditions described above. For transient transformation assays the barley (*Hordeum vulgare*) cultivar Golden Promise was directly sown on soil (see above, Typ ED73), grown under the conditions described above and leaf segments from 7 days old plants were used for the experiments.

9.1.2 Pathogens and infection.

Bgh was propagated on the cultivar "Golden Promise" in a Sanyo (Munich, Germany) growth chamber as described in Section 9.1.1. 14-days-old plants were inoculated by blowing spores from infected plants in an inoculation tower to reach a density of 100 conidia/mm² leaf surface. Second leaves were harvested after 12 h and 32 h after infection and ground in liquid nitrogen to fine powder in a mortar. For transient transformation assays, detached leaves of seven days old Golden Promise plants were fixed on 0.5 % (w/v) water agar in petri dishes and inoculated as described above.

9.1.3 Elicitors.

Flg22 (Felix *et al.*, 1999) was synthesized as described before (Ranf *et al.*, 2011). Chitin from shrimp cells was purchased from Sigma-Aldrich Chemie GmbH (Steinheim, Germany) and ground to fine powder in a mortar. 200 mg of fine powder was shaken in 20 ml MilliQ-H_2O for 16 h. Insoluble chitin fractions were spun down (1900 g, 10 min) and the supernatant was used for the experiments (10 mg/ml).

PAMP treatment was performed using ten leaf discs (LD, 5 mm diameter) from 7-days-old barley plants or from 6-week-old arabidopsis plants in 24-well plates. LD were floated in MilliQ-H_2O for 16 h. After

incubation in fresh water for 30 min LD were elicited with 100 nM flg22 and 100 µg/ml chitin, harvested at 0, 2, 5, 7, 10, 20, 60 min and frozen in liquid nitrogen.

For measuring reactive oxygen species production, 24 LD of 5 mm in diameter from 7 days old barley plants per genotype were incubated in 200 µl MilliQ H_2O for 16 h in 96-well plates. These 24 LD were splitted in 2 x 12 for control LD which were not elicited and for sample LD which were elicited with the PAMPs flg22 and chitin. After 16h incubation, water was evacuated and 100 µl horseradish peroxidase mix (HRP) (2 µg/ml HRP, 10 µM L012) was added for sample LD and 150 µl HRP mix to the control LD. For detailed measuring procedure, refer to Section 9.3.4.

9.2 MOLECULAR BIOLOGY METHODS

9.2.1 MICROARRAYS.

Microarray analysis was carried out based on total RNA extracted using the Trizol method (Chomczynski and Sacchi, 1987) from 14-days-old second barley leaves (WT, *CA RACB*, *RACB* RNAi each 12 h and 32 h after either mock- or *Bgh*-treatment). RNA was solved in MilliQ H_2O and treated with DNaseI according to the manufacturer's manual (RNase-Free DNase set (#79254), Qiagen, Hilden, Germany) before RNA clean up with RNeasy® MinElute® Cleanup (#74204, Qiagen, Hilden, Germany). RNA quality was assessed with an Agilent 2100 Bioanalyzer (Agilent Technologies, Santa Clara, USA). High-quality cRNA was generated with an input of 100 ng RNA using the Agilent`s Low Input Quick Amp Labeling Kit which produces fluorescent cRNA by labeling with cyanine 3-labeled CTP. Four biological replicates per genotype, treatment and timepoint were prepared. The custom array SCRI_Hv35_44k-v1 (Agilent design: 020599) representing 42, 302 barley cDNA contig sequences in a 60mer probe per selected gene in a 4x44k format was generated. Full details of the array can be found in Mayer (2011) and at Array-Express (http://www.ebi.ac.uk/microarray-as/ae/; accession number A-MEXP-1728) (Mayer, 2011). The barley arrays were hybridized at 65 °C for 16 h and subsequently washed and scanned with the Agilent Microarray Scanner according to the manufacturer's manual (One-Color Microarray-Based Gene Expression Analysis Low Input Quick Amp Labeling protocol, Version 6.5, May 2010). Raw data were extracted with the Feature Extraction software v.10.7.3.1 (Agilent Technologies) and imported into Genespring GX (v.12.5). Data were normalized by choosing percentile of 75 % and baseline-to-median algorithms. Subsequently, data were analyzed with 1-way ANOVA statistics ($p < 0.05$) with a Tukey posthoc test and filtered for genes with a 2-fold difference in expression level. Seven arrays had to be excluded as they were outliers. Hence, in WT two biological replicates at 12 h mock-treated and two replicates at 32 h *Bgh*-treated, in three biological replicates in *CA RACB* barley at 32 h untreated and three at 12 h *Bgh*-treated and three replicates in *RACB* RNAi ecotype at 32 h untreated and *Bgh*-treated were used for analysis instead of four biological replicates. Data are available on http://www.ncbi.nlm.nih.gov/geo/, accession number GSE69215.

9.2.2 Quality control of microarray data.

The quality of hybridization was directly checked after the scanning process by means of the Feature Extraction Program of Agilent (Agilent Feature Extraction Software 10.10.1.1). The quality control (QC)

report offers the possibility to analyse reproducibility and reliability of each of the arrays. Hereby a typical report includes “QC headers”, “Spot finding of Four Corners”, “Outlier Stats”, “Spatial Distribution of all Outliers”, “Net Signal Statistics”, “Histogram of Signals Plot”, “Negative Control Stats”, “Local Background Inliers”, “Foreground Surface Fit”, “Multiplicative Surface Fit”, “Reproducibility Statistics”, “Spatial Distribution of Median Signals for each Row and Column”, “1-Color gene expression spike-in signal Statistics”. Details to each of these metrics can be found in the Agilent manual. Agilent defines these metrics to be important to distribute between a good and a bad grid. Helpful points are the “Spot finding of Four Corners” and the “Evaluation Metrics” which is part of the “QC headers”. Fig. 2 exemplifies extracts out of a QC report from one array chip. The values in Fig. 2 A of the evaluation metrics list all mentioned QC points above and classifies into categories from excellent to evaluate with a colour code. In total this chip (grid) is of good quality as indicated by the blue colour and the first value calculated with 1. The histogram in Fig. 2 B shows the signal level and the shape of the signal distribution. Here, the number of intensity points is plotted against the log of the processed signal. The spot finding shown in Fig. 2 C is important to see whether spot centroids have been located properly. Otherwise if off-centres in one or more corners would appear, this grid cannot be used for further analysis. Grids showing more than one red value or a clear visible shift in the histogram were excluded from analysis.

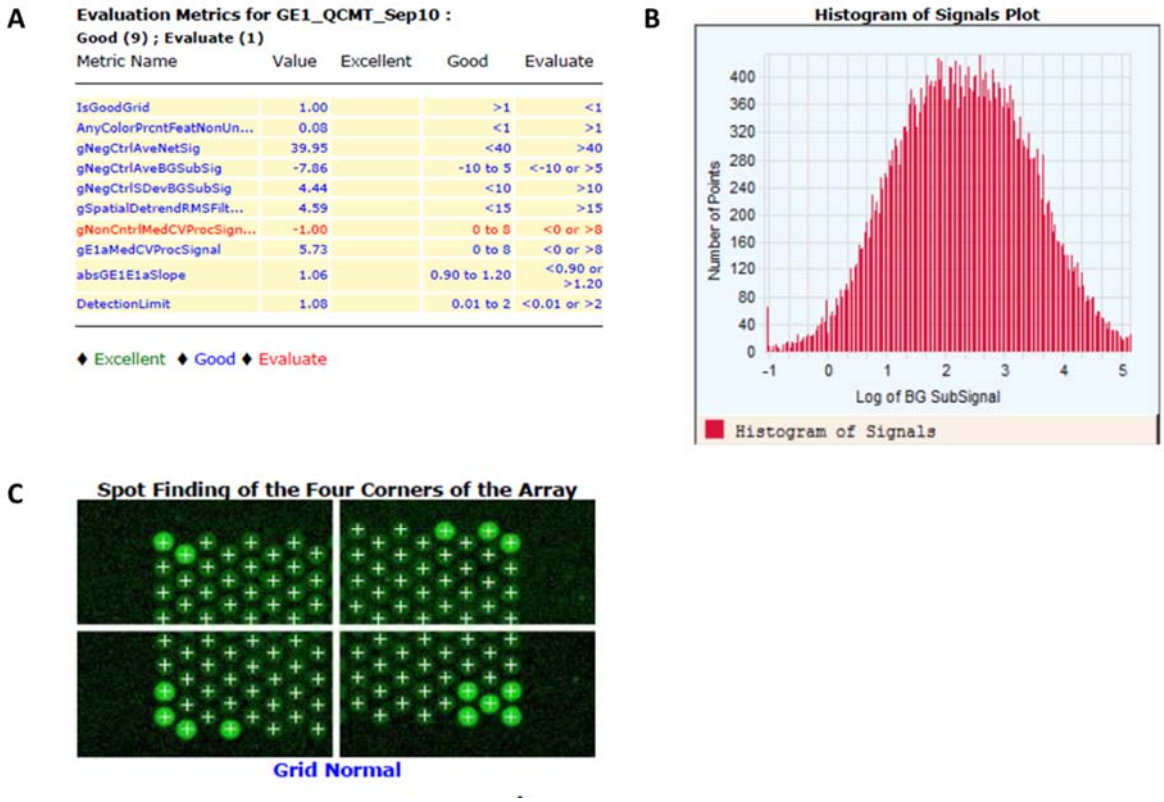

Fig. 2: QC report extracts examples a typical analysed microarray grid. QC reports are calculated via the Feature extraction Software of Agilent directly after the scanning process. Agilent defined several metrics to be important to determine between a good and a bad chip. **A-C** Examples helping the user to evaluate quickly whether the experiment meets the technical requirements for further

analysis. **A** Evaluation matrix listing all values and in a color-dependent range from excellent (green), good (blue) and evaluate (red). **B** Histogram of all the signal points arranged against the logarithm of the BackGround (BG) Subtraction Signal (SubSignal). Distribution of the points should be arranged in a typical histogram curve and not shifted to far to the left or right. **C** In each of the four corners spot centroids are checked to be located properly. If not, off-centres appear and the grid cannot be listed as normal. Mathematics and statistics are determined by Agilent and can be looked for in the manual of the Feature Extraction Software (http://www.chem.agilent.com/Library/usermanuals/Public/G4460-90026_FE_Reference.pdf).

9.2.3 Construction of RNAi and overexpressing constructs for functional assessment of genes and localization studies of proteins.

For transient gene silencing studies by RNAi, 200 – 500 bp fragments were amplified with gene specific primers (Table 1) out of a cDNA pool out of leaves of WT, *CA RACB* and *RACB RNAi* leaves treated with and without *Bgh* at 12 hpi and 32 hpi in a standard PCR approach with Phusion® High-Fidelity DNA Polymerase (Life Technologies, Carlsbad, USA) and checked for off-target specificity with the freely available SiFi program (http://labtools.ipk-gatersleben.de/). Blunt-ended fragments were cloned in antisense-sense orientation into the entry vector pIPKTA38 and subsequently into the destination vector pIPKTA30N by using the Gateway standard lambda-based site-specific recombination (Gateway LR clonaseII, Thermo Fisher Scientific, Waltham, United States) reaction described before (Douchkov *et al.*, 2005).

For generation of OE constructs, coding sequences were amplified from cDNA using specific full-length primers (Table 1). Full-length open reading frames were cloned into pGEMTeasy entry vector by TA cloning (Promega, Madison, USA) and after sequence confirmation subcloned into the pUC18-based plant expression vector pGY1 under the control of the 35S Cauliflower Mosaic Virus (CaMV) promotor (Schweizer *et al.*, 1999) with adequate restriction sites (*Xba*I, *Sph*I or *Sal*I).

To fuse the leucine-rich repeat containing protein (LRR-P) to different fluorescent proteins (LRR-P-GFP or LRR-P-mCherry) for localization studies, the coding sequence was amplified by PCR using specific primers (Table 1) containing *Bpi*I restriction sites for GoldenGate cloning (Engler *et al.*, 2008; Weber *et al.*, 2011). The PCR fragment was cloned into the pUC18-based entry vector pGGEntL-EP-21 (S. Ranf, unpublished) using *Bpi*I restriction-ligation. By using the GoldenGate cloning system (S. Ranf, unpublished) a fragment missing the stop codon was produced by *Eci*I digestion and subsequent blunting of the 3'-overhang with T4-DNA-Polymerase (Thermo Fisher Scientific, Waltham, USA) and subcloned in frame to the N-terminus of the 35S CaMV promotor-driven fluorophore into the destination vectors pGGIn-224C-GFP or pGGIn-225C-mCherry, respectively, using *Esp3*I restriction-ligation.

9.2.4 Isolation and purification of plasmid DNA.

For isolation and purification of plasmid DNA from *Escherichia coli* (*E.coli*) alkaline lysis method was performed with the NucleoSpin Plasmid Extraction Kit of Macherey-Nagel GmbH &Co. KG (Düren,

Germany) performed according to the manufacturer's manual. One colony from a selection plate containing the putative plasmid was inoculated in 3 ml liquid culture with the appropriate antibiotic (LB medium (5 g/l yeast extract, 10 g/l tryptone, 10 g/l NaCl, 15 g/l agar, pH 7) and 50 µg/ml kanamycin for pIPKTA38 in DH5α cells, 50 mg/ml spectinomycin for pGGIn in DH5α cells or 100 mg/ml ampicillin for pGY1, pIPKTA30N and pGGEntL in DH5α cells) and incubated at 37 °C overnight with shaking. DH5α cells were centrifuged for 10 min at 20 000 x g and DNA was isolated out of the pellet. Purified DNA was collected in 40 µl MiliQ H_2O and stored at -20°C until use. For midi-scale extraction the NucleoBond Xtra Midi Kit (Macherey-Nagel) was used. According to the manufacturer`s manual one colony from a selection plate containing the putative plasmid was inoculated in 100 ml LB medium and incubated at 37 °C overnight with shaking. Bacteria were collected *via* centrifugation for 50 min at 4000x*g* at 4°C. Finally, the DNA was dissolved in 100 µl MilliQ H_2O and stored until use at -20 °C.

9.2.5 Total nucleic acid extraction from plant tissue.

Genomic DNA (gDNA) was extracted from 7 days old *CA RACB* overexpressing plants. 0.5 cm leaf pieces of the first leaf were harvested in a 2 ml reaction tube prepared with 3 glass beads (2 mm diameter). Leaf material was frozen in liquid nitrogen and ground with the TissueLyser (Qiagen, Mannheim, Germany) for 1 min at 30 Hz. Ground material was resuspended in 500 µl extraction buffer (200 mM Tris-HCl pH 7.5, 250 mM NaCl, 25 mM EDTA, 0.5 % SDS (w/v)) and mixed vigorously. After 5 min incubation at RT 500 µl chloroform was added and mixed vigorously. After centrifugation for 10 min at 20 000 x *g* the supernatant was taken in a new reaction tube and precipitated with isopropanol for 10 min on ice. Pellet was washed with 70 % (v/v) EtOH and gDNA was spun down at 20 000 x *g* for 5 min and dried at 37°C for 10 min. Finally, the gDNA was dissolved in 40 µl MilliQ H_2O.

Presence of the *CA RACB* construct (Schultheiss *et al.*, 2005) was verified by PCR using the maize ubiquitin promotor-specific primer (Table 1). *RACB RNAi* construct carrying plants were identified phenotypically *via* their lacking root hairs as described in (Hoefle *et al.*, 2011).

9.2.6 RNA extraction from plant tissue.

Pools of second leaves of 3-5 different 14 days old barley plants per genotype and treatment were ground in liquid nitrogen to a fine powder in a mortar. RNA was extracted from 100 mg of the ground material using the Trizol method (Chomczynski and Sacchi, 1987). RNA concentration was measured photometrically at 260 nm using a NanoDrop photometer (Peqlab, Erlangen, Germany) and placed at -20 °C for short term or -80 °C for long term storage.

9.2.7 cDNA synthesis

1 µg total RNA was transcribed into cDNA using QuantiTect Reverse Transcription Kit (Qiagen (Mannheim, Germany). The manufacturer`s protocol was followed except for the gDNA elimination from barley RNA was performed for 10 min and reverse transcription for 30 min. cDNA was stored at -20 °C.

9.2.8 Polymerase chain reaction (PCR).

For genotyping of barley plants or testing of primers for quantitative Real-Time PCR, PCR was performed with 50-100 ng gDNA or 2 µl cDNA in a 20 µl reaction consisting of 2.5 µl 10x reaction buffer, 1.25 µl 2 mM dNTP mix (25 mM dATP, dCTP, dGTP and dTTP), 2.5 µl 10 µM forward and reverse primer each (see 8.2.4 and Table 1), 1 U Biotherm Taq polymerase and 16 µl MilliQ H_2O. PCR conditions used were an initial denaturation step at 95 °C for 5 min followed by 28-35 cycles of denaturation at 95 °C for 30 sec, annealing at 60 °C for 30 sec and elongation at 72 °C for 30 sec/1 kb DNA template and a final 10 min extension step at 72 °C. Barley ubiquitin conjugating enzyme 2 (*UBC2,* AY220735) was used as reference gene for semi-quantitative PCR as this housekeeping gene is constitutively expressed.

For cloning amplification of the PCR fragments was performed with Phusion® High-Fidelity DNA Polymerase (Life Technologies, Carlsbad, USA), Q5® High-Fidelity DNA Polymerase (New England Biolabs GmbH, Ipswich, USA), Herculase II Fusion DNA Polymerase (Agilent Technologies, Santa Clara, USA), KAPA3G DNA Polymerase (VWR International GmbH, Erlangen, Germany) or BIOTAQ ™ DNA Polymerase (Bioline GmbH, Luckenwalde, Germany) according to the manual for reagents composition and PCR conditions. Generally, 1-5 µl cDNA or gDNA was mixed with 10 µM forward and reverse primer each together with the necessary other reagents dependent on each polymerase in a 25 µl or a 50 µl final volume. Bacteria colony PCR was performed as described similar as for genotyping of barley. One colony was picked into a 25 µl final volume of PCR reaction. The PCR war performed with a program consisting of an initial denaturation step at 95 °C for 5 min, 40 cycles of denaturation at 95 °C for 1 min, annealing at 53 °C for 1 min and elongation at 72 °C for 2 min and a final extension step at 72 °C 10 min.

All PCR products were analysed by electrophoresis in a 1 % agarose gel supplemented with ethidium bromide (10 µg/ml, w/v). DNA bands were visualized with an UV-transilluminator (Wealtec, Meadowvale Way Sparks, USA).

For quantitative gene expression analysis a quantitative Real-Time PCR (qPCR) in a Mx3005P cycler (Agilent, Santa Clara, USA) using the Maxima SYBR Green qPCR master mix (2x) (Thermo Fisher Scientific, St. Leon-Rot, Germany) was used. cDNA of either mock- and *Bgh*-treated or PAMP-treated plant material was prepared and reactions were carried out in duplicates with 1 µl cDNA and 330 nM forward and reverse primer each in a 10 µl final volume. Expression values of the candidate genes were normalized to the internal control and housekeeping gene (*UBC2*) using the ΔΔCt method (Livak and Schmittgen, 2001). The PCR program consisted of an initial step at 95 °C for 10 min and 95 °C for 30 s followed by 40 cycles at 55 °C for 30 s and at 72 °C for 1 min. The melting curve analysis was performed at 55 °C – 95 °C. All primers (Table 1) were designed using Primer3 software (Untergasser *et al.*, 2012) and were checked for specificity using the Basic Local Alignment Search Tool (BLAST) and therein with nucleotide blast against *Hordeum vulgare* database (http://blast.ncbi.nlm.nih.gov), OligoCalc (Kibbe, 2007) and semi-quantitative PCR before running RT-qPCR. Standard curves were performed with 10 ng cDNA dilution series (100 ng, 50 ng, 25 ng, 12.5 ng, 6.75 ng) mixed with 330 nM forward and reverse primer each in a 10 µl final volume in triplicates to validate specificity of the primers for the RT-qPCR conditions.

Table 1: Oligonucleotides sequences for PCR.

Gene of interest	Harvest 35 assembly number: P_35_	Accession number	Forward primer (5`→3`)/ reverse primer (5`→ 3`)	T (annealing) [°C]	Product size [bp]	restriction site
RNAi constructs						
LRR-P	15510	AK360562	TCTAGATACCGGAGCAGCG GTCGACTACTGCCCCAAGC	60	451	*Swa*I
COP	24054	AK368392	ATGCATCTACACATGACCAAGA GACCATCTCCAACTCCGACC	60	339	*Swa*I
S-RLK	7436	AK369396	AACCTCACCTACCTGGAGACG CTTTTGAGCTTTGTAAGGTTGC	60	311	*Swa*I
LRR-RLK	26520	AK361450	TGGAGACGCTCGACCTCA GCTTTTGAGCTTTGTAAGGTTG	60	299	*Swa*I
WAK-RLK	42590	AK365606	GCTTTATCGAACATCCCCTCAT CGCACGAGCCATTTGTTAGG	60	235	*Swa*I
DUF26-RLKa	6100	AK368110	ACATCTGTGTTGACCGGATTGC TGCATCGAAGAGAACGGTGT	60	242	*Swa*I
OE constructs						
LRR-P	15510	AK360562	TCTAGATATGGCAGCTCAGACC GGCATGCCTCAGCTTGTAGT	60	689	*Xba*I, *Sph*I
COP	24054	AK368392	TCTAGATATGAGCGGTTTCCTC GGCATGCCTTAGTATAGTTTTACTCT	60	1629	*Xba*I, *Sph*I
WRKY18	23506	DQ840417	TCTAGATTCCATCGGCATG GTCGACTATGCTCGCGTG	60	561	*Xba*I, *Sal*I
WRKY22	25198	AK377066	TCTAGATATGGAGAGCGTGGA GTCGACATATCATGCAAAGAAGC	60		*Xba*I, *Sal*I
			OE construct with fluorescent tag			
LRR-P-GFP HvLRR-P-mCherry	15510	AK360562	TGAAGACTTAATGGCAGCTCAGACCG G TGAAGACTTACTAGCTTGTAGTCTTGA GCG	60	675	*Bpi*I, *Esp3*I
			qRT-PCR primers			
UBC2	46110	M60175	TCTCGTCCCTGAGATTGCCCACAT TTTCTCGGGACAGCAACACAATCTTCT	58	263	
Gene of interest	**Harvest 35 assembly number: P_35_**	**Accession number**	**Forward primer (5`→3`)/ reverse primer (5`→ 3`)**	**T (annealing) [°C]**	**Product size [bp]**	**restriction site**
PR1b	704	Z26333	AAGCTGCAAGCGTTCGCC AGGTGTTGGAGCCGTAGTC	60	184	

PR3	14580	AK364132	CTACACGTACGACGCCTTCAT GTGGCCTTGCTTATCTCTTCC	60	195	
PR5	14133	AK371265	CACGGACATCACCAAGGATT TTGCCCTTGAAGAACATTGAG	60	153	
PR10	15827	AK360974	AGGGCGACAAGGTAAGTGG CATCTTGAGCAGGTCGAGGTA	60	182	
JIP23	14320	AB251339	TGTTGCAGACTATGCCATGAA TGCCAATCGTTGTACTTAGCC	60	168	
JIP60	1209	AK372562	TTCTTCTTCCGGGCTGTAAAT GTACGCTGAGCTACCCAGACA	60	151	
LRR-P	15510	AK360562	TCTTCAGTTGTCCCAGTTGAG GTGTGGAAGGACCCCAAC	60	166	
COP	24054	AK368392	TCGCGGACAATTAAGACACC TGTCCATTCATTACTTTTTGTGAAA	60	180	
S-RLK	7436	AK369396	ATGACCAGTAGAATAATAACAACGGA ACATCAGTGGAGGCGGC	60	190	
LRR-RLK	26520	AK361450	AAGATCTCCAGCAGCGTGAT AATTCAGAGAGCACCATTGGA	60	125	
WAK-RLK a	21250	AK365606	ATTCCACCATCGACGAGC TATCACAGGAAAATGGGATTGAC	60	227	
WAK-RLK b	12191	AK362513	TCTCGCAGTTTCTTAGCTCTGA TGCTAATATGTGTGGCACTGG	60	240	
WAK-RLK c	50253	AK362513	ATTACTATGATGAATTGCTCGTTGA GCATATCTGGAGCTACCCTCTC	60	262	
DUF26-RLK a	39909	AK252276	TTCTTTCCATGTTGCCCTTC TCTGGAGTGTGTGCACATCG	60	162	
DUF26-RLK b	6100	AK368110	AACACCGTTCACGATCTTCAG TGTACGAGTATATGCCAAACCTG	60	104	
DUF26-RLK c	10485	AK253014	AGAGAGGCTGCTCATCTATGAG TGAGGTCACGATGGACTACTTT	60	179	

Gene of interest	**Harvest 35 assembly number: P_35_**	**Accession number**	**Forward primer (5`→3`)/ reverse primer (5`→ 3`)**	**T (annealing) [°C]**	**Product size [bp]**	**restriction site**
WRKY2	15932	AJ853838	GACAGCAAGCGCGTCC CACCTTCTGCCCGTACTTC	60	132	

WRKY3	9124	AK359706	ATCAAGGTCAAGAGGGTCTGC TCACCTTCTGCCCGTACTTC	60	97
WRKY18	23506	DQ840417	GTGGAGGAAGTACGGCAAGA AACCCCCTCATACATCGTCA	60	148
WRKY20	3498	AK363451	GCAAGTACGGCAAGAAGTCC TGGCGTAGTAGATGGTGCTG	60	180
WRKY22	25198	AK377066	TTCGTTTTTGGGACAAGGAG GCTTCCTCCATTTTCATCCA	60	84
MPK3-like	2237	MLOC_17814	ATAGTAGGCCTCCGAGACGTG TTCAGGTCGCGATGGATC	60	209
MPK4-like	2346	AK366765	TGATTCAAGCCTGGGATTTC GATGCAGAGCCTCATCAACA	60	185
MPK6-like	46412	AK355058	GCTTTATCGGAGGAGCACTG GCAAGCCCAAAATCACAAAT	60	155
Bacteria colony check primer					
M13/pGEMT			GTTTTCCCAGTCACGAC AACAGCTATGACCATGA	53	320
pGY1			TGACGCACAATCCCACTAT AGAGAGACTGGTGATTTCAGC	53	136
pIPKTA38			AGCAGGCTTTAAAGGAACC TGTACAAGAAAGCTGGGTCT	53	109
pIPKTA30N att I			GATGACGCACAATCCCACTATCCT TCAAATTAAACAAATGCAGTATGAAGA	53	401
pIPKTA30N att II			GGATAGCCCTCATAGATAGAGTACTAA CTAA ATGAGCGAAACCCTATAAGAACCCTA	53	444
Barley genotyping					
CA RACB	1790	AJ344223	AACCAGATCTCCCCCAAATC GTTGGGTCTTCGAGCTGCAT	58	1070
RACB RNAi	1790	AJ344223	GGCTTGCTCCATCTTGTGATC GTCGGCACCTCCGCTTC	58	636
CA RAC1	19046 20494	AJ518933	ATCCGCTGGAGAGGAGAGG TCAGCGGGCATGCCT	58	666

9.2.9 Particle bombardment.

Leaves of 7-days-old wild-type barley plants were transiently transformed *via* biolistic delivery in epidermal cells with gold particles. Gold stock solution was prepared as followed: 27.5 mg of 1 micron gold (Biorad, Munich, Germany) were mixed in 1 ml MilliQ H_2O and incubated for 30 s in an ultrasonic bath. Afterwards particles were centrifuged for 30 s at 20 000 *g*, the supernatant was discarded and the gold particles were washed with 1 ml MilliQ H_2O and 1 ml 100 % EtOH twice. Particles were dried at 50 °C, resuspended in 50 % glycerol and stored at -20 °C until further use. Transient transformation

was carried out with the particle delivery system PDS-1000/HeBiolistic Particle Delivery (Biorad, Munich, Germany). First, barley leaves were cut and laid down with the adaxial side up onto petri dishes containing 0.5 % (w/v) water agar. Leaves were bombarded with gold particles coated with the desired plasmids. To destroy gold clusters, gold particles were solubilized in an ultrasonic bath for 10 min and 1 µg of the plasmid containing the gene of interest was mixed with 0.5-1 µg plasmid carrying the reporter gene GFP or mCherry. 11 µl/reaction of gold particles were added to the plasmids and for a better precipitation of the plasmids onto the gold particles 14 µl/reaction of 1 M calcium nitrate (pH 10) was added dropwise to the mixture during vortexing. The mixture was incubated for 30 min at room temperature with inverting from time to time. The gold-plasmid mixture was washed with 1 ml 70 % EtOH and with 1 ml 100 % EtOH before finally adding 6 µl 100 % EtOH/shoot. In between the washing procedure, the mixture was vortexed and centrifuged at 20 000 g for 30 s. The washed solution was then evenly distributed on macrocarriers and the barley leaves containing petri dishes were placed in the particle delivery system. 26 Hg vacuum was applied and gas pressure was regulated *via* rupture discs of 1200 psi (pounds per square inch). All accessories such as macrocarriers and rupture discs were obtained from Biorad (Munich, Germany). In the case of overexpressing constructs bombarded barley leaves were incubated for 4 h and in the case of RNAi constructs leaves were incubated for one day in a plant chamber (see 8.1.1) before inoculation with *Bgh* (100 spores/mm²).

9.2.10 Gene function assessment by transient transformation.

To test gene function of test plasmids (containing either the RNAi or the OE construct) 7-days-old barley leaves were transiently transformed with 1 µg of the test plasmid together with 1 µg pGY1::GFP, pGY1::mCherry or pGY1::RAC1-CFP (Hoefle *et al.*, 2011; Huesmann *et al.*, 2012) as transformation markers and inoculated as described in 8.1.2. For microscopic analysis transiently transformed barley leaves were shortly washed in MilliQ H_2O and fungal chitin was stained for 1 min in 0.3 % (w/v) calcuoflor solution (see 8.4.1) as described (Hueckelhoven *et al.*, 2003; Schultheiss *et al.*, 2002).

To test whether LRR-P is silenced efficiently 1 µg per shot of each of the constructs pIPKTA30N-LRR-P (Harvest35 identifier P_35_15510) or pIPKTA30N empty vector together with pGGIn-LRR-P-GFP and the transformation marker pGY1-mCherry were transiently transformed into 7-days-old detached barley leaves. mCherry-expressing cells were inspected two days after bombardment for presence or absence of LRR-P-GFP fluorescence by microscopy. In total at least 50 interactions per construct in three independent experiments were evaluated and penetration efficiency was calculated as the number of all penetrated cells divided by the number of attacked cells multiplied with 100 and used as the relative frequency of cells with haustoria in percent. For testing RNAi efficiency of the LRR-P TIGS construct 300 cells were counted in total in three independent experiments in each of the variants.

9.3 BIOCHEMICAL METHODS

9.3.1 Protein extraction from plants.

Total proteins were extracted in 80 µl of 2x extraction buffer (50 mM Tris-HCl pH 7.5, 100 mM NaCl, 20 mM EGTA, 30 mM ß-glycerophosphat, 30 mM 4-pNitrophenylphosphat, 20 mM $MgCl_2$, 4 mM NaF, 4 mM Na_3VO_4, 4 mM Na_2MoO_4, 10 mM DTT, 0.2 % (v/v) Tween20, 1% (w/v) protease inhibitor) on ice. Extracts were centrifuged at 20 000 x *g* for 10 min at 4 °C and the cleared supernatant transferred into a fresh reaction tube. 1 µl of the lysat was used for calculating the protein concentration *via* Bradford test (Bradford, 1976; Kruger, 1994) using the Bio-Rad protein assay reagent (BioRad, Munich, Germany). 50 µg protein extracts were mixed with 5x SDS Loading buffer (60 mM Tris-HCl pH 6.8, 2% (v/v) SDS, 10 % (v/v) glycerol, 5 % (v/v) β-mercaptoethanol, 0.01 % (v/v) bromophenol blue), heat-denatured at 95 °C for 10 min and applied for immunoblot analysis.

9.3.2 Sodium dodecyl sulphate (SDS)-PAGE.

Total proteins were separated by SDS-PAGE (Laemmli, 1970) using 6 % stacking gels (7.9 ml H_20, 6.7 ml 30 % acrylamide mix, 5.0 ml 1.5 M Tris (pH 8.8), 200 µl 10 % SDS, 200 µl 10 % ammonium persulfate, 8 µl N, N, N´, N´ tetramethylethylenediamine (TEMED) for 4 gels in total) and 10 % separation gels (6.8 ml H_20, 1.7 ml 30 % (v/v) acrylamide mix, 1.25 ml 1.5 M Tris (pH 6.8), 100 µl 10 % (w/v) SDS, 200 µl 10 % (w/v) ammonium persulfate, 1 µl TEMED for 4 gels in total). 50 µg of total protein was separated and electrophoresis was carried out at 100 V for 120 min in 1x Laemmli buffer (10 x stock solution: 30 g (w/v) Tris-Base, 144 g glycine, 10 g SDS, pH 8.3) in a Mini Protean III Cell (BioRad, Munich, Germany).

9.3.3 Immunoblot analysis.

For western blot analysis proteins were electrophoretically transferred onto Protran nitrocellulose membrane (Whatman, Springfield Mill, UK) at 1 mA/cm^2 for 1 h using a SemiDry blotter (Trans-Blot SD, BioRad, Munich, Germany). Transfer buffer contained 0.5 M Tris, 0.8 M glycine, 0.4% (w/v) SDS and 20 % (v/v) methanol. After transfer the membrane was incubated in 5 ml Pierce-Protein free T20 (Tris-buffered saline pH 7.4, 0.04 % (v/v) Tween20) blocking solution for 1 h to block remaining binding sites. For detection of phosphorylated MAPKs the membrane was incubated with anti-pTEpY (α-phospho-p44/42-ERK, Cell Signaling Technology, Cambridge, United Kingdom) in a 1:1000 dilution in 5 ml fresh protein buffer for 16 h at 4 °C. As secondary antibody anti-rabbit IgG-HRP conjugate (Cell Signaling Technology, Cambridge, United Kingdom) was used in a 1:80 000 dilution and applied for 1-2 h with shaking at RT. 1x TBS (87.6 g NaCl, 12.1 g Tris, pH 7.6, 0.05 % (v/v) Tween20) was used as washing buffer between each step up to three times. Chemiluminescence detection was performed using SuperSignal West Femto Maximum Sensitivity Substrate (Pierce, Rockford, USA) (Saijo, 2009). Equal protein loading and transfer was determined by total protein staining with amido black (0.1 % (w/v) amido black, 25 % (v/v) isopropanol, 10 % (v/v) acetic acid).

9.3.4 ROS accumulation

Reactive oxygen species (ROS) accumulation was assayed by luminescence after H_2O_2-dependent oxidation of luminol. 24 leaf discs (LD) (5 mm diameter) from 7-days-old barley plants per genotype were floated in 200 µl MilliQ H_2O for 16 h in 96-well plates. These 24 LD were split in 2 x 12 for control LD which were not elicited and for sample LD which were elicited with the PAMPs flg22 and chitin. After 16h incubation, water was evacuated and 100 µl horseradish peroxidase (HRP) mix (2 µg/ml HRP, 10 µM L012) was added for sample LD and 150 µl HRP mix to the control LD.100 nM flg22 and 100 µg/ml chitin was applied. Luminescence was measured in 1 min intervals with a TecanReader (infiniteM200, Tecan, Männedorf, Switzerland) for 30 min.

9.4 CELL BIOLOGICAL AND HISTOCHEMICAL METHODS

9.4.1 Staining methods

9.4.1.1 WGA staining of fungal structures.

Wheat germ agglutinin-tetramethylrhodamin (WGA-TMR, Invitrogen Molecular Probes GmbH Karlsruhe, Germany) binds to fungal chitin. To investigate haustorium development of *Bgh* on *Hordeum vulgare*, inoculated leaves were harvested 16, 24, 32, 34, 37, 48 h after inoculation (100 spores/mm²), discoloured in 70% EtOH and washed in MilliQ H_2O to remove the EtOH and equilibrated for 6 minutes in 1x PBS buffer (80 g (w/v) NaCl, 2 g KCl, 7.65 g $Na_2HPO_4x2xH_2O$, pH 7.4). The leaves were placed into the staining solution (0.01 µg/µl WGA-TMR and 0.01 µg/µl bovine serum albumin (BSA) in 1x PBS buffer (50 µl WGA-TMR, 50 µl BSA, 4900 µl 1xPBS)) and vacuum infiltrated twice at -0.8 bar. After 24-48 h incubation in the dark at 4°C, haustorial growth was analysed by confocal laser-scanning microscopy (Leica Microsystems CMS GmbH, Mannheim, Germany). WGA-TMR was excited at 561 nm and detected between 570-615 nm.

9.4.1.2 Calcofluor staining of fungal structures.

Calcofluor binds to chitin and is used to stain fungal cell walls. After transient transformation of the test plasmids together with pGY1-GFP as transformation marker and subsequent inoculation with *Bgh* (see chapter 8.2.8 and 8.2.9) 7-days-old detached barley leaves were stained for 1-2 min in 0.3 % calcofluor and then shortly washed in MilliQ H_2O containing Tween20. Visualization was performed with standard fluorescence microscopes using the GFP filter (495 nm – 530 nm) and the DAPI filter (358 nm – 461 nm) for detection of fungal structures.

9.4.2 Subcellular localization of LRR-P-GFP.

Localization of LRR-P-GFP or LRR-P-mCherry (LRR-P, Harvest 35 identifier P_35_15510) was visualized after particle bombardment (see above) together with 1 µg pGY1-mCherry or 0.8 µg pGY1-GFP as an additional transformation marker of seven-days-old barley WT leaves by confocal laser scanning microscopy (CLSM, Leica TCS SP5, Leica Microsystems, Mannheim, Germany). GFP was excited with a laser line of 488 nm and detected at 500-550 nm whereas mCherry was excited with a laser line of 561 nm and detected at 570-620 nm with the highly sensitive hybrid detector. LRR-P-GFP was best

expressed 20-24 h after bombardment. For *Bgh*-dependent localization detached leaves were inoculated 4 h after bombardment with 100 spores/mm² and analysed after two days.

To test for autofluorescence lambda scanning was performed. For the single-channel lambda scan of the GFP-labelled fusion construct the detection range was set to 110 nm (490-600 nm) with a band width of 20 nm and a λ detection step size of 5 nm. For the mCherry-labelled fusion construct the detection size was set to 100 nm (570-670 nm).

9.5 BIOINFORMATIC METHODS

9.5.1 Sequence and phylogenetic analysis.

To determine cloning success 20 – 100 ng of a plasmid containing the gene of interest was sent with the appropriate primers (see Table 1, colony PCR) to Eurofins Genomics (Ebersberg, Germany) and was sequenced using the Sanger-based cycle sequencing technology with ABI3730XL sequencing devices. Data analysis and vector map generation was done with GEntle (http://gentle.magnusmanske.de/), SnapGene (http://www.snapgene.com/; GSL Biotech LLC, Chicago, USA) or pDRAW32 (http://www.acaclone.com/).

Protein sequence alignments were carried out with ClustalW2 (Goujon *et al.*, 2010; Larkin *et al.*, 2007) and visualized using JalView (Waterhouse *et al.*, 2009). Data were analysed for phylogeny using the Maximum Likelihood (ML) algorithm by using a matrix of pairwise distances estimated under the Jones-Thornton-Tayler (JTT) model (Tamura and Nei, 1993) in Molecular Evolutionary Genetics Analysis (MEGA6) (Tamura *et al.*, 2013). Sequences were obtained from GenBank (http://www.ncbi.nlm.nih.gov/genbank/, National Center for Biotechnology Information, U.S. National Library of Medicine, Bethesda, USA) or Ensembl Plants (Kersey *et al.*, 2014).

Table 2: **Protein accession numbers of *Arabidopsis thaliana* (At), *Oryza sativa* (Os), *Hordeum vulgare* (Hv, MLOC) are listed used for sequence alignments.**

protein	accession number	protein	accession number	protein	accession number
HvMPK3-like (TEY motif)	MLOC_17814	OsMPK15 (TDY motif)	LOC_Os11g17080	ZmBAK1c	AFW58459
HvMPK4-like (TEY motif)	MLOC_5653	HvLRR-P	BAJ91771	AtPRK2a	AT2G07040
HvMPK6-like (TEY motif)	AK376245	HvBAK1a	AEE44134	LeShy	AAR27431
HvMPK1-like a (TEY motif)	MLOC_44271	HvBAK1b	BAK05837	LeSTIG	AAR27430
HvMPK1-like b (TEY motif)	MLOC_74277	HvBAK1c	BAK03316		
HvMPK4 (TEY motif)	AK252980	HvSERKa	BAJ89901		
OsMPK1 (TEY motif)	LOC_Os06g06090	HvSERKb	ABN05373		
OsMPK3 (TEY motif)	LOC_Os02g05480	HvSERKc	BAK05837		
OsMPK4 (TEY motif)	LOC_Os06g48590	HvSERKd	BAK03316		
OsMPK5 (TEY motif)	LOC_Os03g17700	HvSERKe	MLOC_59982		
OsMPK6 (TEY motif)	LOC_Os10g38950	HvPAN1	BAJ89657		
OsMPK8 (TDY motif)	LOC_Os01g47530	HvPAN1-like	BAK01563		
OsMPK9 (TDY motif)	LOC_Os01g43910	ZmBAK1a	AFW57132		
OsMPK11 (TDY motif)	LOC_Os06g26340	ZmBAK1b	AFW71975		

protein	accession number	protein	accession number	protein	accession number
AtMPK1 (TEY motif)	AT1G10210	ZmBAK1d	AFW62723		
AtMPK2 (TEY motif)	AT1G59580	ZmSERK1	AJ277702		
AtMPK3 (TEY motif)	AT3G45640	ZmSERK2	AJ277703		
AtMPK4 (TEY motif)	AT4G01370	ZmSERK2-like	KJ004522		
AtMPK5 (TEY motif)	AT4G11330	ZmPAN1	ACI95776		
AtMPK6 (TEY motif)	AT2G43790	ZmPAN2	DAA42750		
AtMPK7 (TEY motif)	AT2G18170	AtBAK1	AT4G33430		
AtMPK8 (TDY motif)	AT1G18150	AtSERK1	AT1G34210		
AtMPK11 (TEY motif)	AT1G01560	AtSERK2	AT1G34210		
AtMPK12 (TEY motif)	AT2G46070	AtSERK3	AT4G33430		
AtMPK13 (TEY motif)	AT1G07880	AtSERK5	AT2G13800		
AtMPK14 (TEY motif)	AT4G36450	AtPAN1a	AT2G01210		
AtMPK16 (TDY motif)	AT5G19010	AtPAN1b	AT1G25320		
AtMPK17 (TDY motif)	AT2G01450	AtPAN1-like1	AT2G42290		
AtMPK20 (TDY motif)	AT2G42880	AtPAN1-like2	At3G57830		

9.5.2 Microarray data analysis

Pathway analysis was performed using the freely available program MapMan version 3.5.1 (Thimm *et al.*, 2004). LOG2 values of all regulated genes were classified into MapMan bins (functional categories) according to their annotation by mapping against the arabidopsis genome and its MapMan bin annotation (performed by Karl Kugler, Helmholtzzentrum München) resulting in a *Hordeum vulgare* MapMan bin file. Significant pathways were evaluated by use of the Wilcoxon rank sum test. Hierarchical clustering was done using again MapMan tool by measuring Euclidean distances.

9.5.3 Statistics

Microarray expression data were normalized by choosing percentile of 75 % and baseline-to-median algorithms. Subsequently, data were analysed with 1-way ANOVA statistics ($p < 0.05$) with a Tukey posthoc test and filtered for genes with a 2-fold expression level.

For verification of microarray data, qRT-PCR data were correlated to microarray data using the Spearman`s rank sum test with R statistics (http://www.r-project.org/) based on the mean of all biological replicates (minimum of three independent biological experiments). For all other experiments statistical analysis was performed using a two-sided unpaired Student`s t-test.

10. RESULTS

10.1 EARLY PLANT IMMUNE RESPONSE

The barley RAC/ROP protein RACB supports invasion of *Bgh* into epidermal cells of barley (Schultheiss *et al.*, 2002). Several RACB interacting proteins were identified holding crucial roles within the barley powdery mildew interaction (Hoefle *et al.*, 2011; Huesmann *et al.*, 2012; Reiner *et al.*, 2015; Schultheiss *et al.*, 2008). However, the exact mechanism of RACB function is not clear yet. It is possible that RACB a) influences the early immune response negatively or b) regulates structural or metabolic factors which are important for establishment of the fungus itself (Hueckelhoven *et al.*, 2013; van Schie and Takken, 2014).

To understand whether barley *RACB* negatively influences pattern-triggered immunity (PTI), ROS accumulation and MAPK activation were analysed as potential output responses. First, putative barley MAPK homologs were identified by bioinformatics and functionally described. Second, ROS accumulation and MAPK activation were measured in *RACB*-transgenic barley. Third, the expression of pathogenesis-related genes was additionally tested by qRT PCR with and without *Bgh* infection.

10.1.1 Barley MAPK homologs found in phylogenetic analysis

Based on MAPK protein sequences of AtMPK3, AtMPK4 and AtMPK6, involved in immunity, barley homologs were searched using the BLAST LINK function on NCBI database (http://www.ncbi.nlm.nih.gov/pubmed). This identified three potential barley MAPK homologs, MPK3-like, MPK4-like and MPK6-like. Sequence analysis (Fig. 3) of in total 35 barley, rice and arabidopsis MAPKs showed high conservation of typical amino acid motifs of MAPKs. From 35 analysed sequences - based on nomenclature of Doczi *et al.* (2007) and Singh *et al.* (2012) - 12 share the TDY motif whereas the 22 share the TEY motif important for dual phosphorylation of threonine and tyrosine (Ferrell and Bhatt, 1997; Nuehse *et al.*, 2000). Only one sequence has a MEY motif, not typical for plant MAPKs (OsMPK2). All barley sequences found shared the TEY motif. Considering the phylogenetic relationships of these MAPKs, three main clusters (Fig. 4) appeared. In the first subcluster of cluster 1 AtMPK4 appear together with AtMPK5, 11, 12 and 13, OsMPK2, OsMPK6 and HvMPK4-like. Members of this cluster are suggested to be involved in biotic and abiotic stress and associated with developmental processes (Beckers *et al.*, 2009; Bethke *et al.*, 2009; Lieberherr *et al.*, 2005; Taj *et al.*, 2014; Xiong and Yang, 2003). The well-known arabidopsis MAPKs AtMPK3 and AtMPK6 can be found in the second subcluster of cluster 1, together with the barley HvMPK3-like and HvMPK6-like, the AtMPK10 and the rice MAPKs OsMPK1and OsMPK5. The third cluster represents MAPKs with up to now unknown function, except for OsMPK3 and OsMPK4 which positively regulate the JA signalling pathway (Wang, 2013) and salt stress tolerance (Wang *et al.*, 2014a) as well as HvMPK4 which negatively regulates biotic stress to *Magnaporthe grisea* (Abass and Morris, 2013). The fourth cluster contains TDY-carrying MAPKs with unknown functions.

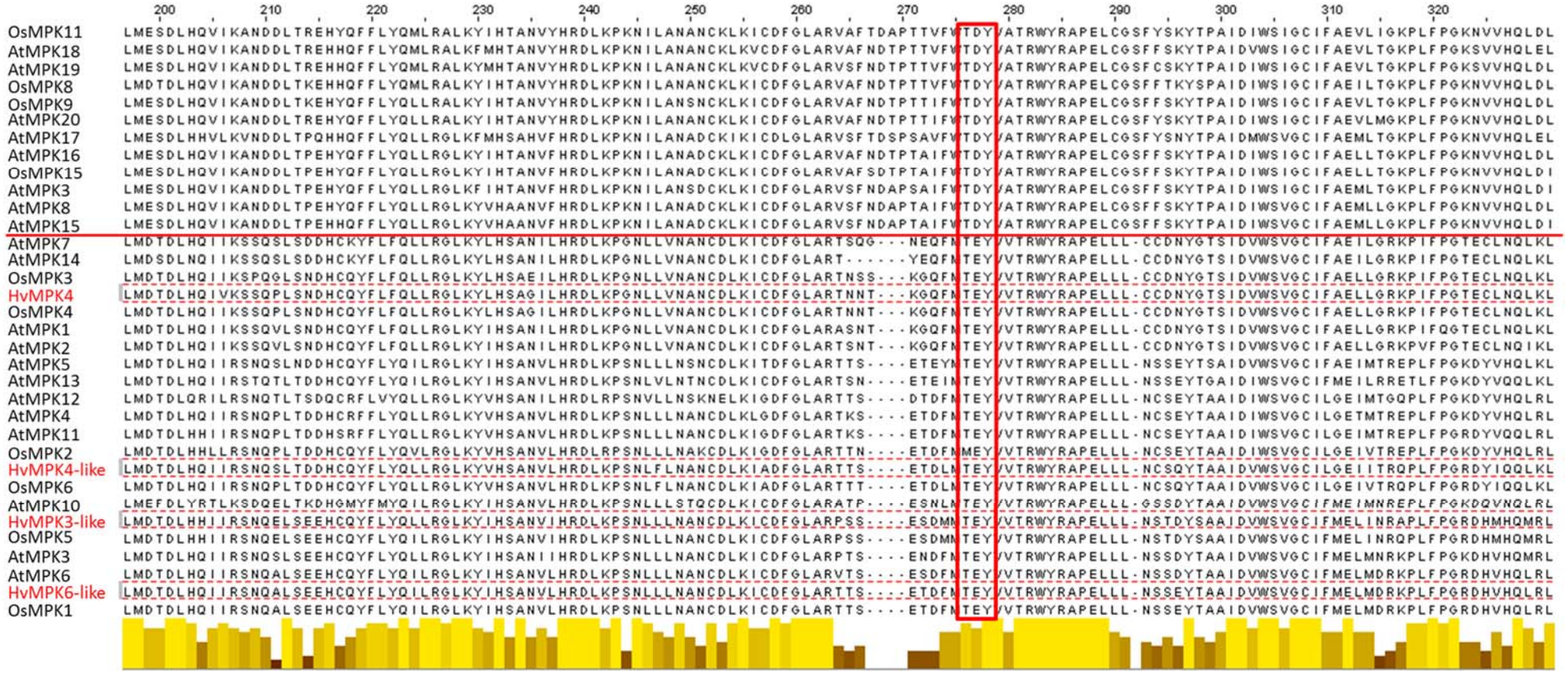

Fig. 3: Alignment of several barley, rice and arabidopsis MAPK protein domain sequences showing high conservation. This alignment extract shows 35 MAPK protein sequences aligned to each other by pairwise comparison performed in ClustalW2 (Larkin *et al.*, 2007) and Jalview (Waterhouse *et al.*, 2009). Red labelled MAPKs are barley protein sequences. 22 MAPKs sharing the TEY phosphorylation motif whereas 12 the TDY phosphorylation motif. Sequences were obtained from Genbank or EnsemlPlants: HvMPK4 (AK252980; was transcribed into protein sequence with the *Triticeae* full-length CDS database http://trifldb.psc.riken.jp/v3/index.pl), HvMPK3-like (MLOC_17814), HvMPK4-like (MLOC_5653), HvMPK6-like (BAK07440), AtMPK1 (At1g10210), AtMPK2 (At1g59580), AtMPK3 (At3g45640), AtMPK4 (At4g01370), AtMPK5 (At4g11330), AtMPK6 (At2g43790), AtMPK7 (At2g18170), AtMPK8 (At1g18150), AtMPK9 (AT3G18040), AtMPK10 (AT3G59790), AtMPK11 (At1g01560),

AtMPK12 (At2g46070), AtMPK13 (At1g07880), AtMPK14 (At4g36450), AtMPK15 (AT1G73670), AtMPK16 (At5g19010), AtMPK17 (At2g01450), AtMPK18 (AT1G53510), AtMPK19 (AT3G14720), AtMPK20 (At2g42880), OsMPK1 (LOC_Os06g06090), OsMPK2 (LOC_Os08g06060), OsMPK3 (LOC_Os02g05480), OsMPK4 (LOC_Os06g48590), OsMPK5 (LOC_Os03g17700), OsMPK6 (LOC_Os10g38950), OsMPK8 (LOC_Os01g47530), OsMPK9 (LOC_Os01g43910), OsMPK11 (LOC_Os06g26340), OsMPK15 (LOC_Os11g17080). MAPK nomenclature refers to literature (Doczi *et al.*, 2007; Singh *et al.*, 2012). Amino acids numbers correspond to OsMPK11.

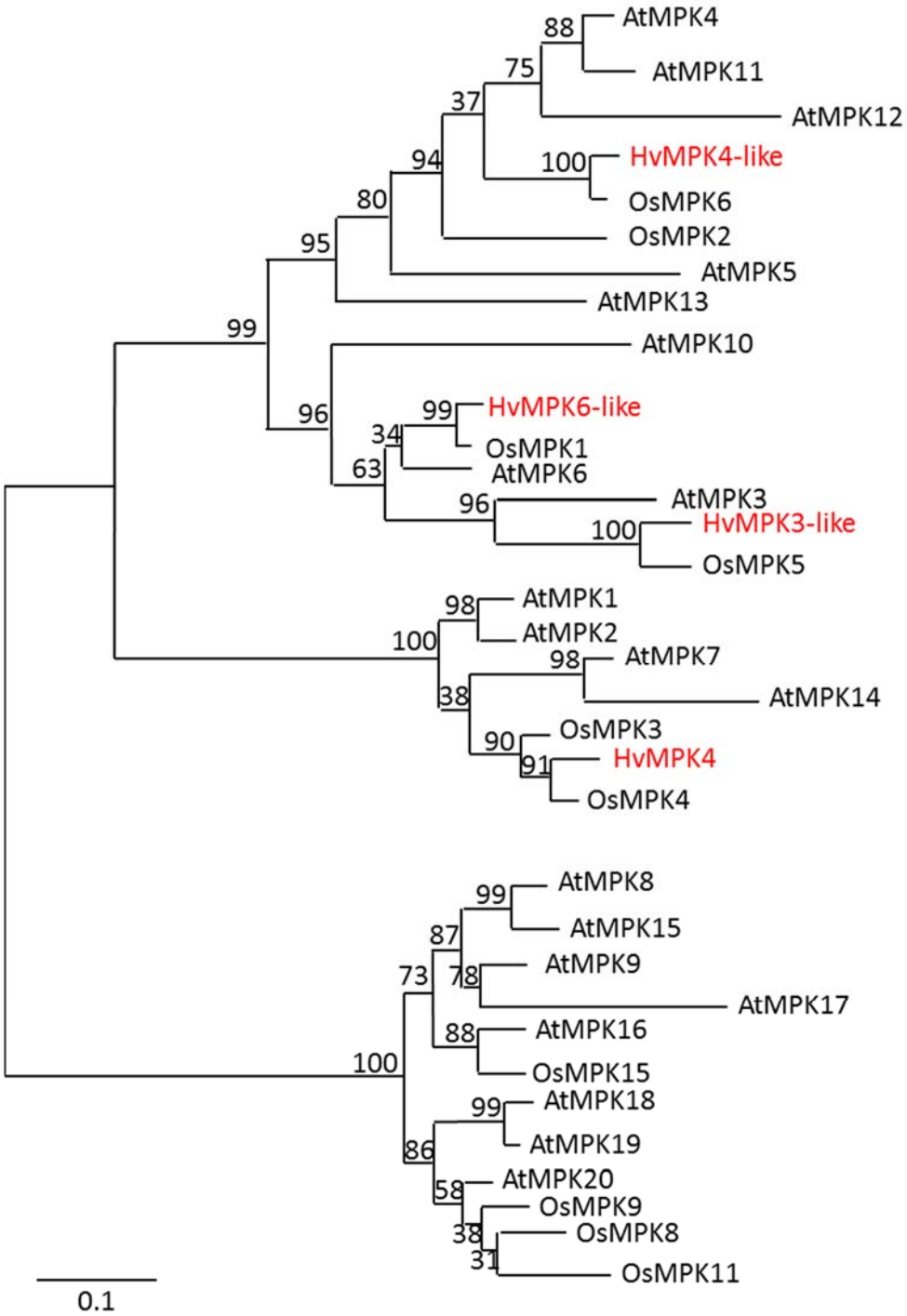

Fig. 4: Phylogenic clusters of barley MAPK homologs and known arabidopsis and rice MAPKs. MAPK proteins involved in abiotic and biotic stress of arabidopsis were compared to the corresponding rice and barley homologs. Alignments were carried out with ClustalW (Larkin *et al.*, 2007) and data were analysed using the Maximum Likelihood (ML) algorithm by using a matrix of pairwise distances estimated under the Jones-Thornton-Tayler (JTT) model (Tamura and Nei, 1993) in Molecular

Evolutionary Genetics Analysis (MEGA6) (Tamura *et al.*, 2013). The tree is drawn to scale 0.1 with branch lengths measured in the number of substitutions per site. Phylogeny test was done with the bootstrap method (Efron, 1979) with 500 replications (Pattengale *et al.*, 2010). Analysis was performed with MAPK protein sequences obtained from Genbank of arabidopsis, rice and barley: HvMPK3-like (MLOC_17814), HvMPK4-like (MLOC_5653), HvMPK6-like (BAK07440), AtMPK1 (At1g10210), AtMPK2 (At1g59580), AtMPK3 (At3g45640), AtMPK4 (At4g01370), AtMPK5 (At4g11330), AtMPK6 (At2g43790), AtMPK7 (At2g18170), AtMPK8 (At1g18150), AtMPK11 (At1g01560), AtMPK12 (At2g46070), AtMPK13 (At1g07880), AtMPK14 (At4g36450), AtMPK16 (At5g19010), AtMPK17 (At2g01450), AtMPK20 (At2g42880), OsMPK1 (LOC_Os06g06090), OsMPK3 (LOC_Os02g05480), OsMPK4 (LOC_Os06g48590), OsMPK5 (LOC_Os03g17700), OsMPK6 (LOC_Os10g38950), OsMPK8 (LOC_Os01g47530), OsMPK9 (LOC_Os01g43910), OsMPK11 (LOC_Os06g26340), OsMPK15 (LOC_Os11g17080). MAPK nomenclature refers to known literature (Doczi *et al.*, 2007; Singh *et al.*, 2012).

10.1.2 Barley MAPK homologs function in basal resistance and susceptibility.

To validate that barley MAPKs with high similarity to arabidopsis MAPKs function in resistance or susceptibility to *Bgh*, transient-induced gene silencing (TIGS) experiments were performed. Vectors containing the RNAi constructs of three barley MAPK homologs were constructed and delivered into seven days old detached WT leaf segments transiently *via* gold particles using a particle gun, and subsequently densely inoculated with *Bgh* conidia (Fig. 5). Penetration events (successful haustorium establishment or stopped attempts) were evaluated by microscopy of single transformed cells (Douchkov *et al.*, 2005; Hueckelhoven *et al.*, 2003) 48 h after inoculation with *Bgh*. Barley epidermis cells, transformed with *HvMPK6-like* and *HvMPK3-like* TIGS constructs, developed an enhanced relative susceptibility phenotype (+ 40 % more haustoria), whereas cells bombarded with *HvMPK4-like* RNAi developed a more resistant phenotype (- 35 %) in relation to the empty vector control (set as 100% in Figure 5). These data suggest that barley MAPK homologs are involved in regulating immunity as proposed for related arabidopsis MAPKs (Bethke *et al.*, 2009; Petersen *et al.*, 2000; Pitzschke *et al.*, 2009; Qiu *et al.*, 2008a).

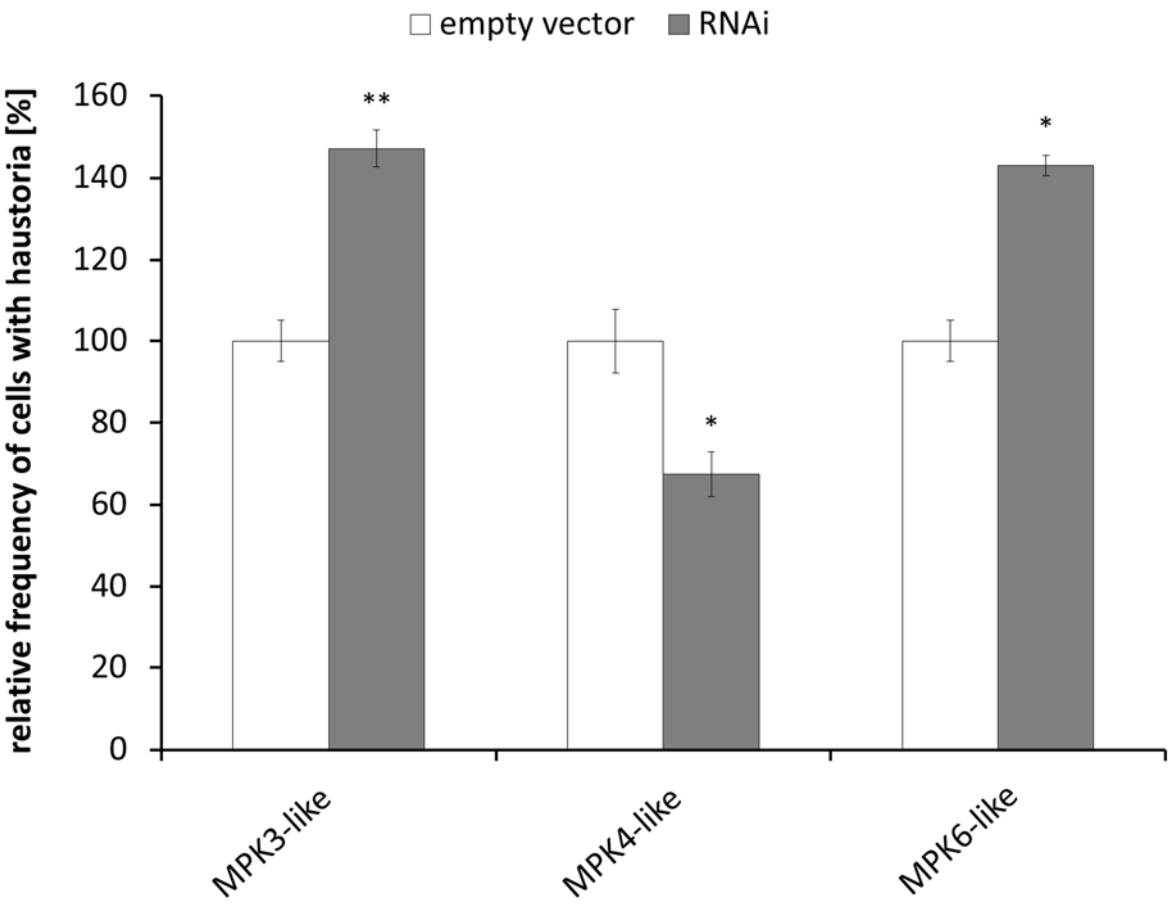

Fig. 5: Barley MAPK homologs influence the barley-*Bgh* interaction. A transient-induced gene silencing (TIGS) approach of barley MAPK homologs was used to analyse the influence of *Bgh* on seven days old wild type barley leaves bombarded with the pIKTA30N::35S vector carrying RNAi constructs of the barley MAPK homologs MPK3-like, MPK4-like and MPK6-like. Gold particle delivery was conducted together with an expression vector for green fluorescent protein (pGY1-GFP) to identify transformed cells. Leaf segments were inoculated with 100 spores/mm² 1 day after bombardment and microscopically analysed 48 h after inoculation. Frequencies of cells with haustoria were counted as the number of all penetrated transformed cells divided by the number of all attacked transformed cells multiplied with 100. For display of the relative influence of the RNAi constructs, haustoria frequency of the empty vector control was set to 100 %. A minimum of 50 interactions was counted per experiment and gene construct. Bars indicate standard errors of three independent biological experiments and significance is shown as * with a p-value of < 0.05 or ** with a p-value of <0.01 according to a two-sided unpaired Student`s t-test performed on the non-transformed raw data.

10.1.3 MAPK activation is not affected by RACB.

As an early PAMP response, MAPK activation can be detected via immunoblot analysis of the phosphorylated TEY-motif of MAPKs which is present in the AtMPK3, AtMPK4 and AtMPK6 (Ranf *et al.*, 2011) and the putative barley orthologs. To see if MAPKs are activated in response to PAMPs, phosphorylated MAPK (MAPK-p) were detected in arabidopsis and barley leaf discs treated with typical elicitors such as the bacterial flagellin peptide flg22 (Felix *et al.*, 1999) and chitin. PAMP-induced signals from phosphorylated MAPKs were observed in arabidopsis with two to three bands visible, whereas in barley protein extracts only two bands were visible (Fig. 6 A). Table 3 lists the calculated molecular weights of the arabidopsis MAPKs and the barley homologs. This suggested that the two stronger bands corresponded to the MPK6 and MPK4 and the fainter one to MPK3 of both arabidopsis and barley, proposing for the first time that barley reacts to PAMPs by MAPK activation.

Table 3: Calculated molecular weights of barley and arabidopsis MAPKs. The three MAPKs 3, 4, and 6 were calculated for their molecular weights in kDa using a freely available online tool (EXpasy, http://web.expasy.org/compute_pi/).

MAPKs	Hv [kDa]	*A.th* [kDa]
3	38.7	42.7
4	42.9	42.8
6	44.2	45

To analyse the influence of *RACB* on early PAMP responses, leaf discs of the three barley genotypes (WT, *CA RACB* line 17/1-11, *RACB RNAi* line B16/2-4) were used for analysis of MAPK activation. The transgenic status and the impact of *Bgh* of the over-expressing *CA RACB* line 17/1-11 and the *RACB RNAi* knock-down line B16/2-4 was confirmed in former studies (Hoefle *et al.*, 2011; Schultheiss *et al.*, 2005). All three genotypes showed similar MAPK activation with an increase from 5 to 20 minutes after elicitation with flg22 and chitin, and a subsequent signal declines at 40 to 60 min. In these assays mostly only one MAPK-p band was detected (Fig. 6 B-C). As the MAPK activation pattern was similar in all three barley lines, I conclude that MAPK activation is likely not dependent on *RACB*.

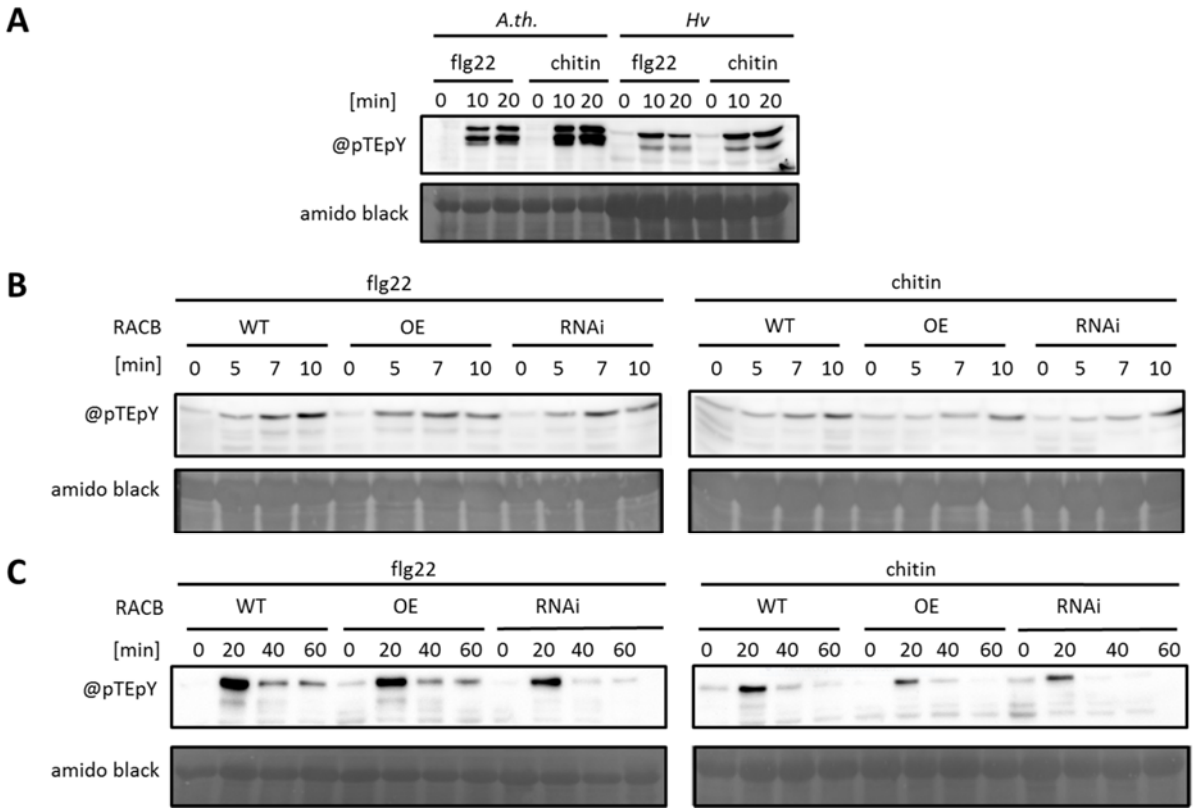

Fig. 6: PAMP-triggered MAPK phosphorylation is not affected in *RACB*-transgenic lines. A MAPK activation of *Arabidopsis thaliana (A.th.)* or *Hordeum vulgare* (*Hv)* leaf discs after elicitation with flg22 or chitin with a MAPK antibody detecting the phosphorylated TEY-motif (α-phospho-p44/42-ERK). **B-C** PAMP-triggered MAPK activation results in similar patterns independent of over-expression (CA) or knock-down (RNAi) of *RACB*. Leaf discs were prepared from eight week old *A.th* or 14 days old barley plant with 30 leaf discs of three plants. Elicitors (100 nM flg22; 10 µg mL^{-1} chitin) were added at 0 min and proteins were extracted either early (5, 7, 10 min) or later (20, 40, 60 min). Proteins were extracted from 100 mg powdery plant material. Amido black was used as loading control during immunoblot analysis.

Additionally, gene expression of barley *MAPKs* was studied after elicitation with flg22 (100 nM), chitin (10 µg/mL^{-1}) after 0, 20 and 60 min or with *Bgh* (100 spores/mm^2) at 12 hpi and 32 hpi. *MPK3-like* expression was increased after 20 and 60 min compared to *MPK4-like* and *MPK6-like* when treated with the two PAMPs but no differences were observed that were caused by *RACB*-misexpression; all barley MAPK homologs showed a constant expression level (Fig. S1). At 12 h and 32 h after *Bgh*-infection barley *MPKs* showed variable gene expression largely without significant influence of genotype or inoculation. Only at 12 hpi (mock samples), the *CA RACB* line showed a significantly lower expression of *MPK3-like* compared to wild type (Fig. 7A/B). Together, misexpression of *RACB* did not consistently influence *MPK3*/ *-4*/ *-6-like* gene expression in barley.

A

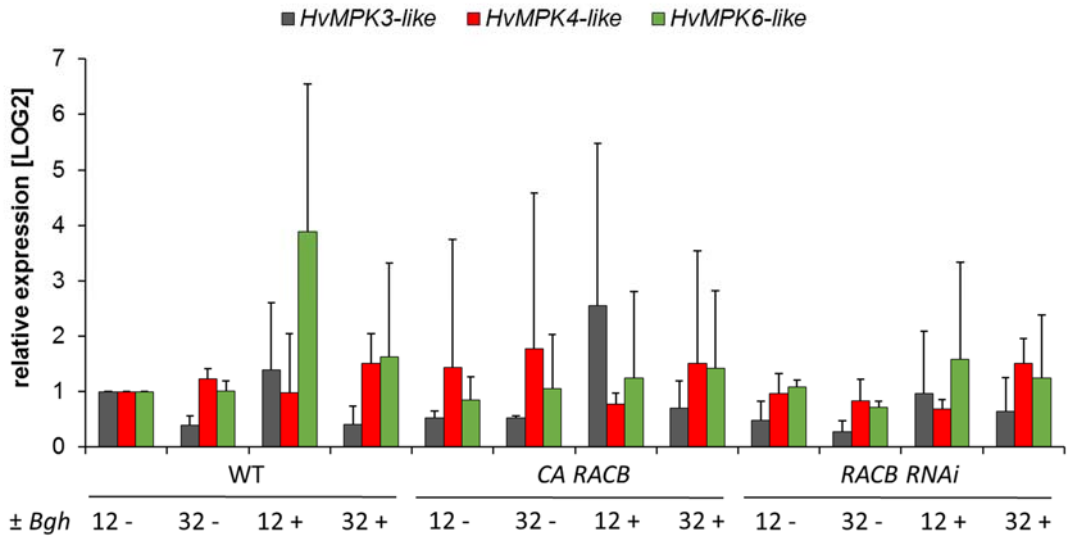

B

		p-value						
		influence of *Bgh* compared to mock			influence of *RACB*-transgene compared to WT			
		WT	*CA RACB*	*RACB RNAi*	*CA RACB* mock	*RACB RNAi* mock	*CA RACB Bgh*	*RACB RNAi Bgh*
12 hpi	*HvMPK3-like*	0.629	0.368	0.454	**0.024**	0.122	0.458	0.566
	HvMPK4-like	0.982	0.655	0.432	0.775	0.864	0.728	0.637
	HvMPK6-like	0.201	0.637	0.652	0.603	0.413	0.262	0.287
32 hpi	*HvMPK3-like*	0.941	0.567	0.494	0.365	0.510	0.324	0.706
	HvMPK4-like	0.534	0.605	0.285	0.779	0.087	0.998	0.964
	HvMPK6-like	0.556	0.323	0.487	0.911	0.050	0.366	0.392
12 hpi + 32 hpi	*HvMPK3-like*	0.570	0.274	0.225	0.315	0.076	0.286	0.814
	HvMPK4-like	0.705	0.478	0.564	0.634	0.167	0.844	0.594
	HvMPK6-like	0.122	0.322	0.359	0.856	0.341	0.191	0.177

Fig. 7: Constitutive and *Bgh*-induced MAPK gene expression is not affected in *RACB*-transgenic barley lines. A. RNA was extracted out of a pool of three second leaves of 14 days-old WT, CA *RACB* over-expressing and *RACB RNAi* plants which were either mock-treated (-) or treated with 100 spores/mm² *Bgh* after 12 hpi and 32 hpi. Calculation was performed according to the ΔΔ Ct method (Pennington *et al.*, 2015) and normalized to untreated WT mock at 12 hpi. Error bars show standard deviation over biological replications in the plus direction. Three biological repetitions were performed. Accession numbers of analysed genes: *UBC2* used as normalizer (M60175), *MPK3-like* (MLOC_17814), *MPK4-like* (AK357723), *MPK6-like* (AK376245).**B** For significance, p-value was calculated with the two-sided paired student`s t-test at 12 hpi, 32 hpi and 12 hpi + 32 hpi. The p-values < 0.05 are marked in bold.

Together, data suggest that barley MAPKs are involved in interaction with *Bgh* but the susceptibility factor *RACB* does neither influence expression of tested *MPK* genes nor activation of barley MPKs.

10.1.4 The PAMP-triggered ROS burst is not affected in *RACB* transgenic lines

Reactive oxygen species (ROS) production is a typical early PTI response (Nicaise *et al.*, 2009) and can be regulated *via* RAC/ROP GTPases (Wong *et al.*, 2007). Also, barley reacts to flg22 with a typical transient production of ROS (Proels *et al.*, 2010). Therefore, barley genotypes WT, *CA RACB* (line 17/1-11*)* and *RACB RNAi* (line 16/2-4) were tested for their ability to respond to different elicitors by producing ROS (Fig. 8). Flg22 was used as positive fungus-unrelated PAMP control. ROS was measured by peroxidase-catalysed oxidation of luminol by ROS, which was measured as relative luminescence units. A typical ROS burst was observed when leaf discs were elicited with flg22 with a similar pattern in all three plant genotypes. With the fungus-related PAMP chitin, there was also a typical ROS burst measurable. The amounts of ROS generated in response to chitin were similar in all tested plant lines as well.

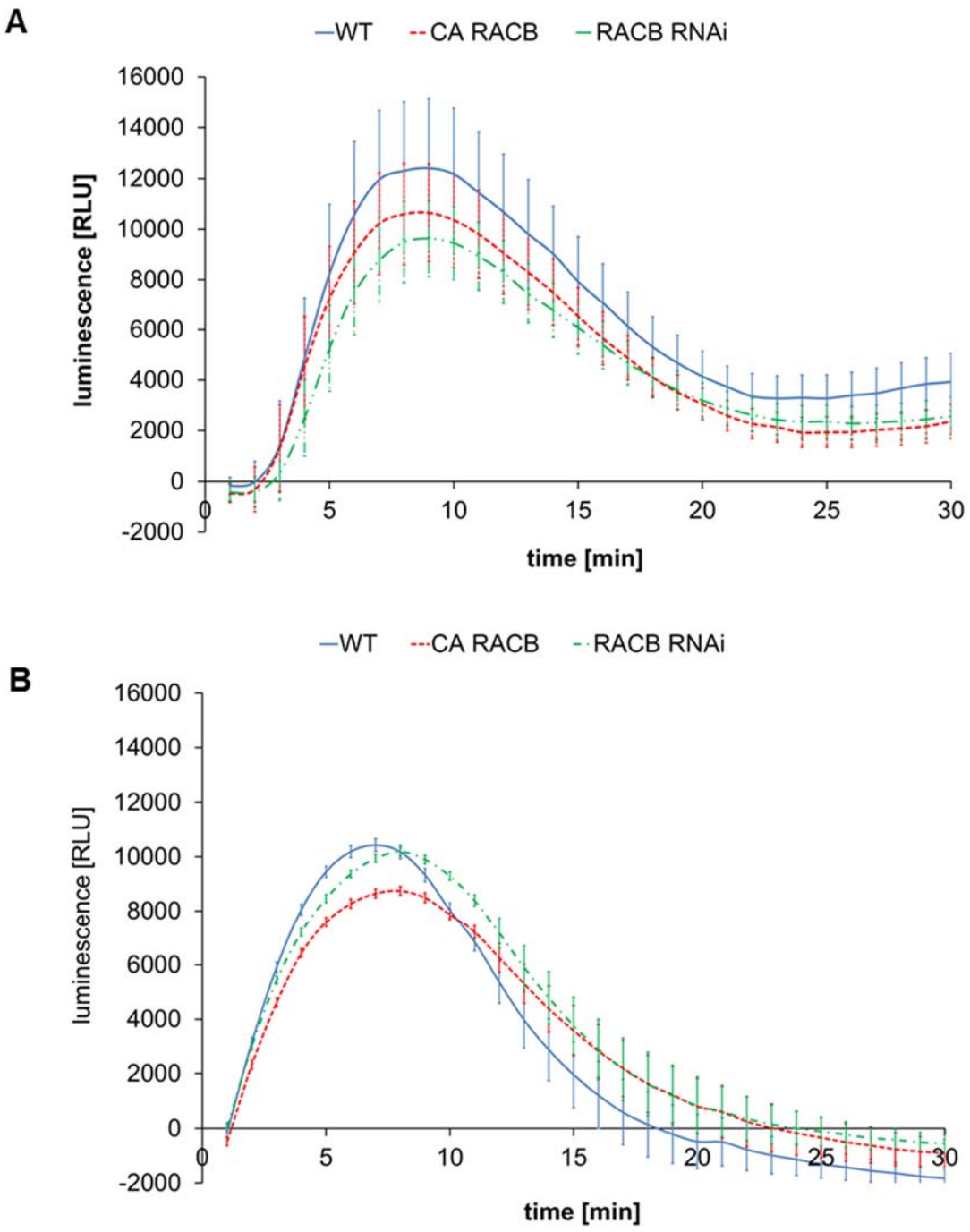

Fig. 8: PAMP-triggered ROS burst is unaffected in *RACB*-transgenic barley. A flg22 (100 nM)-triggered ROS accumulation is unaffected by over-expression of barley *CA RACB* or by silencing of *RACB*. **B** Chitin (10 µg mL^{-1})-triggered ROS production is unaffected by over-expression of barley *CA RACB* or by silencing of *RACB*. Elicitors were added at 0 min and ROS was measured by peroxidase-catalysed oxidation of luminol, measured as relative luminescence units (RLU) up to 30 min. Leaf discs (LD) of 14 days old barley plants (24 LD of 5 mm diameter of three plants) were used. Error bars present standard deviations over three biological replicates.

10.1.5 Barley pathogenesis-related gene expression is not influenced by *RACB*.

As a typical plant immune response gene expression of defence genes such as pathogenesis-related genes (*PR*) or jasmonate-induced genes (*JIPs*) was analysed in barley *RACB* transgenes with and without *Bgh*-challenge (Fig. 9). *PR1b*, *PR3*, *PR5* and *PR10* were studied after dense inoculation with conidia of *Bgh* 12 hpi and 32 hpi. These times represent stages of fungal penetration attempts and of haustorium expansion (see below Fig. 10) which both are influenced by *RACB* (Hoefle *et al.*, 2011). All *PR* genes were up-regulated by *Bgh* in WT plants. Both transgenic lines reacted similar to WT after *Bgh* challenge with the expression of PR genes. In super-susceptible *CA RACB* plants *PR1b*, *PR3* and *PR5* additionally showed an enhanced constitutive expression level. Also, Jasmonate-induced protein genes *JIP23* and *JIP60* (Kogel *et al.*, 1995; Rustgi *et al.*, 2014) were constitutively expressed independent of inoculation with *Bgh*. However, these results thus cannot explain modified susceptibility phenotypes in the *RACB* transgenic genotypes.

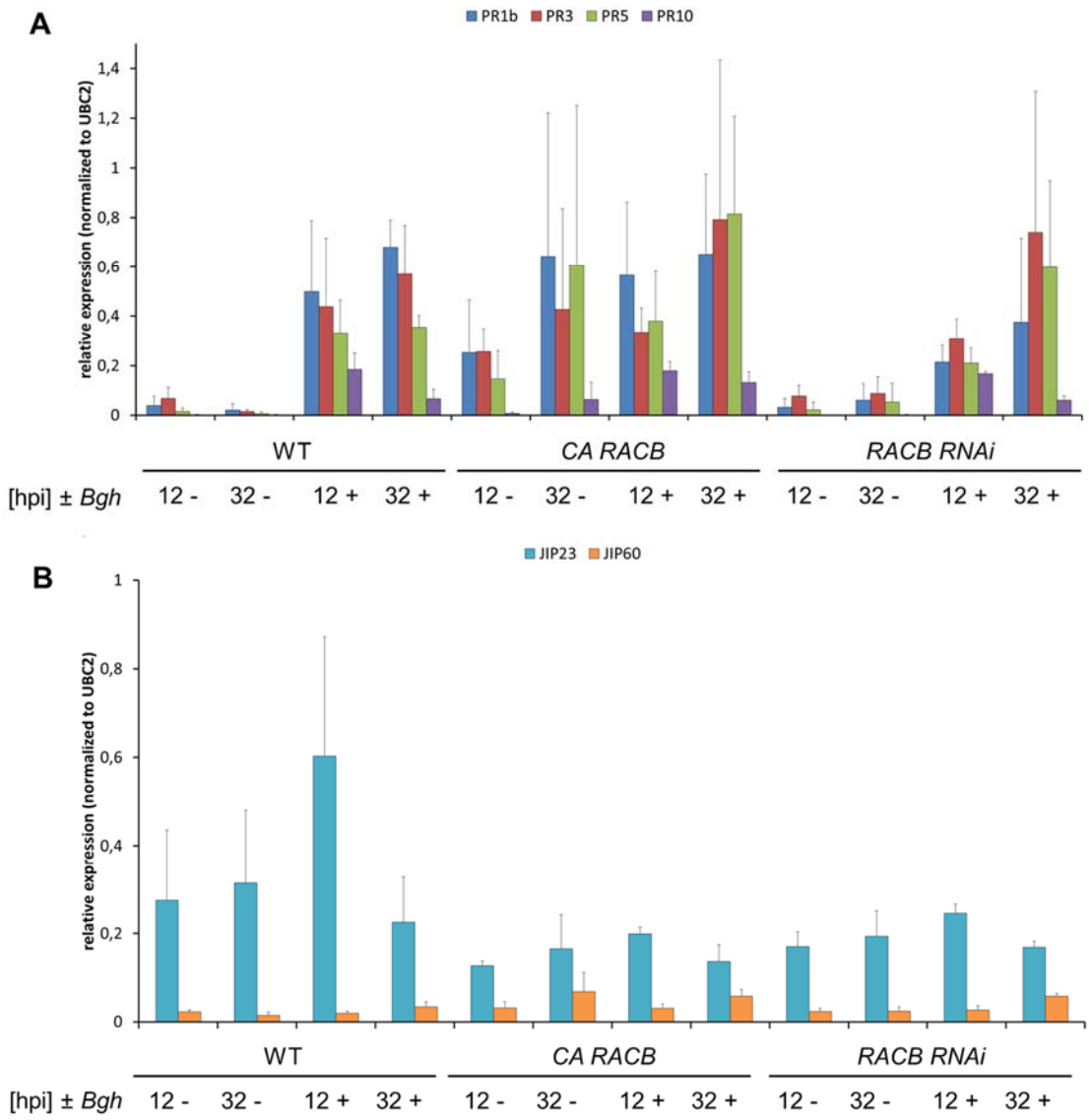

Fig. 9: Defence gene expression provides no explanation for the pathogenesis phenotypes- of *RACB*-transgenic barley. WT, *CA RACB* over-expressing and *RACB RNAi* plants were either mock-treated (-) or treated (+) with *Bgh* after several time points and collected for gene expression analysis. **A** Pathogenesis-related *(PR*) genes are slightly over-expressed in mock-treated *CA RACB* plants. *Bgh*-triggered expression of PR-genes is only weakly affected by the transgenes. **B** Jasmonate-induced protein (JIP) genes are constitutively expressed in all genotypes and stages of interaction with *Bgh* tested. **C** For significance p-value was calculated with the two-sided student`s t-test. Significant p-values below 0.05 are marked in bold. 14 days old barley plants were inoculated with 100 spores/mm² and harvested after 12 hpi and 32 hpi. A pool of three second leaves of three leaves per genotype was used. qRT-PCR was carried out with 10 ng cDNA. The average of three biological repetitions relative to that of constitutively expressed *UBC2* is shown. Calculation was performed according to the ΔΔ Ct method (Pennington *et al.*, 2015). Error bars show standard

deviation over biological replications in the plus direction. Accession numbers of analysed genes: *UBC2* used as normalizer (M60175), *PR1b* (Z26333), *PR3* (AK364132), *PR5* (AK371265), *PR10* (AK360974), *JIP23* (AB251339), *JIP60* (AK372562).

10.2 TRANSCRIPTOMICS

A direct influence was not observed of *RACB* on early PTI responses and *PR*-gene expression that would explain its function in susceptibility. In metazoans and yeast, however, RACB-related RHO proteins are major players of stress-related gene expression (Marinissen *et al.*, 2001; Nie *et al.*, 2012; Perez and Cansado, 2010). Therefore, a transcriptomic approach was used to investigate global gene expression of transgenic barley in interaction with *Bgh*. I used microarrays to address the question what kinds of genes are expressed in the interaction with the fungus. 44k microarray hybridizations were performed and at first analysed globally in a pathway analysis to get an overview of the regulated pathways and to find pathways specifically regulated by *RACB*. In a stringent analysis of the microarray data I generated a candidate list of genes which were functionally analysed.

I used the custom-made SCRI_Hv35_44k-v1 Agilent microarray consisting of 42, 302 barley sequences in a 60mer probe per selected gene in a 4x44k format with a design based on the HARVEST35 assembly (Agilent design: 020599) of the barley transcriptome (http://www.ncbi.nlm.nih.gov/geo/, accession number: GSE69215) (Chen *et al.*, 2011). To find differentially expressed genes in different stages of the pathogen`s invasion process, several times were assessed in pre-experiments to find interesting stages of the interaction for transcriptome analysis. RACB influences both fungal penetration and haustorium expansion. According to the life cycle of *Bgh,* 12 hours after inoculation was set as first time point - just when the fungus penetrates. At that time point the fungus builds a mature appressorium (Hueckelhoven *et al.*, 1999). For determining a second time for transcriptome analysis, haustorium expansion data were collected at different stages in the haustorium initial forming phase and subsequent haustorium expansion phase (16, 24, 32, 34, 37, 48 hours post inoculation (hpi)). Collected barley leaves were discoloured in 70% EtOH for 24 hours and then fungal chitin was stained with wheat germ agglutinin-tetramethylrhodamin (WGA-TMR) for 24-48 h (Fig. 10 A). Haustoria were imaged using a confocal laser scanning microscope. Haustoria grew over time from 16 µm (16 hpi) up to 65 µm (48 hpi) (Fig. 10). The growth rate curve was calculated by the mean increase in length of a minimum of 30 measured haustoria divided by the time span analyzed to define the growth rate per hour. Growth rate curve demonstrated a constant growing phase until 34 hpi with a following slight drop-down phase. Since a later point was searched where the haustorium is expanding within the cell but has not reached its full size, I decided 32 hpi to be the second time point for future transcriptome analyses. At 32 hpi the haustorium expansion was still in progress and about to increase compared to later time points when the growing progress has decelerated (Fig. 10).

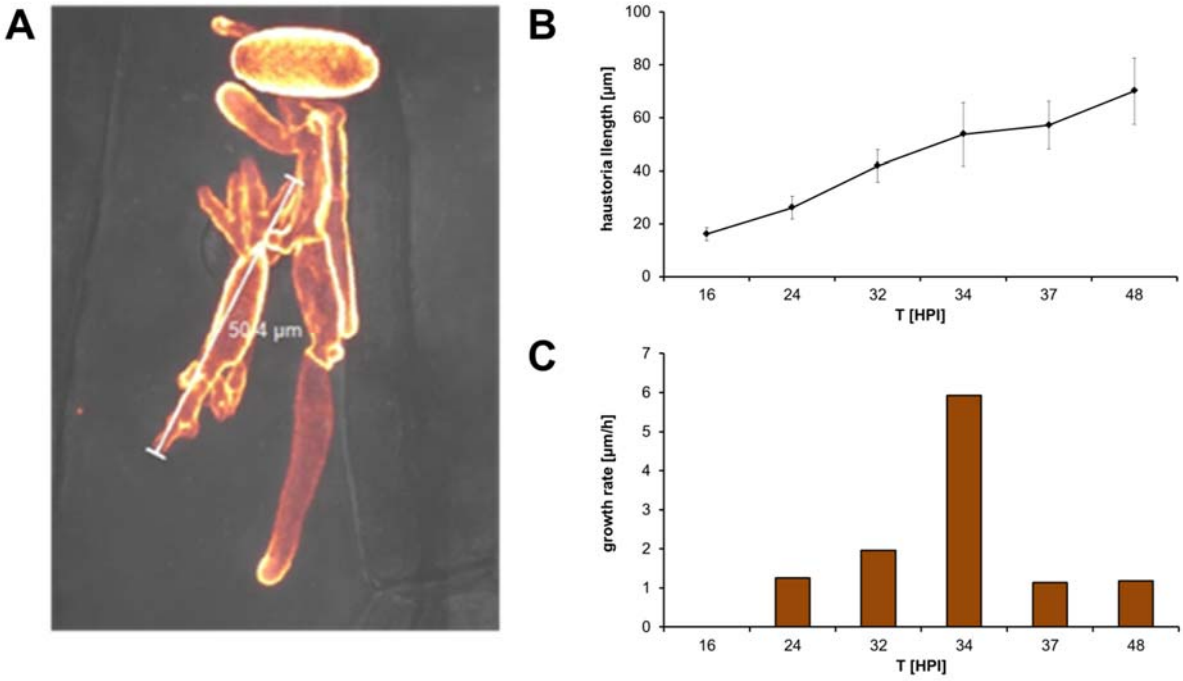

Fig. 10: *Bgh* haustoria expansion over time. A Typical haustorium formed after 34 h after inoculation, stained with WGA-TMR for 48 h before microscopic evaluation. **B**. Haustoria growth was measured in WT plants at six different time points (16, 24, 32, 34, 37, 48 hpi). A minimum of 30 haustoria was measured per time point in three independent biological experiments. Size is given in µm. Bars indicate standard errors of three independent biological experiments. **C** The growth rate was calculated with the following formula exemplified for the growth rate at 24 hpi: (mean of 40 haustoria at 24 hpi - mean of 40 haustoria at 16 hpi)/(24h-16h).

Therefore, WT, *CA RACB* and *RACB RNAi* plants with and without *Bgh*-challenge at 12 h and 32 hpi were analysed in a transcriptome analysis according to the manufacture´s manual as described in section 9.2.1. The aim was to find those genes that were significantly regulated by *RACB* and *Bgh* at both times.

10.2.1 Principal component analysis suggests a reliable data set.

Principal component analysis (PCA) can be used to assess the quality of the experiment statistically. Huge data sets can be structured and simplified. Hereby, many variables get approximated to a small number of linear combinations (principal components) (Pearson, 1901). PCA clusters the means of biological replicates according to treatment and time points (Fig. 11). The mean values of the three genotypes are sorted after their signal intensities. Fig. 11 A shows the PCA analysis of the early infection state 12 hpi. Mock-treated samples clustered together as well as the *Bgh*-treated samples. *Bgh*-treated samples were shifted to the left compared to mock-treated samples confirming a major influence of the treatment. That the three genotypes (WT, *CA RACB*, *RNAi RACB*) showed distances between each other is likely due to the different *RACB*-transgene impacts. A similar profile was observed for the 32 hpi state (Fig. 11 B), where also a cluster on the right part of the diagram presents mock-treated samples, which were closer to each other than at 12 hpi. The *Bgh*-treated samples also shifted away from the mock-treated samples. The *Bgh*-treated *CA RACB* OE (line 17/1-11) seemed to

be more different from the other two lines (WT GP and *RACB RNAi* line 16/2-4) which might be caused by influence of *CA RACB* on gene expression but also by the fact that at 32 hpi the fungus is already in its growing stage and likely more fungus is growing on *CA RACB* barley. Hence, this exceptional position is perhaps explained by fungal influence on gene expression in the super-susceptible *CA RACB* plants. Together, this suggests that data are useful because clusters can be explained by genotype and treatment at both times.

A

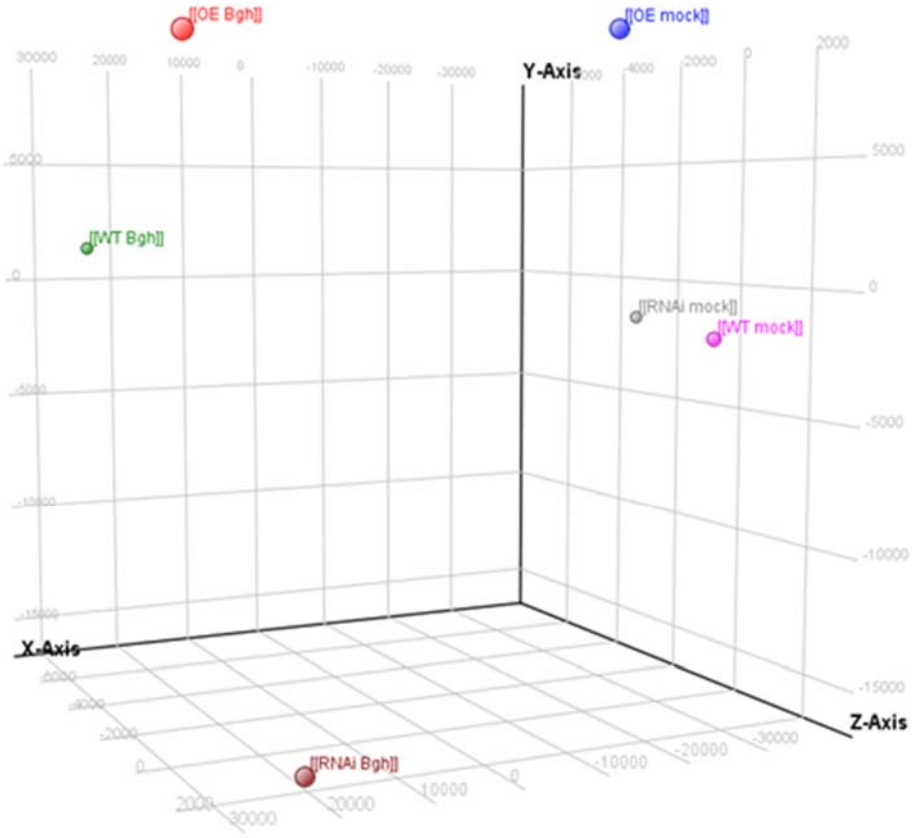
[[OE Bgh]]
[[OE mock]]
Y-Axis
[[WT Bgh]]
[[RNAi mock]]
[[WT mock]]
X-Axis
Z-Axis
[[RNAi Bgh]]

B

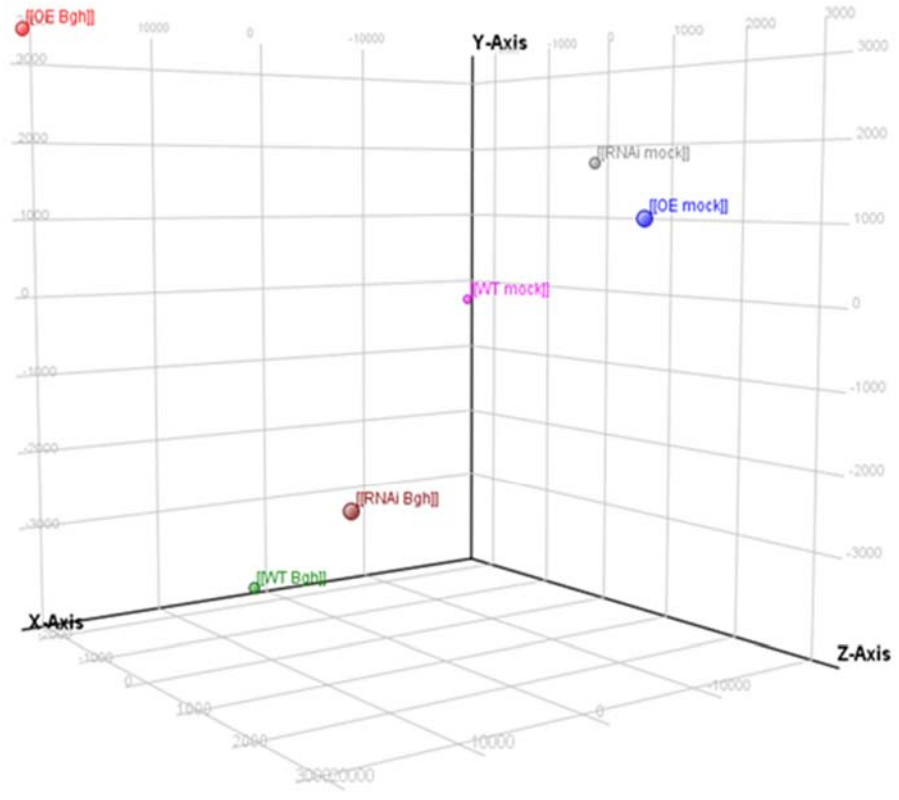
[[OE Bgh]]
Y-Axis
[[RNAi mock]]
[[OE mock]]
[[WT mock]]
[[RNAi Bgh]]
[[WT Bgh]]
X-Axis
Z-Axis

Fig. 11: Principal component analysis (PCA) of biological replicates of WT, *CA RACB* (OE) and *RACB RNAi* plant lines 12 hpi and 32 hpi forming distinct clusters. A PCA of 12 hpi. Signal intensity of the biological replicates was calculated and plotted as mean values within the principal components. **B** PCA of 32 hpi. Biological replicates for 12 hpi: 2x WT mock, 4x WT *Bgh*, 4x OE mock, 3x OE *Bgh*, 4x RNAi mock, 4x RNAi *Bgh*; Biological replicates for 32 hpi: 4x WT mock, 2x WT *Bgh*, 3x OE mock, 4x OE *Bgh*, 3x RNAi mock, 3x RNAi *Bgh*.

10.2.2 Overexpression and knockdown of *RACB* have a great influence on different pathways after pathogen attack.

To analyse data properly in regard to genes modulated by a) *RACB*, b) *Bgh* or c) *RACB* and *Bgh*, different comparisons were chosen at each time for detailed gene expression analysis (Fig.12):

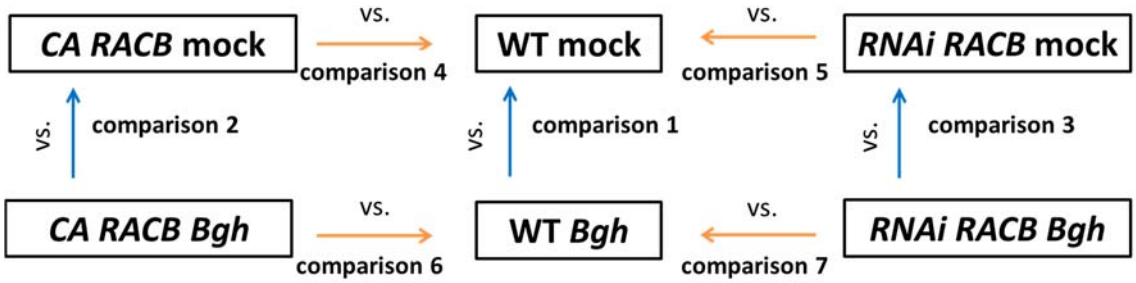

Fig. 12: Chosen comparisons for analysis of microarray data. Seven comparisons were chosen to analyse the influence of *Bgh* (blue arrows) or genotypes (orange arrows) on global gene expression.

Thousands of genes were differentially expressed after inoculation with *Bgh* or in single *RACB*-transgenic barley plants (fold change cut-off of 2-fold and a false discovery rate (FDR) corrected p-value of < 0.05). It is not clear at what time points more genes were regulated. Interestingly, when *CA RACB Bgh* was compared to WT *Bgh* much more genes were regulated at 32 hpi than at 12 hpi. This might be explained by the support of successful fungal development by *CA RACB* (Schultheiss et al. 2005). In most comparisons more transcripts were up-regulated than down-regulated (Table 4).

Table 4: Number of differentially regulated genes in different comparisons dependent on *RACB*-genotype, *Bgh*-treatment and time. Genes were selected with a fold change cut-off of 2-fold and a false discovery rate (FDR) corrected p-value of < 0.05.

comparison	number of differentially regulated genes					
	all regulated genes		up-regulated genes		down-regulated genes	
	12 hpi	32 hpi	12 hpi	32 hpi	12 hpi	32 hpi
WT *Bgh* vs. WT mock	5636	3086	3477	2230	2159	856
CA RACB Bgh vs. *CA RACB* mock	3904	3495	2522	2111	1382	1564
*RNA*i *RACB Bgh* vs. RNAi *RACB* mock	6547	4291	3520	2814	3027	1477
CA RACB Bgh vs. WT *Bgh*	903	2400	558	1381	345	1019
RNAi RACB Bgh vs. WT *Bgh*	867	874	412	638	455	236
CA RACB mock vs. WT mock	2015	2408	1581	1595	434	813
RNAi RACB mock vs. WT mock	661	388	275	180	386	208

An overlap of *CA RACB*-influenced and *Bgh*-influenced gene expression was observed in the total lists of significantly regulated genes (Table 4). Of 2015 *CA RACB*-influenced genes at 12h 1485 were also regulated by *Bgh* (74%). 1210 of these genes were up-regulated by both *CA RACB* and *Bgh*, whereas 249 were down-regulated by both *CA RACB* and *Bgh* and only 26 genes were oppositely regulated by *CA RACB* and *Bgh*. Hence, most genes overlapping between *CA RACB*-regulated genes and *Bgh*-regulated genes are regulated by both factors with the same tendency. Vice versa, of 5636 *Bgh*-regulated genes in WT 25.5 % (1485 genes) were regulated by *CA RACB* without infection. At 32 hpi 2408 genes were de-regulated in mock-treated *CA RACB* plants. 1109 genes were also regulated by *Bgh* (46 %). 647 of these genes were up-regulated by both *CA RACB* and *Bgh*, whereas 462 genes were down-regulated by *CA RACB* and *Bgh*. Together, *CA RACB* expression provoked expression of a set of genes that resembles a subset of the *Bgh*-regulated genes within the barley transcriptome. Pre-activation of this gene set by the *CA RACB* transgene without infection might explain why fewer genes were additionally regulated by *Bgh* in the *CA RACB* genotype when compared to the wild-type or *RACB RNAi* plants. Together, *CA RACB* and *Bgh* support expression of strongly overlapping sets of genes.

MapMan software supports calculation of whether the response of genes in a particular pathway differs from the overall response of all other genes that have been recorded. This is done by using a Wilcoxon rank sum test and the FDR correction of Benjamini Hochberg (1995). Table 5 lists significance

levels (corrected p-values) for pathway regulation of selected pathways under influence of *Bgh* and/or the *RACB* transgenes (comparisons: WT *Bgh* vs. WT mock, *CA RACB* mock vs. WT mock, *RACB RNAi* mock vs. WT mock, *CA RACB Bgh* vs. *CA RACB* mock, *RACB RNAi Bgh* vs. *RACB RNAi* mock, *CA RACB Bgh* vs. WT *Bgh* and *RACB RNAi Bgh* vs. WT *Bgh* at 12 hpi and 32 hpi (presented as value 12 hpi/ value 32 hpi)). Pathways were selected because they showed significant regulation and potential functional links to RAC/ROP G protein signalling. This pathway extract exemplified that many pathways were pathogenesis-dependently and *RACB*-dependently regulated. All pathways shown were significantly (marked in bold in Table 5) regulated in the comparisons dependent on the *RACB*-transgene itself *CA RACB* mock vs. WT mock and *RNAi RACB* mock vs. WT mock. All of them were also *Bgh*-regulated in WT *Bgh* vs. WT mock and/or *CA RACB Bgh* vs. *CA RACB* mock and/or *RNAi RACB Bgh* vs. *RNAi RACB* mock comparison. At 12 h more pathways seemed to be significantly regulated compared to 32 h. Furthermore, pathways in the *CA RACB Bgh* vs. WT *Bgh* comparison were obviously not significantly regulated at 12 hpi in any of the selected pathways.

Table 5: Pathway regulation by *Bgh* or *RACB* in barley at 12/32 hpi. *Bgh*- and *RACB*-dependent comparisons are shown for different selected pathways which belong to those pathways with a number of genes above 50. Bold marked numbers symbolize significantly regulated pathways with false discovery rate corrected p-value < 0.05 (Wilcoxon rank sum test). Analysis was carried out with MapMan (Usadel *et al.*, 2005; Usadel *et al.*, 2009). P-values below 0.001 are displayed as 0.000.

		FDR-corrected p-value (12 hpi/32 hpi)						
pathway	number of transcripts in pathway	WT *Bgh* vs. WT mock	*CA RACB* mock vs. WT mock	*RACB RNAi* mock vs. WT mock	*CA RACB Bgh* vs. *CA RACB* mock	*RACB* RNAi *Bgh* vs. *RACB RNAi* mock	*CA RACB Bgh* vs. WT *Bgh*	*RACB* RNAi *Bgh* vs. WT *Bgh*
cell wall	493/493	**0.031/0.000**	**0.039/0.000**	**0.000/0.001**	0.337/0.503	0.916/0.017	0.945/**0.000**	**0.000/0.000**
cell organisation	575/577	**0.023/**0.526	0.491/0.383	**0.004/**0.464	0.604/0.344	0.695/0.960	0.762/0.383	**0.004/**0.808
vesicle transport	247/244	**0.000/0.000**	**0.000/0.000**	**0.000/0.000**	**0.000/**0.503	**0.000/0.000**	0.246/**0.000**	**0.000/0.000**
DNA synthesis/chromatin structure/ histone	181/182	**0.000/**0.600	**0.009/**0.383	**0.024/**0.199	0.337/0.503	**0.000/**0.153	0.246/0.383	**0.024**/0.388
RNA/regulation of transcription	1849/1842	0.830/0.600	**0.000/0.000**	**0.015/0.000**	**0.000/0.000**	**0.000/**0.594	0.945/**0.000**	**0.015/0.000**
signalling	1710/1703	**0.000/0.000**	**0.000/0.000**	**0.000/0.000**	**0.000/**0.176	**0.000/0.000**	0.440/**0.000**	**0.000/0.244**
signalling/calcium	246/247	**0.000/0.000**	**0.000/0.000**	**0.006/0.000**	**0.000/**0.783	**0.003/0.000**	0.945/**0.000**	**0.006/**0.350
signalling/G-proteins	273/272	**0.002/0.014**	0.276/**0.006**	**0.000/**0.464	0.337/0.503	0.931/**0.001**	0.978/**0.006**	**0.000/**0.388
signalling/receptor kinases	798/792	**0.000/0.000**	**0.000/0.000**	0.463/**0.003**	**0.000/0.000**	**0.000/0.000**	0.246/**0.000**	0.463/0.449
stress	987/984	**0.000/0.526**	**0.039/0.011**	0.463/**0.039**	**0.000/**0.451	**0.000/0.000**	0.260/**0.000**	0.463/0.858

10.2.3 Clustering of *RACB*- and *Bgh*- dependently regulated transcripts.

To visualize the expression patterns of the selected pathways listed in Table 5, clustering can be used as a tool to group genes with related expression patterns. Genes within one group (cluster) are more similar in expression to each other than to those in other groups/clusters. One can also observe how these genes behave in terms of different treatment or in different plant genotypes. Following selection criteria with a fold-change cut-off FC>2 and a FDR of < 0.05 to extract significantly regulated genes, a total of 9105 transcripts were counted for 12 hpi and 6649 transcripts for 32 hpi to be differentially regulated. Lists were generated for each 12 hpi and 32 hpi summing all expression sets (Fig. 12, Table 4) together in one list to collect effects of both *Bgh* and *RACB* (*CA RACB Bgh* vs. *CA RACB* mock, *CA RACB Bgh* vs WT *Bgh*, *CA RACB* mock vs WT mock, *RACB RNAi Bgh* vs. *RACB RNAi* mock, *RACB RNAi Bgh* vs. WT *Bgh*, *RACB RNAi* mock vs. WT mock, WT *Bgh* vs WT mock). Due to the fact that RACB as G-protein is involved in signalling cluster analysis was performed with MapMan for subsequent highlighting of signalling pathway genes. The obtained clusters were inspected in regard to the chosen comparisons in Fig. 12 to label clusters with transcripts modulated by a) *Bgh*, b) *RACB* or c) *Bgh* and *RACB*. Distinct clusters were observed for each time point (coloured boxes in Fig. 13): Clusters containing genes observed in the comparisons dependent on *Bgh*-challenge are labelled with green boxes, displaying regulation in the comparisons 1-3 (compare Fig. 12); Clusters containing genes observed in the comparisons dependent on the *RACB*-transgene, are labelled with yellow boxes presenting differential regulation in the comparisons of different *RACB*-genotype 4-7. Red boxes indicate differential regulation both in non-infected *RACB*-transgenic barley and in WT *Bgh* vs. WT mock. At 12 hpi two clusters displayed up-regulation in the two *Bgh*-dependent comparisons (green boxes) and two clusters were recorded to be *RACB*-dependent (yellow box) with no regulation in *Bgh* comparisons. Three clusters were classified to be *Bgh*- and *RACB*-dependently regulated (red boxes) where up-regulation in *CA RACB* and vice versa down-regulation in *RACB RNAi* and additional up-regulation in WT *Bgh* vs. WT mock was observed. Seven clusters showed none of the described expression types. At 32 hpi two clusters were *Bgh*-dependent (green boxes), two *RACB*-dependent, five *CA RACB*- and *Bgh*-dependent (red boxes) and five showed other patterns. The early time point showed more clusters with *RACB*-dependency and less *Bgh*-dependency compared to the later time point. From the three modules of regulation a) *Bgh*-dependent, b) *RACB*-dependent and c) *Bgh*- and *RACB*-dependent, c) was the most often observed type for both times indicating an important set of transcripts in the barley barley powdery mildew interaction. Each cluster contains a minimum of 100 transcripts. Out of all regulated transcripts a lower number of signalling components where counted per cluster and highlighted in blue in Figure 13. Table S1 includes all transcripts numbers and the appropriate signalling transcripts numbers per cluster at both time points (6 % of all transcripts are signalling transcripts at both time points).

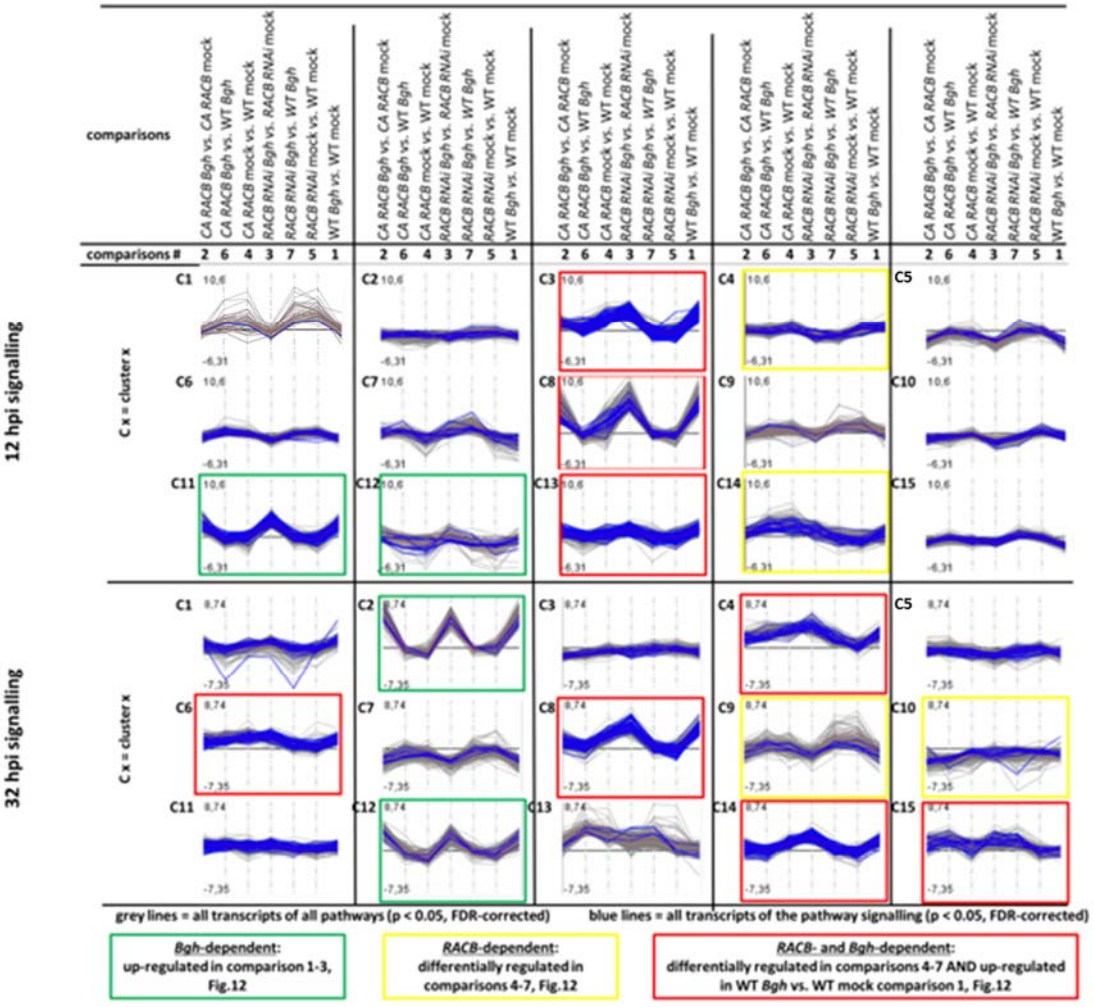

Fig. 13: Cluster analysis of differentially regulated genes shows *RACB* and *Bgh* influence on gene expression. 9105 significantly regulated transcripts at 12 hpi and 6649 at 32 hpi were displayed for their expression patterns in MapMan. Fold changes in expression levels (LOG2-transformed) were clustered equally after Euclidean clustering dividing in 15 clusters. Each cluster (marked as C x) contains a different number of transcripts. Vertical dotted numbered lines display the seven different comparisons described in Fig. 12: *CA RACB Bgh* vs. *CA RACB* mock, *CA RACB Bgh* vs WT *Bgh*, *CA RACB* mock vs. WT mock, *RACB RNAi Bgh* vs. *RACB RNAi* mock, *RACB RNAi Bgh* vs. *WT Bgh*, *RACB RNAi* mock vs. WT mock and WT *Bgh* vs. WT mock. Grey lines present all transcripts of all pathways whereas blue lines display transcripts belonging to the pathway signalling. Green, yellow and red boxes correspond to the three main categories of regulation possible in the described array study: green = *Bgh*-dependent transcripts; up-regulated in WT *Bgh* vs. WT mock (comparison 1 in Fig. 12), *CA RACB Bgh* vs. *CA RACB* mock (comparison 2 in Fig. 12), *RACB RNAi Bgh* vs. *RACB RNAi* mock (comparison 3 in Fig. 12); yellow = *RACB*-dependent transcripts; differentially regulated in *CA RACB Bgh* vs. WT *Bgh* (comparison 6 in Fig. 12) and *RACB RNAi Bgh* vs. WT *Bgh* (comparison 7 in Fig. 12) or in *CA RACB* mock vs. WT mock (comparison 4 in Fig. 1s) and *RACB RNAi* mock vs. WT mock

(comparison 5 in Fig. 12); red = *Bgh* & *RACB*-dependent transcripts; differentially regulated in comparisons 4-7 and up-regulated in comparisons 1.

10.2.4 Receptor-like kinases are highly differentially regulated.

Since signalling RLKs were pathway-regulated in many comparisons (Table 5), I took a closer look into this group of genes out of the list of 9105 genes at 12 hpi and of the list of 6649 genes at 32 hpi to see what types of RLKs are differentially and significantly regulated in at least one out of the seven comparisons displayed in Fig. 12 (Fig. 14). Regulated genes in the *RACB*-specific comparisons *CA RACB* mock vs. WT mock and *RACB RNAi* mock vs. WT mock (4 and 5 in Fig. 12) were displayed. Fig. 14 presents regulated genes as red dots and down-regulated genes as blue dots. The RLK classes of LRR-RLK, WAK-RLK, DUF26-RLK and S-RLK are found to be mostly differentially regulated with the strongesten tendency to LRR-RLKs.

In sum, pathway analysis and data display suggests a high impact of *RACB* on expression of receptor-like kinases.

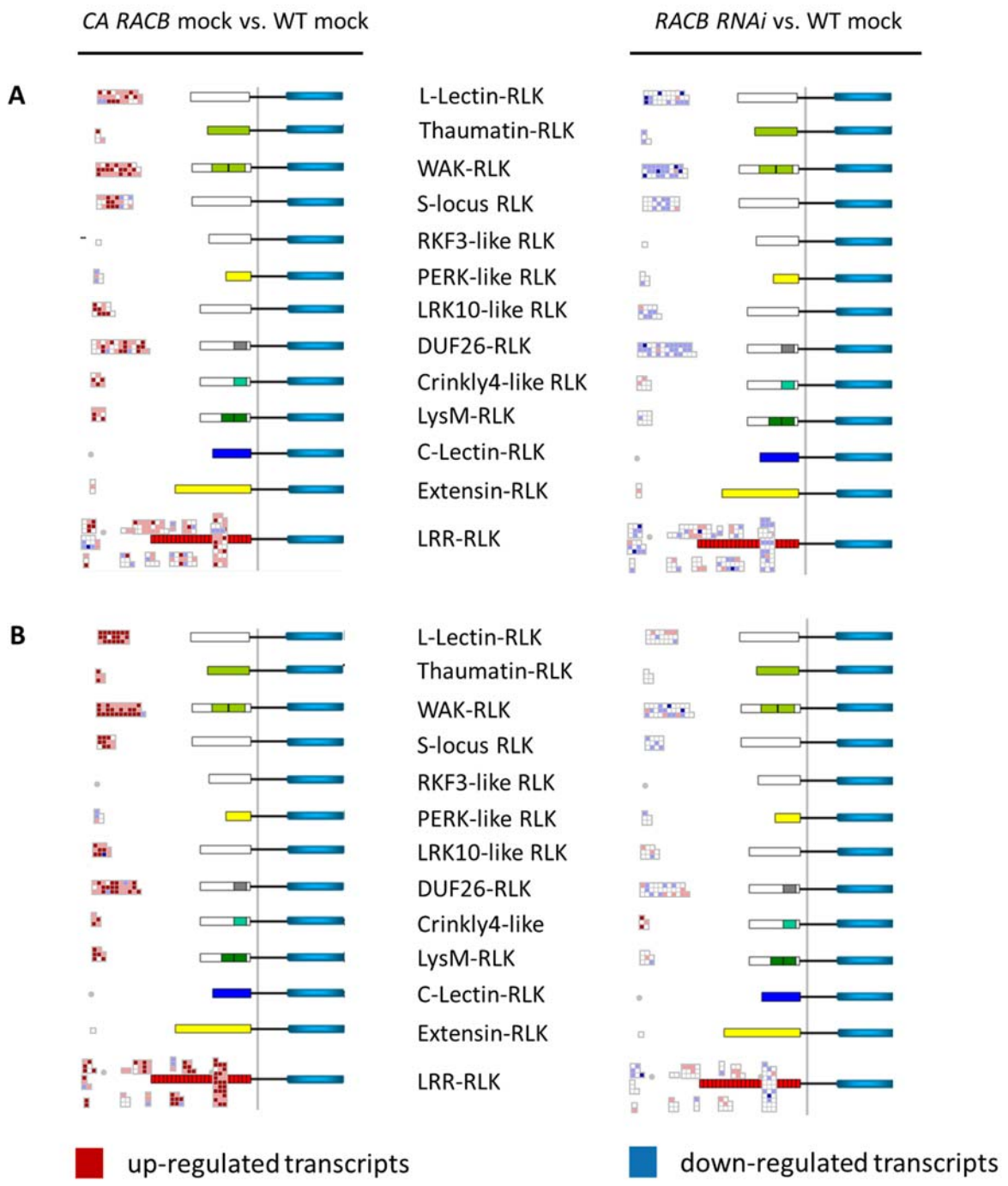

Fig. 14: Receptor-like kinases are differentially regulated in *RACB* transgenic barley plants. MapMan display of the 12 h (**A**) and 32 h (**B**) microarray data set revealed up-regulation of receptor-kinases in super-susceptible *CA RACB* line and down-regulation in resistant *RACB RNAi* line. Genes are coded as dots and up-regulation is displayed in red and down-regulation in blue. Values are displayed as LOG2 in the range of -2 (dark blue) to +2 (dark red). L-Lectin: legume-lectin, WAK: wall-associated kinase, RKF; receptor-like kinase in flowers, PERK: proline-rich, extensin-like receptor kinase, LRK10: Lr10 disease resistance locus receptor kinase, C-Lectin: C-type lectin, LRR: leucine-rich repeat.

10.2.5 Verification of microarray data and generation of a candidate list.

To verify microarray data, RT-qPCR was chosen as an independent method. Several genes were selected based on their annotation and their strongly differential regulation: three wall-associated kinases (WAK-RLK a-c), three DUF26-RLK (a-c) presenting the RLK family and five WRKY transcription factors (WRKY2, WRKY3, WRKY18, WRKY20, WRKY22) since WRKYs are highly regulated genes in regard to defence. WRKY2 was published as negative regulator of resistance to *Bgh* (Eckey *et al.*, 2004) and was therefore used as positive control. Additionally, genes were selected, which showed regulation at both time points at stringent filter settings (FC >2, FDR $p < 0.05$). Based on the 12 hpi mock comparisons 4 and 5 (4 = *CA RACB* mock vs. WT mock and 5 = *RACB RNAi* mock vs. WT mock) a list of 142 genes was created (Table S2) that contained only genes that were contrarily regulated in these comparisons. For 32 hpi mock, the corresponding list contained 15 genes only (not shown). Next, the 142 genes were reduced to those 113 genes (Table S3), which additionally were significantly regulated after *Bgh*-challenge in the wild-type (Fig. 15A, Table S3). The corresponding gene list for 32 hpi contained only 10 genes (Fig. 15B; Table S4). Fig. 15 shows a common up-regulation by *Bgh* and *CA RACB* of the same transcripts which are additionally down-regulated by *RACB RNAi*. This up-regulation might indicate that in the super-susceptible *CA RACB* plants those genes are already over-expressed which support susceptibility to *Bgh* during infection.

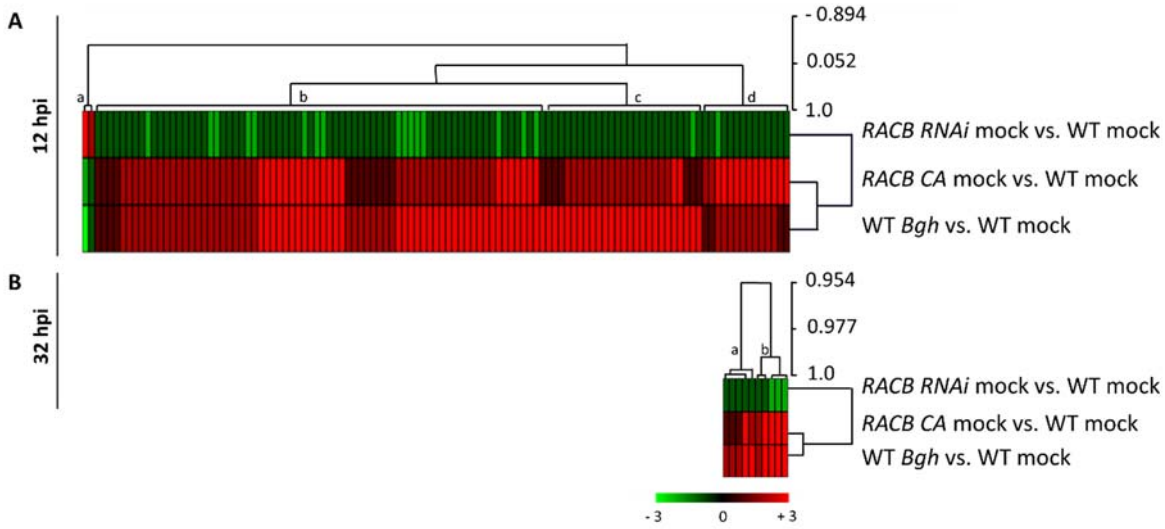

Fig. 15: Hierarchical clustering of stringently *RACB*- and *Bgh*-regulated genes at 12 hpi and 32 hpi. **A** Heatmap of oppositely regulated 113 genes in untreated *CA RACB* and *RACB RNAi* transgenic barley plants are additionally *Bgh*-regulated at 12 hpi. **B** Heatmap of oppositely regulated 10 genes in untreated *CA RACB* and *RACB RNAi* transgenic barley plants are additionally *Bgh*-regulated at 32 hpi. Heatmap and hierachical clustering (Eisen et al., 1998) clustering was done with multiple experiment viewer (TMEV, http://www.tm4.org/mev.html). Gene expression values are displayed as Log2-fold changes within a range of -3 (green) and +3 (red). Genes are listed according to their clusters (see suppl. Table S3 for 12 hpi and Table S4 for 32 hpi).

To address the aim of finding genes for functional analysis, which are de-regulated at both times by misexpression of *RACB* the list 142 genes (12 hpi mock) was compared to the list of 15 genes (32 hpi

mock). This comparison showed that all 15 genes that were stringently *RACB*-regulated at 32 h (mock) were also stringently *RACB*-regulated at 12 h (mock). From this list of 15 genes I arbitrarily selected six genes for functional analysis because they had interesting annotations and/or expression patterns. I selected five receptor-like kinases or receptor-like proteins: *LRR-P* (P_35_15510), *DUF26-RLK b* (P_35_6100), *WAK-RLK a* (P_35_21250), *LRR-RLK* (P_35_7436) and *S-RLK* (P_35_26520). LRR-P (P_35_15510) is possibly a leucine-rich repeat protein or a LRR-receptor-like protein. DUF26-RLK b (P_35_6100) has a domain of unknown function. LRR-RLK is a receptor like kinase similar to OsXA21 (LRR-RLK) and S-RLK is a receptor like kinase containing a S- lectin domain. I further selected *COPINE* (COP, P_35_4054), a gene encoding a Ca^{2+}-dependent phospholipid-binding protein, which is suggested to be involved in Ca^{2+} signalling, which is important during pathogen attack (de Silva *et al.*, 2011; Zhang *et al.*, 2014). These six genes are the candidate genes I focussed on for functional characterization (Table S5, Fig. 17). WAK-RLK a (P_35_21250) failed during cloning procedure for TIGS analysis and was replaced by WAK-RLK (P_35_42590, accession number AK365606) as randomly selected RLK control (Fig. 17).

For confirmation of array results, qPCR was performed for 17 genes in a minimum of three biological replicates and compared to microarray data via correlation analysis with the Spearman`s rank sum test. Fig. 16 shows qPCR results for 12 and 32 hpi in all comparisons (1-7, compare Fig. 12). Microarray data (Fig. 16 A, 16 D) showed up-regulation in *Bgh*-dependent WT *Bgh* vs. WT mock, *CA RACB Bgh* vs. *CA RACB* mock and *RNAi RACB Bgh* vs. *RNAi RACB* mock comparison of all genes. This was also true for the *CA RACB* mock vs. WT mock and *CA RACB Bgh* vs WT *Bgh* comparison. Vice versa down-regulation in *RACB RNAi* mock vs. WT mock and RACB RNAi *Bgh* vs. WT *Bgh* comparison was observed for most of the tested genes. Interestingly, LRR-RLK, WRKY2 and WRKY22 were found to be up-regulated in all comparisons at 12 hpi but LRR-RLK and WRKY2 were strongly down-regulated in the *RACB RNAi* mock vs. WT mock comparison at 32 hpi whereas WRKY22 still was up-regulated in all comparisons. It is also mentionable that DUF26-RLK b, WAK-RLK b and WAK-RLK c turned from a differentially regulated expression pattern at 12 h into a complete up-regulated pattern at 32 hpi. qPCR data confirmed microarray data largely with a similar expression pattern. Differences appeared for WAK-RLK c at 12 hpi where the strong down-regulation in *RACB RNAi* mock vs. WT mock was not observable in the mean of three biological experiments even though up-regulation was moderate. Same pattern was found for COP, WRKY3 and WRKY20. WRKY3 was also up-regulated in WT *Bgh* vs. WT mock comparison compared to down-regulation in microarray data. LRR-RLK appeared to be down-regulated in *RACB RNAi* mock vs. WT mock in qPCR data.

At 32 hpi expression of all tested genes differed largely between microarray and qRT-PCR data (Fig. 16 D-F). Especially the *RACB RNAi Bgh* vs. WT *Bgh* expression set showed strong down-regulation compared to up-regulation in microarray data. Some genes, which were up-regulated in the comparison *RACB RNAi* mock vs. WT mock in the arrays, were strongly down-regulated according to RT-qPCR (DUF26-RLK b, DUF26-RLK c, WAK-RLK b, WAK-RLK c).

To summarize, qPCR data correlated to microarray data within a range of 50 % to 90 % at 12 hpi (Fig. 16 C, Table S7) except for DUF26-RLK a which is below 50 %. At 32 h qPCR data correlated within a

range of 50 % to 70 % except for COP and WRKY20 which correlated with a value below 50 %. Correlation values below 50 % might indicate strong biological variance. By tendency, most genes showed similar expression pattern in independent biological experiments.

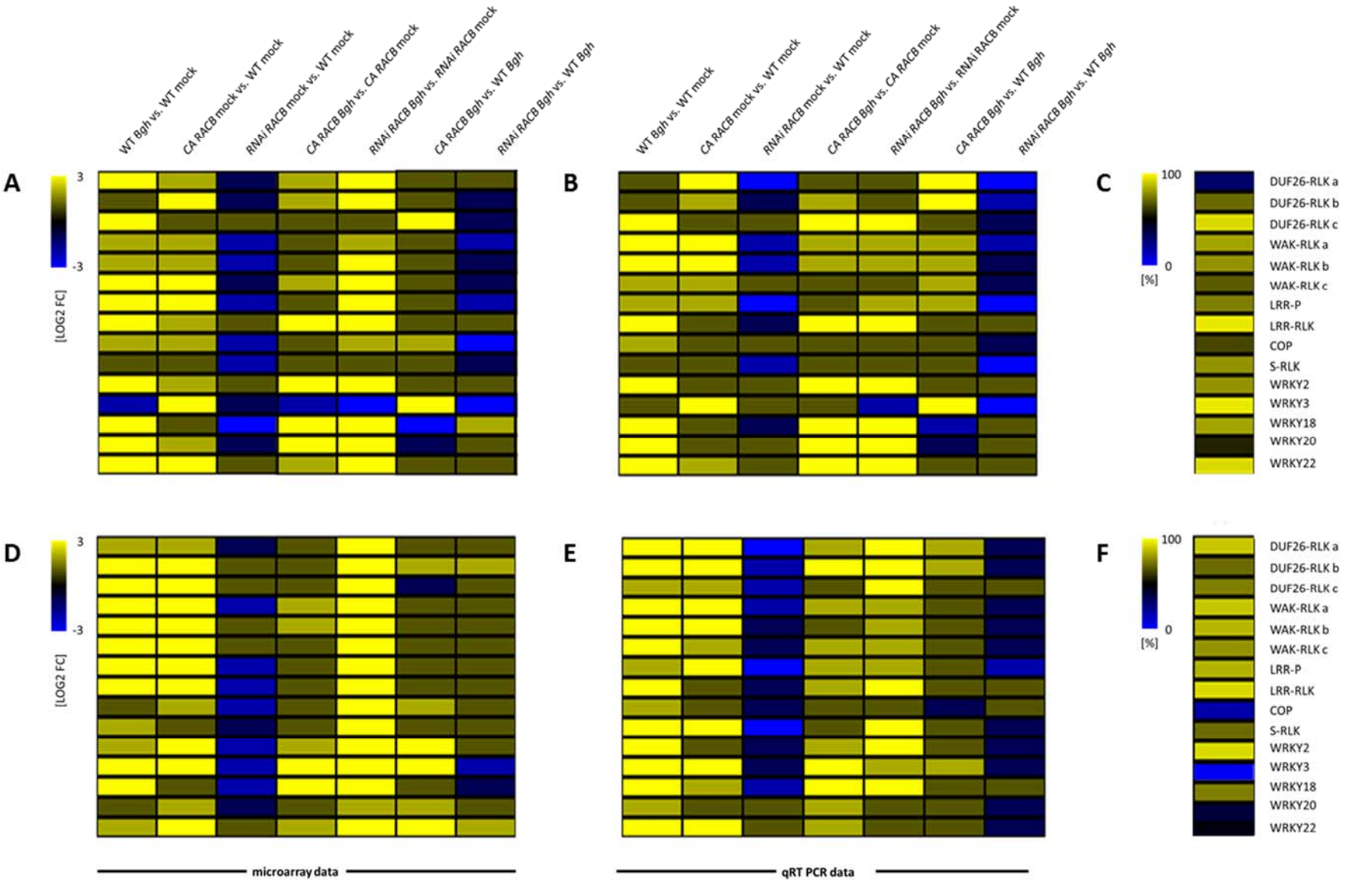
A
B
C
D
E
F
WT Bgh vs. WT mock
CA RACB mock vs. WT mock
RNAi RACB mock vs. WT mock
CA RACB Bgh vs. CA RACB mock
RNAi RACB Bgh vs. RNAi RACB mock
CA RACB Bgh vs. WT Bgh
RNAi RACB Bgh vs. WT Bgh
3
-3
[LOG2 FC]
100
0
[%]
DUF26-RLK a
DUF26-RLK b
DUF26-RLK c
WAK-RLK a
WAK-RLK b
WAK-RLK c
LRR-P
LRR-RLK
COP
S-RLK
WRKY2
WRKY3
WRKY18
WRKY20
WRKY22
microarray data
qRT PCR data

Fig. 16: Confirmation of differential expression of selected genes modulated by *Bgh* and *RACB*. qPCR results confirm microarray data in all gene expression sets at 12 hpi (**A-C**) and 32 hpi (**D-F**). Expression of candidate kinases *WAK-RLK a* (P_35_21250), *WAK-RLK b* (P_35_12191) and *WAK-RLK c* (P_35_50253), *DUF26-RLK a* (P_35_6100), *HvDUF26-RLK b* (P_35_39909) and *DUF26-RLK c* (P_35_10485), *LRR-P* (P_35_15510), *S-RLK* (P_35_7436), *LRR-RLK* (P_35_26520), *COP* (P_35_24054), *WRKY2* (P_35_15932), *WRKY3* (P_35_9124), *WRKY18* (P_35_23506), *WRKY20* (P_35_3498) and *WRKY22* (P_35_25198) is shown as heatmap comparing microarray data (**A**) and qRT-PCR data (**B**). Relative expression is shown as LOG2 value and was normalized to the house-keeping gene *UBC2* (P_35_46110). Data are mean values of three biological experiments each. Correlation analysis (**C**) performed with the free available statistic programm R and the Spearman`s rank sum test therein is given in per cent. Mean of the three biological replicates of qRT PCR data were correlated to microarray data over all seven comparisons at each time point. Colour in C and F presents correlation from 0 % (dark blue) up to 100 % (light yellow).

10.2.6 TIGS of *RACB*-regulated genes identifies potential susceptibility factors.

For the functional analysis candidate genes (FC cut-off > 2, FDR corrected p-value <0.05, *RACB* and *Bgh* modulated at both times), I used the final candidate gene list (bold in Table S5) containing the five of the six candidate genes *LRR-P, LRR-RLK, S-RLK, COP, DUF26-RLK b.* The sixth candidate gene *WAK-RLK a* was replaced by *WAK-RLK* (P_35_42590) and served as randomly selected control of receptor-like kinases (see also explanation on page 68). To assess the function of these six candidate genes, which had similar expression patterns at 12 hpi and 32 hpi, a transient-induced gene silencing (TIGS) approach described earlier (Douchkov *et al.*, 2005; Ostertag *et al.*, 2013) was performed. Leaf segments expressing a GFP reporter and a TIGS construct for induction of RNAi in single cells were inoculated with *Bgh* one day after ballistic transformation. In repeated independent experiments attacked cells with or without visible haustoria were counted under a fluorescence microscope to calculate relative percentage of cells with haustoria when compared to an empty vector control set as 100 %. TIGS resulted in significantly reduced haustoria frequency for *LRR-P* (-33 %), *S-RLK* (-37 %) and *LRR-RLK* (-50 %) whereas TIGS effects for the other candidate genes were not significant (Fig. 17).

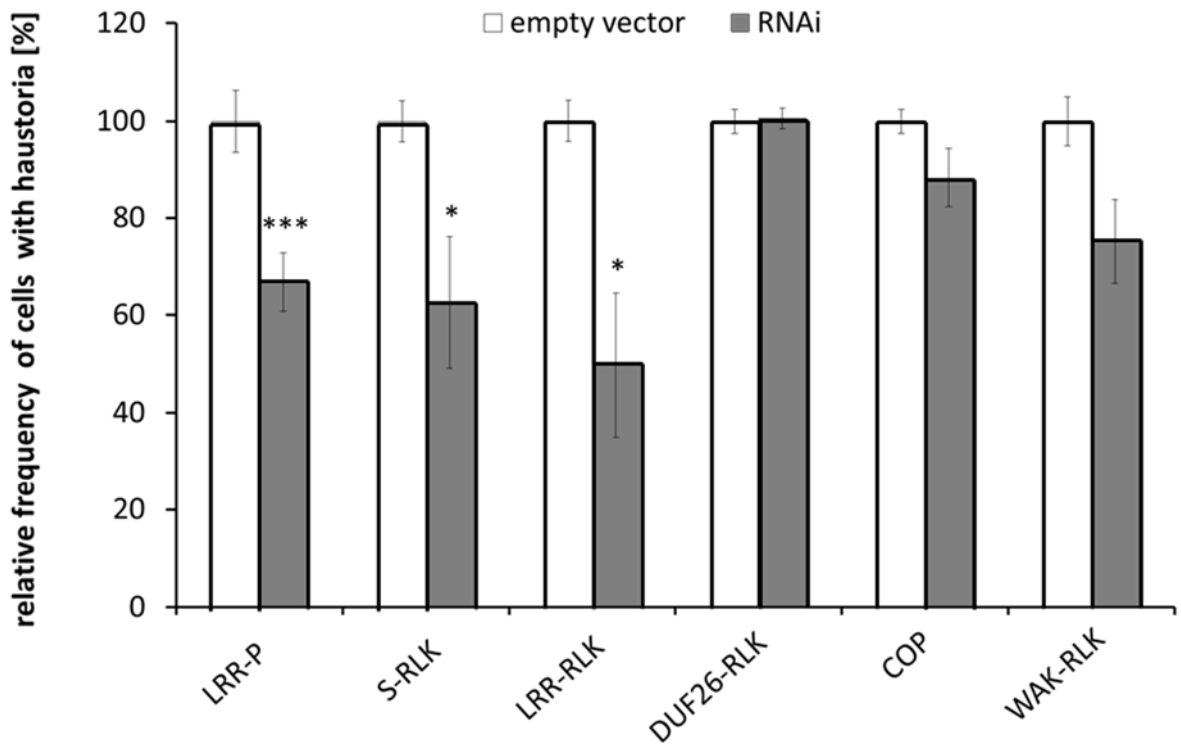

Fig. 17: Transient-induced gene silencing identifies new susceptibility factors. Ballistic transformation of leaf segments of seven days old WT Golden Promise plants with the different RNAi constructs carrying pIPKTA30N vector and *Bgh* inoculation after one day and

subsequent microscopical evaluation two days after inoculation showed a significant reduced single cell susceptibility phenotype for LRR-P, S-RLK and LRR-RLK. Haustoria frequency of the control was set to 100 % and error bars derive from the variance of individual repetitions to the mean. Bars represent standard errors. Asterisks indicate significant differences (t-test: *** p-value < 0.001, ** p-value < 0.01 and * p-value <0.05).

10.2.7 LRR-P genetically interacts with the susceptibility factor RACB in barley.

I went on analysing the LRR protein (LRR-P, P_35_15510) because LRR proteins, and LRR-RLKs are potentially involved in RAC/ROP signalling (Humphries *et al.*, 2011; Kawano *et al.*, 2014). First, the silencing efficiency of the *LRR-P RNAi* construct was tested. This confirmed its ability to knock-down the expression of a *LRR-P-GFP* fusion protein co-expressed with mCherry in epidermal cells of barley leaf segments (Fig. 18 A). Control cells, bombarded with the empty RNAi-vector pIPKTA30N, *LRR-P-GFP* fusion construct and mCherry as transformation marker, showed 70 % co-expression of *LRR-P-GFP* and mCherry. Cells, bombarded with the *LRR-P* carrying RNAi vector pIPKTA30N, *LRR-P-GFP* fusion construct and mCherry as transformation marker showed a reduced co-expression rate of 28 % verifying the functionality of the RNAi construct (Fig. 18 A). After successful cloning of the *LRR-P* over-expression construct with and without fluorescent tag (GFP), the effects of these constructs were analysed in a minimum of three independent over-expression experiments in which seven days old detached barley epidermal cells were transiently transformed and densely inoculated with *Bgh* spores. Eighty interaction sites on transformed cells were counted per experiment. Both constructs, *LRR*-P and *LRR-P-GFP* enhanced susceptibility by + 35 % (*LRR-P* OE) and + 44 % (*LRR-P-GFP OE*) (Fig. 18 B) compared to the empty vector (EV) control, which was set to 100 %. To analyse genetic interaction of *LRR-P* with *RACB*, the *LRR-P* OE and *LRR-P*-RNAi construct was co-expressed with different variants of *RACB* (*CA RACB*, *RACB* RNAi). Co-expression of *LRR-P* OE with *RACB* RNAi induced resistance (- 47 % relative haustoria formation) indicating that over-expression of LRR-P cannot induce susceptibility when *RACB* is silenced. When LRR-P was transiently silenced by RNAi a resistant single cell phenotype was observed (- 33 % relative haustoria formation). This was over-compensated when *LRR-P RNAi* was co-expressed with the activated susceptibility factor RACB. Despite silencing of *LRR-P*, *CA RACB* enhanced fungal success in haustoria formation by + 30 %. In total this data propose on the one hand that *LRR-P* acts as a susceptibility factor due to the fact that it induced susceptibility when over-expressed and resistance when silenced. On the other hand, data showed that *LRR-P* is genetically dependent on *RACB* in its function in susceptibility. Control experiments (Fig. S2) of single expression of *CA RACB*, *RACB RNAi* and dominant-negative (DN) *RACB* correspond to published function of activated RACB as a susceptibility factor (Schultheiss *et al.*, 2003).

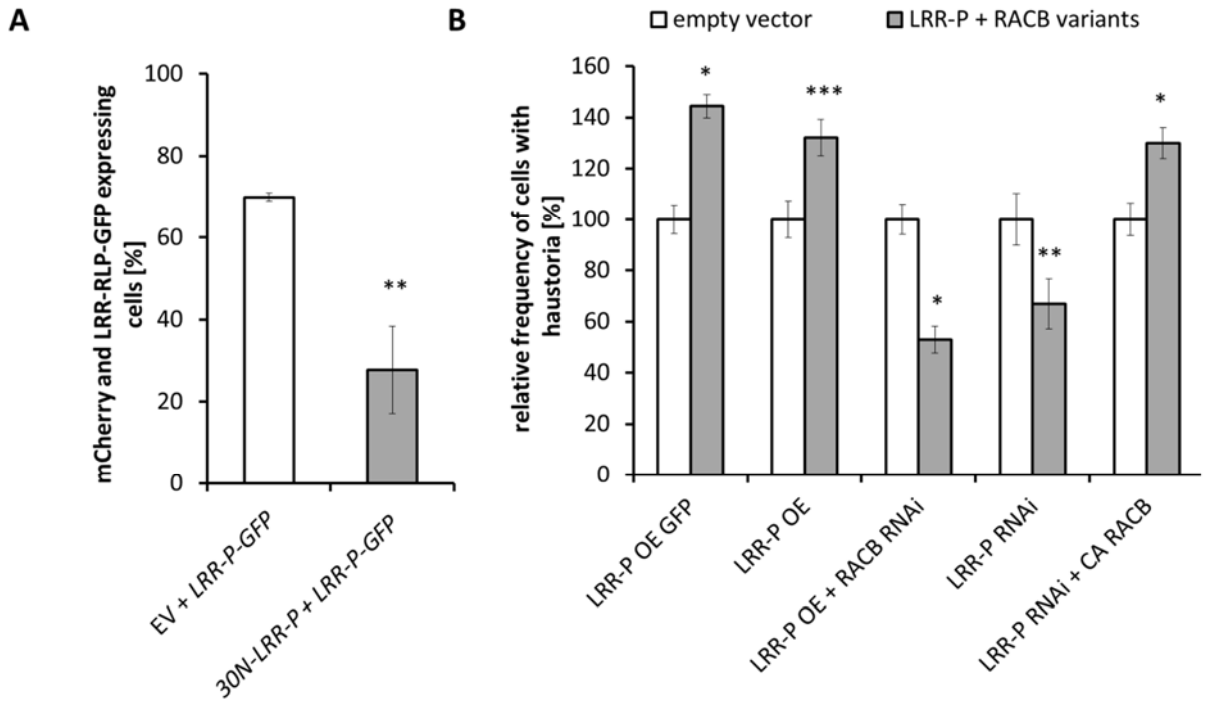

Fig. 18: Simultaneous misexpression of *LRR-P* and *RACB* suggest genetic interactions between corresponding gene functions. TIGS and overexpression experiments were performed in seven days old WT Golden Promise leaf segments after gold particle delivery of the test constructs together with pGY1::35S-GFP as transformation marker. Leaves were inoculated 4 h (or one day for RNAi) after bombardment with *Bgh* and were microscopically evaluated 48 h after bombardment. **A** Functionality of the pIPKTA30N::35S-*LRR-P* RNAi construct is displayed as the ability to knock-down the pGGIn-*LRR-P-GFP* fusion construct. Here, additionally mCherry was co-bombarded and red-fluorescing cells were analysed to an additional presence of the GFP fusion protein. In three independent experiments 100 cells were analysed two days after gold particle delivery. EV = empty vector. **B** *LRR-P* penetration efficiency when overexpressed (OE; pGY1::35S-LRR-P OE) or knocked-down (RNAi; pIPKTA30N::35S-LRR-P-RNAi). *LRR-P OE* or *LRR-P RNAi* co-bombarded with different variants of *RACB*. Haustoria rate is counted as the number of all penetrated cells divided by the number of attacked cells multiplied with 100. Bars represent standard errors. *, **, *** represent significance at p –value < 0.05, 0.01 and 0.001, according to a two-sided unpaired Student`s t-test performed on the non-transformed raw data. LRR-P-RNAi data correspond to those in Figure 17.

10.2.8 Localization of fluorescence-tagged LRR-P.

Overexpression of *LRR-P* leads to more susceptible leaf cells and vice versa knock-down of *LRR-P* to more resistant cells after ballistic transformation and inoculation with *Bgh.* To get a better understanding of LRR-P function, the subcellular localization of LRR-P was analysed before and during contact with *Bgh*. Since *LRR-P* was annotated as having a secretory leader peptide *GFP* was fused C-terminally to LRR-P in order to not interfere with the protein processing. *LRR-P-GFP* was transiently

transformed into detached barley leaves together with mCherry as cytoplasmic marker or *CA RAC1-CFP* as plasma membrane marker. Additionally, LRR-P-GFP and a marker were combined with CA RACB to check subcellular localization 20-25 h after particle bombardment by confocal laser scanning microscopy. The green fluorescing LRR-P protein localized to the cytoplasm or the endoplasmic reticulum (ER) therin and was distributed diffusely throughout the whole cell (Fig. 19 A). Partial plasma membrane association was imaged after plasmolysis induced with glycerol, which led to LRR-P-GFP-labelling of Hechtian strands (Fig. 19 B). Hechtian strands are useful as characteristic of plasma membrane proteins when protoplast shrinkage occurs after the plasma membrane peals away from the cell wall (Oparka, 1994). Hechtian strands were coloured with the green-fluorescing LRR-P, which seemed still to be attached to the membrane. Additionally, CA RAC1-CFP served as positive membrane control because as an active RAC/ROP protein it is attached to the plasma membrane (Huesmann *et al.*, 2012). Co-expression resulted in similar localization represented as an overlay of signals from the green (LRR-P GFP) and the cyan-fluorescing (CA RAC1-CFP) proteins at the plasma membrane (Fig. 19 C; D). Plasmolysis control experiments confirmed membrane association as Hechtian strands were whitish-coloured indicating that LRR-P-GFP and CA RAC1-CFP were both associated with the plasma membrane (Fig. 19 D). An interesting localization was observed for CA RAC1-CFP and LRR-P-GFP after *Bgh*-challenge (Fig. 19 C+D): Both the proteins accumulated around the penetration site and the membrane (labelled with red arrows) suggesting that LRR-P might be secreted.

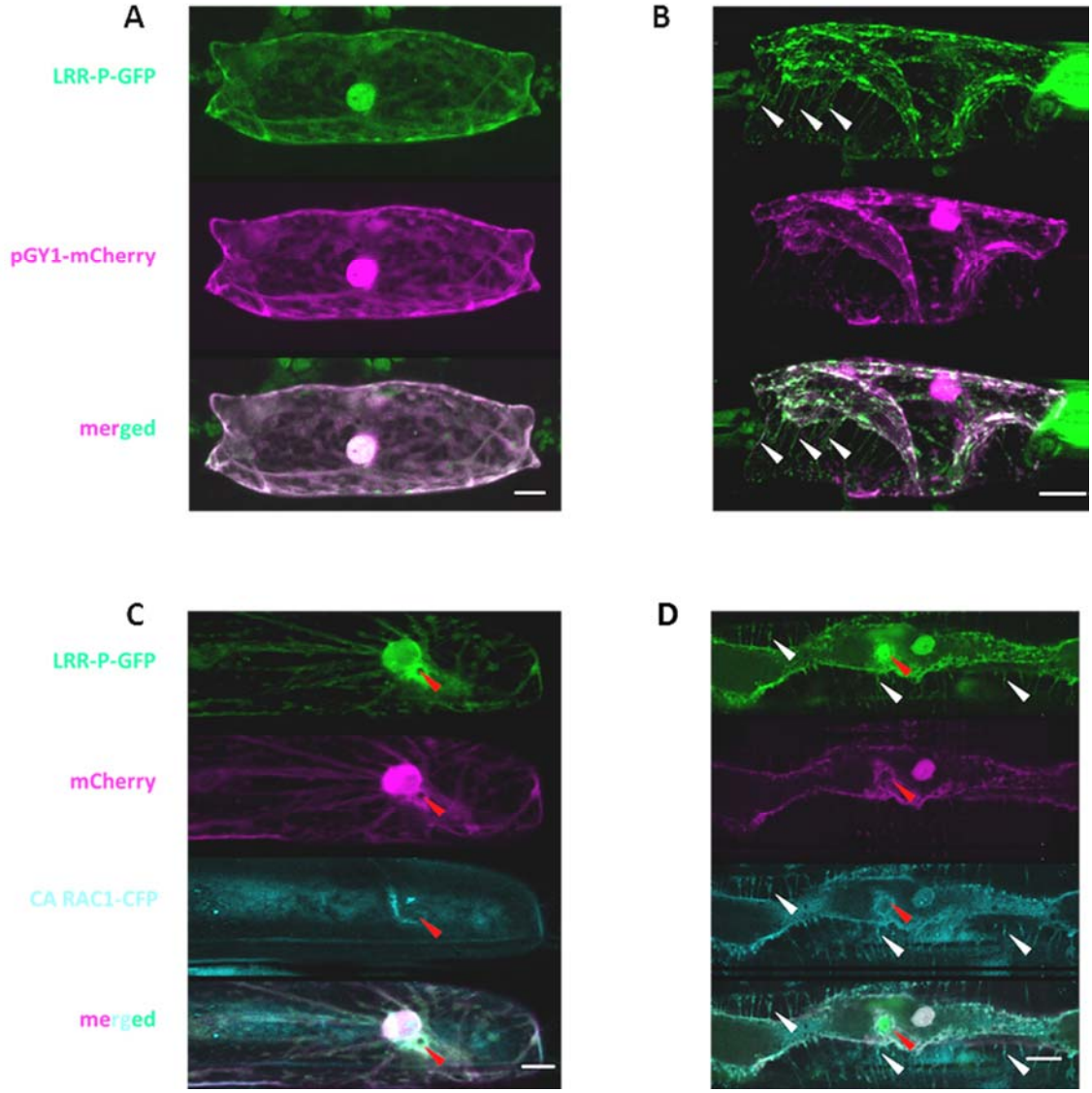

Fig. 19: LRR-P-GFP shows a complex subcellular localization pattern. A Diffuse cytoplasmic localization of LRR-P-GFP. **B** Clearly visible Hechtian strands of LRR-P-GFP after plasmolysis with 50 % glycerine for 1 min. **C** Localization of LRR-P-GFP is observed together with CA RAC1-CFP at the membrane. **D** Clearly visible Hechtian strands of LRR-P-GFP after plasmolysis with 50 % glycerine for 1 min. mCherry or CA RAC1-CFP was used as cytoplasmic or membrane transformation marker. Together with pGGIn::35S-LRR-P-GFP (P_35_15510) the plasmids (1 µg each) were transiently transformed by ballistic delivery of gold particles into 7 days old epidermal leaves. Microscopic observation was performed using the CLSM (Leica TCS SP5, Leica Microsystems, Wetzlar, Germany). GFP was excited with a laser line of 488 nm and detected at 500-550 nm whereas mCherry was excited with a laser line of 561 nm and detected at 580-650 nm. White arrows indicate examples of Hechtian strands visible by LRR-P association to the membrane (**B** and **D**) and red arrows indicate the fungus penetration site (**C** and **D**). Scale bar: 20 µm.

To analyse the potential effect of *Bgh* and of RACB, detached barley leaves transiently expressing *LRR-P-GFP*, mCherry and with or without *CA RACB* were inoculated 4 hours after bombardment with fungal spores for subsequent imaging. Subcellular localization was observed in the cytoplasm or at the ER therein (Fig. 20 A) as seen before without *Bgh* (Fig. 19 A) (Fig. 20 E-F) as well as "dots" perhaps presenting the secretory pathway in form of the Golgi apparatus. Membrane localization and LRR-P "dots" became visible under co-expression of *CA RACB*. In non-inoculated cells, LRR-P GFP appeared along cortical net like structures and as dots throughout the whole cell and surrounded the nucleus (Fig. 20 C-D). When barley cells were transiently transformed with LRR-P-GFP together with CA RACB and were challenged with *Bgh*, many more LRR-P-GFP green fluorescing dots were visible. These dots accumulated largely around the penetration site (labelled with red arrows) (Fig. 20 E-F). This goes in line with results from Fig. 19 C-D where *LRR-P GFP* co-expressed with *CA RAC1* CFP appeared surrounding the nucleus. These data propose that LRR-P could be a secreted protein, which partially remained within the secretory pathway when *CA RACB* is co-expressed.

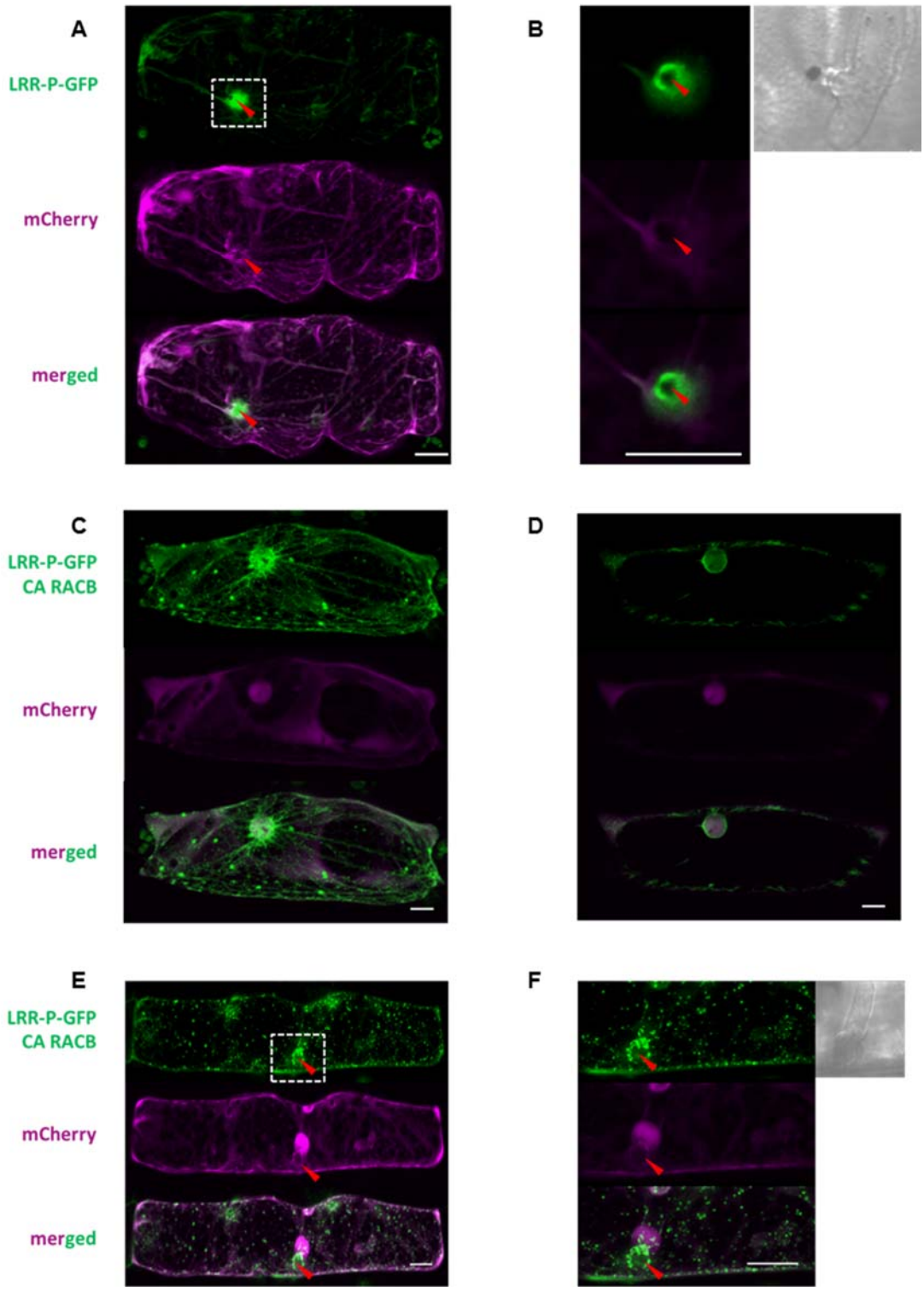

Fig. 20: LRR-P-GFP subcellular localization changes when it is co-expressed with *CA RACB*.
A pGGIn::35S-LRR-P-GFP transiently transformed barley cells were inoculated with *Bgh* resulting in cytoplasmic localization. **B** Zoom-in at penetration attempt shows clearly accumulation of LRR-P-GFP. **C-D** Co-expression of *CA RACB* results along net-like structures and surrounding the nucleus without *Bgh* and in more dot-like structures with *Bgh* (**E-F**). **F** Zoom-in of E at the penetration site.

7 days old barley leaves were transiently transformed with *LRR-P-GFP* +/- *CA RACB* via ballistic transformation and challenged with *Bgh* 4 hours after bombardment. Subcellular localization was examined 20-25 h after bombardment with confocal laser scanning microscopy. White colour in the merged pictures indicates co-localization. Red arrows indicate penetration sites. White dotted boxes present zoom-in pictures of **B** and **E**. Scale bar: 20 µm.

10.2.9 LRR-P is related to the SERK family.

To obtain a phylogenetic relationship of LRR-P, the protein sequence of LRR-P was blasted against protein sequences available on NCBI. Interestingly, arabidopsis proteins with the highest similarity to LRR-P are AtSERK RLKs. For instance, amino acids 27-185 of AtSERK2 share 68% identity to amino acids 21-179 of LRR-P. Hence, LRR-P might resemble an ectodomain of SERK-like RLKs. The queries with a similarity > 40% for found barley, corn and arabidopsis sequences were chosen and aligned with ClustalW and data were analysed using the Maximum Likelihood (ML) (Zhang and Nei, 1997; Zuckerkandl and Pauling, 1965) algorithm by using a matrix of pairwise distances estimated under the Jones-Thornton-Tayler (JTT) model (Tamura and Nei, 1993) in Molecular Evolutionary Genetics Analysis (MEGA6) (Tamura et al., 2013). After phylogenetic analysis (Fig. 21) three clusters resulted of which the first one contains arabidopsis somatic embryogenesis receptor-like kinase (SERK) proteins 1 and 2, and three maize SERKs and two potential barley SERK proteins. The second cluster includes AtSERK3/AtBAK1 (Chinchilla *et al.*, 2007; Li *et al.*, 2002), AtSERK4 and AtSERK5, two potential LRR-Ps of arabidopsis and one of barley. HvLRR-P (P_35_15510) was found to build the third cluster with similar barley LRR-Ps but related to the whole SERK family. Like the SERKs, NIKs belong to the LRR-RLK subclass II and are involved in perception of viral signals (Fontes *et al.*, 2004; Santos *et al.*, 2010). The arabidopsis NSP-interacting kinase 1 (AtNIK1) builds an outgroup showing that the barley LRR-RLPs are more related to the SERK family. LRR-RLKs of the subclass II –including SERK and NIK proteins – act in immunity (Chen *et al.*, 2014; Chinchilla *et al.*, 2007; Mariano *et al.*, 2004; Roux *et al.*, 2011); phylogenic data suggest a relationship of HvLRR-P to SERK proteins with similar functions.

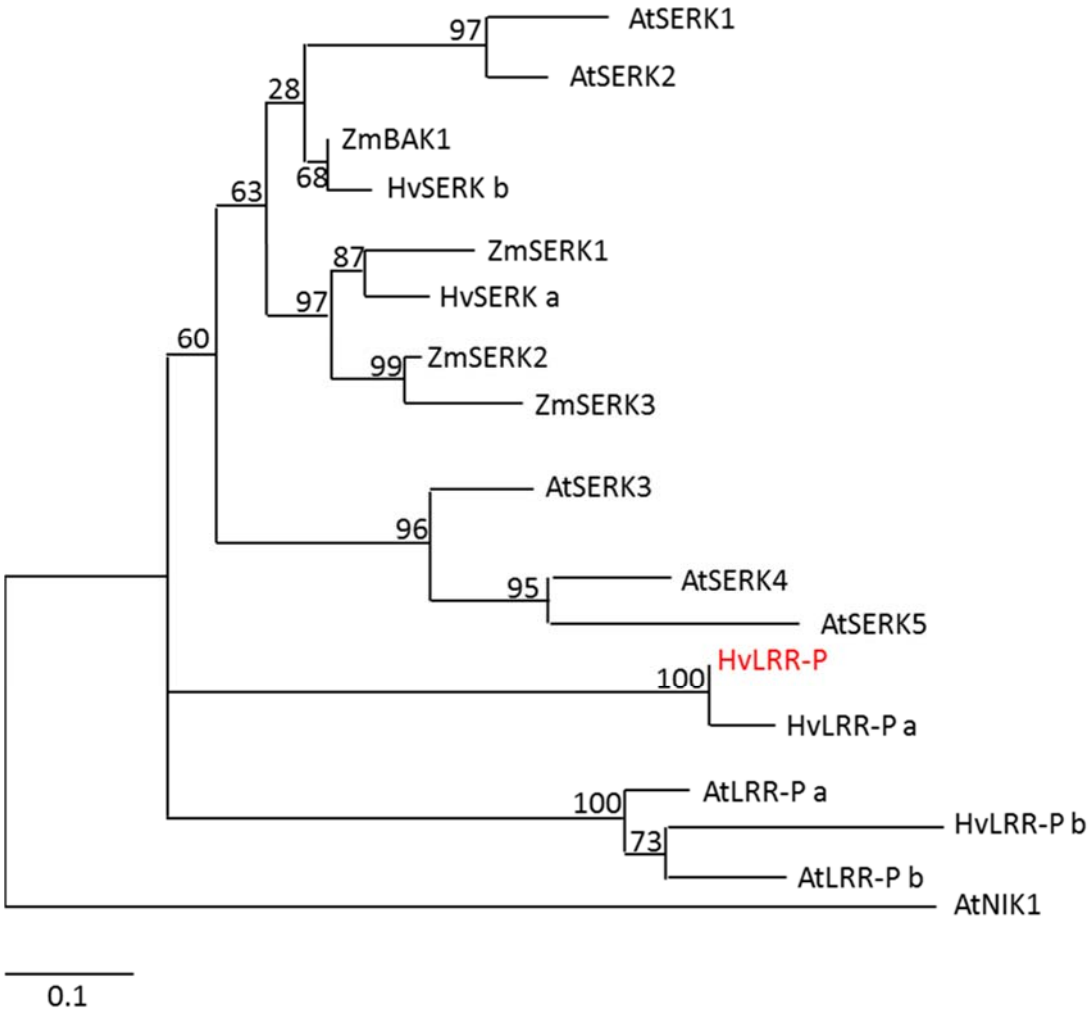

Fig. 21: Phylogenic relationships of LRR-P. Phylogenetic analysis clusters LRR-P within SERK proteins of arabidopsis, maize and barley. HvLRR-P (marked in red) (P_35_15510; BAJ91771) was compared to several protein sequences of barley (Hv), arabidopsis (At) and maize (Zm). For similarity HvLRR-P protein sequence was blasted against the barley and arabidopsis genome and sequences with a similarity of > 40% was chosen. Alignments were carried out with ClustalW and data were analysed using the Maximum Likelihood (ML algorithm by using a matrix of pairwise distances estimated under the Jones-Thornton-Tayler (JTT) model (Tamura and Nei, 1993) with a superior log likelihood value in Molecular Evolutionary Genetics Analysis (MEGA6) (Tamura et al., 2013). The tree with the highest log likelihood (-2736.75) is displayed and next to the branches is the percentage of trees in which the associated taxa clustered together shown. The tree is drawn to scale with branch lengths measured in the number of substitutions per site. Phylogeny test was done with the bootstrap method (Efron, 1979) with 500 replications (Pattengale *et al.*, 2010). All positions containing gaps and missing data were eliminated. 18 amino acid sequences were used for analysis: ZmSERK1 (CAC37638), ZmSERK2 (CAC37639), ZmSERK3 (CAC37642), ZmBAK1 (AFW57132), HvLRR-P (BAJ91771), HvLRR-P a (BAJ98355), HvLRR-P b (BAK03440), HvSERK a (BAK03316), HvSERK b

(AEE44134), AtLRR-P a (AED92930), AtLRR-P b (AEE77824), AtSERK1 (AEE35238), AtSERK2 (AEE31686), AtSERK3 (-AAK68074), AtSERK4 (AEC06259), AtSERK5 (AEC06260), AtNIK (AED92233).

11. DISCUSSION

The interplay between a host plant and a pathogen relies on very specific molecular mechanisms during the whole infection process. Loss-of-function of specific host proteins can result in enhanced resistance whereas over-expression can result in higher susceptibilty. Such proteins are called susceptibility factors (SFs) encoded by susceptibility (*S)*-genes. These genes support the invasion of pathogens. They can either negatively influence the first layer of defence – the early plant immune response – or can be structural and metabolic components important for the fungal establishment (Hueckelhoven *et al.*, 2013; van Schie and Takken, 2014). Therefore SFs can be used by the pathogen for maintaining its own life cycle (Dobon *et al.*, 2015). For barley the susceptibility factor RAC/ROP GTPase RACB supports the accommodation of fungal structures via its function in cell polarity and is believed to be involved in microtubule organization or destabilization during infection with the powdery mildew fungus (Hoefle *et al.*, 2011; Reiner *et al.*, 2015; Scheler *et al.*, 2016). To analyse the function of RACB as SF, basal immunity of barley with focus on the first plant responses after perception of PAMPs by plant surface sensors, such as ROS production, activation of MAPKs and regulation of defence gene expression was analysed (Fig. 5, Fig. 6, Fig.7, Fig. 8, Fig. 9). The idea was based on the fact that the RAC/ROP protein OsRAC1 was found to be implicated in PTI (Akamatsu *et al.*, 2013; Kawano *et al.*, 2014). *OsRAC1*-deficient plants showed a reduced ROS production and the expression of defence-related genes was suppressed compared to WT rice plants. Biotic stress induced by *Magnaporthe oryzae* resulted in susceptible *OsRAC1*-RNAi plants indicating a potential function of OsRAC1 in resistance. In contrast to rice where the RAC/ROP protein OsRAC1 plays a role during PTI, my data suggest that the barley SF RACB is not taking over a key role during PTI. Transgenic barley plants (*CA RACB* line 17/1-11 and *RACB RNAi* line 16/2-4) were analysed for ROS accumulation (Fig. 9) and MAPK activation (Fig. 6) with no significant influence of RACB. However, additional biotic stress experiments on the barley MAPK homologs showed differences on fungal establishment in barley *Bgh*-infected epidermal cells (Fig. 5).

Additionally, function of *RACB* was analysed in regard to gene expression. A transcriptomic approach with 44k microarrays was performed, comparing wild-type plants and plants over-expressing constitutively active *RACB (CA RACB)*, or plants characterized by a RNAi-mediated knockdown of *RACB (RACB RNAi)*. To cover major plant-fungus interaction stages during the infection process, two time points were evaluated; one in an early phase when the infection process is started, at 12 hpi, and one in a later stage of fungal establishment when the haustorium is maturing (Hueckelhoven *et al.*, 1999), at 32 hpi. The second time point was evaluated by comparing the different growth rates of the haustorium at several time points (Fig. 10). 32 hpi turned out to be most promising for strong gene activation as the time span between 32 hpi and 34 hpi showed the highest growth rate suggesting that susceptibility related genes were expressed around that stage. Conducted pathway analysis showed that both activated RACB- and *Bgh*-challenge similarly support the expression of RLKs (Table 5, Fig. 13). Six differentially expressed candidate genes were tested for their putative function in interaction with *Bgh* by TIGS in epidermal barley leaves (Fig. 17). Three out of six candidate genes caused reduced

susceptibility to fungal penetration upon their downregulation by transient RNAi. One of them, encoding a leucine-rich repeat containing protein (LRR-P; Harvest35 assembly accession 35_15510), was further characterized in transient over-expression and genetic interaction experiments (Fig. 18). In total my data suggest that *RACB* influences the expression of RLKs and further proteins partially acting in susceptibility to *Bgh* rather than controlling basal immunity.

11.1 RACB IS NOT INVOLVED IN EARLY PLANT IMMUNE RESPONSES.

The RAC/ROP GTPase RACB of barley is a susceptibility factor characterized to be involved in plant development and cytoskeleton organisation (Hoefle *et al.*, 2011; Opalski *et al.*, 2005; Pathuri *et al.*, 2008; Scheler *et al.*, 2016; Schultheiss *et al.*, 2005). Data from rice suggest a strong regulating function of rice RAC/ROP proteins: rice plants over-expressing the closely related *OsRACB* are more susceptible against *Magnaporthe grisea* (Jung *et al.*, 2006). Another relatec RACB/ROP protein, the rice *OsRAC1* is known to positively regulate typical PTI responses such as MAPK activation and ROS production by NADPH oxidases (Akamatsu *et al.*, 2013; Kawano *et al.*, 2014). Other rice RAC/ROP proteins such as OsRAC4, OsRAC5 or OsRACB act as negative regulators of blast resistance (Chen *et al.*, 2010). Based on these regulating functions of the rice RAC/ROP proteins, barley RACB was investigated for its impact during the early plant immune response, since nothing was known.

11.1.1 RACB HAS NO INFLUENCE ON EXPRESSION OF MAPK OR PATHOGENESIS-RELATED DEFENCE GENES.

In this work phylogenetic analysis (Fig. 4) revealed three barley MAPKs, which I named MPK3-like, MPK4-like and MPK6-like because of their similarity to the *Arabidopsis thaliana* MAPKs MPK-3, -4 and -6. In contrast to arabidopsis and rice where roughly 20 MAPKs are known (Meng and Zhang, 2013), barley MAPKs are hardly annotated. For barley, only HvMPK4 was identified to be involved in resistance against *Magnaporthe grisea* when knocked-out (Abass and Morris, 2013). HvMPK4 was named based on OsMPK4 showing an amino acid similarity of 93 % (Table S8). HvMPK4-like, characterized in this work, was named based on AtMPK4 showing the highest amino acid similarity of 79 % (Table S8). HvMPK4 and HvMPK4-like showed only a similarity of 52 % on amino acid level. As shown in Fig. 4 OsMPK3 and OsMPK4 cluster together with AtMPK1 and HvMPK4 and the not-characterized AtMPK7 and AtMPK14 but not with HvMPK4-like.

The expression levels of the three barley MAPK homologs (*HvMPK3-like, HvMPK4-like and HvMPK6-like*) were tested (Fig. 7) during *Bgh*-challenge. The barley MAPKs were not consistently *RACB*-modulated in transcript abundance with and without *Bgh*-treatment suggesting that *MAPK* expression might not be triggered by *Bgh* and/or *RACB*. This is different to the already characterized *HvMPK4*. Expression of *HvMPK4* was increased after *Magnaporthe grisea* challenge (Abass and Morris, 2013). Nevertheless, *HvMPK4* was named based on *OsMPK4* and *HvMPK4-like* was named based on its nearest arabidopsis homolog *AtMPK4* explaining the differences between the two barley MAPK homologs.

Furthermore, I investigated whether *RACB*-transgenic lines displayed changes in the expression of defence genes (Fig. 9) which are marker genes during pathogenesis (Bigeard *et al.*, 2015; Janda *et al.*, 2014). Pathogenesis-related (*PR*) proteins are induced after pathogen attack and can be used as control genes for the molecular infection status (Schultheiss *et al.*, 2003; van Loon *et al.*, 1994). Apparently, *CA RACB* supported constitutive expression of some of the *PR*-genes. However, in the non-infected status more susceptible *CA RACB* barley plants over-expressed these *PR* genes, whereas less susceptible *RACB RNAi* plants lowered *PR* gene expression to the similar level of WT plants. These findings were not observed for the non-infected status with *Bgh* (Fig. 9), which is contradictory to publications where *PR* genes were correlated to infection with a pathogen (Molitor *et al.*, 2011; Peterhaensel *et al.*, 1997) and cannot explain the reduced susceptibility of *RACB RNAi* plants (Hoefle *et al.*, 2011). Noteworthy, defence gene expression in arabidopsis plants expressing a dominant-negative version of the RAC/ROP protein ROP6 was also enhanced in the non-infected status. After infection with the powdery mildew fungus *Golovinomyces orontii,* those plants were more resistant to the fungus. In these studies it was determined that defence gene expression acts uncoupled from the fungal infection (Poraty-Gavra *et al.*, 2013). The rice RAC/ROP protein OsRAC1 was shown to modulate defence gene expression during PTI. In that system fungal-derived chitin gets recognized by the chitin receptor OsCERK1. A huge complex consistent of the RAC/ROP protein OsRAC1, OsRacGEF1 and several other factors such as OsMPK3 and OsMPK6 trigger the resistance to pathogens in rice. After perception of the PAMP by OsCERK1, OsRAC1 gets activated. In its active form OsRAC1 interacts with the MAPKs OsMPK3 and OsMKP6. Subsequently, both MAPKs can interact with the transcription factor RAC Immunity 1 (RAI1) which triggers the expression of elicitor-responsive genes such as OsWRKY19 or the phenylalanine ammonia-lyase gene 1 (PAL1). This systems shows that the RAC/ROP protein OsRAC1 enhance gene expression in biotic stress situations induced by PAMP treatment (Kim *et al.*, 2012). Based on the result found in this work, the RAC/ROP protein HvRACB slightly modulates defence gene expression.

Additionally, other marker genes for early plant immune responses were analysed. Jasmonate-responsive genes are known to be involved in immune responses (Ballare, 2011; Kogel *et al.*, 1995). Two members of these control genes were analysed in barley. Both JIPs *HvJIP23* and *HvJIP60* were also not *RACB*-dependently regulated even though a slight enhanced expression in *CA RACB* plants was observed for JIP23 (Fig. 9). *JIP60* expression was only enhanced at 12 h after *Bgh* infection. *JIP60* it also claimed as a ribosome-inactivating protein cleaving plant polysomes in their subunits during protein synthesis in barley leaf tissue in barley. Thereby, *JIP60* is not only a defense gene but also a marker for regulating protein synthesis (Reinbothe *et al.*, 1994). Enhanced *JIP23* expression in barley was up to now found in the scutellar node, root tip and the leaf base of the primary leaf showing a tissue-specific expression (Hause *et al.*, 1996). High levels of *JIP23* in barley roots colonized by an arbuscular mycorrhizal fungus was found to be correlated to the stronger sink function of colonized roots compared to non-colonized roots (Hause *et al.*, 2002). JIP23 is not a marker gene for infection of barley leaves but can be used as negative control for such analyses.

Summarizingly, gene expression analysis of the marker genes *PR*, the early plant immune response is slightly modulated by *CA RACB.* No significant differences were observed for *JIP* genes in the different *RACB* lines (WT, *CA RACB* line 17/1-11 and *RACB RNAi* line 16/2-4), although the slight differences in the expression of the marker gene JIP23 were observed. At least, *RACB* does not seem to negatively influence defence gene expression. Hence, RACB´s function in susceptibility can also not be explained via a role in negative control of host defense gene expression.

11.1.2 Barley MAPK homologs involved in susceptibility and resistance.

Data of this study suggest that barley MAPKs are involved in regulating defence when barley is attacked by *Bgh.* The effect of *Bgh* on all three barley MAPK homologs *MPK3-like*, *MPK4-like* and *MPK6-like* was evaluated with a standard TIGS assay. Transient silencing of *MAPKs* (Fig. 5) led to enhanced susceptibility (+ 40 % more haustoria compared to control leaves) in the cases of *MPK3-like* and *MPK6-like*. For *HvMPK4-like* transient silencing led to an enhanced resistance by a reduced number of established haustoria within the barley epidermal cells (- 35 %) compared to the control was observed.

The three barley homologs analysed within this study (HvMPK3-like, HvMPK4-like and HvMPK6-like) could act similar to their homologs in arabidopsis and rice. AtMPK3 supports resistance to the necrotrophic fungus *Botrytis cinerea* (Bethke *et al.*, 2009; Galletti *et al.*, 2011; Pitzschke *et al.*, 2009) and the mutant *Atmpk4* increases resistance to a bacterial (*Pseudomonas syringae* pv. *tomato* DC3000 strain) and to an oomycete (*Phytophthora parasitica*) pathogen (Petersen *et al.*, 2000). Although this allows no direct comparison, as the barley MAPKs analysed in this work were investigated for their effect upon the biotrophic fungual pathogen *Bgh*, a similar mode of action is possible. Additionally, both AtMPK3 and AtMPK6 are also involved in developmental processes such as stomata formation or ethylene biosynthesis or root hair formation (Gudesblat *et al.*, 2007; Sheikh *et al.*, 2013; (Lopez-Bucio *et al.*, 2014; Walia *et al.*, 2009; Wang *et al.*, 2008). For rice, only OsMPK4 expression was shown to be increased after challenging with the biotrophic fungus *Magnaporthe grisea* (Reyna and Yang, 2006) which is more related to HvMPK4 than HvMPK4-like. OsMPK3 and OsMPK6 are both involved in immune responses such as defence gene expression and antimicrobial compounds synthesis after MAMP signals (Kishi-Kaboshi *et al.*, 2010). Additionally, OsMPK6 was found as activator and repressor of resistance to the bacterial pathogen *Xanthomonas oryzae* pv. *oryzae* (Shen *et al.*, 2010).

As plant MAPKs carry the TXY motif as shown for the mammalian ERK MAPK pathway (Morrison, 2012), it is possible that the MAPK family of plants could act in a comparable way as in mammals. The mammalian ERK signalling pathway is one of the three components for intracellular signal transduction pathways. c-Jun N-terminal kinases (JNK), ERK and p38 transduce extracellular signals via a multistep processes for triggering the stress response (Bodai and Marsh, 2012). The ERK signalling pathway is – similar to plants- mainly involved in diseases and a variety of studies are available showing its impact on development of several diseases such as cancer, Parkinson`s disease, Alzheimer`s disease and others (Kim and Choi, 2010; Kyriakis and Avruch, 2012; Qi and Elion, 2005). In terms of functions in interaction with microbes, my data on barley MAPK phylogeny and function firstly suggest a partially conserved function of plant MAPKs but also some similarities to mammalian MAPK signalling.

11.1.3 *RACB* is not involved in MAPK activation or in ROS accumulation.

For barley, RBOH oxidases were shown to have an impact on developmental processes and during interaction with *Bgh* (Proels *et al.*, 2010). A direct interaction between RAC/ROP proteins and RBOH oxidases was shown for OsRAC1 and OsRBOHB (Wong *et al.*, 2007). Similar to what was described by Proels et al. (2010), I recorded a typical ROS production in response of barley to PAMPs. However, neither *CA RACB* expression, nor the suppression of *RACB* expression greatly influenced the ability of barley to quickly respond to the fungal PAMP chitin, or to the bacterial PAMP flg22 in standard ROS assays (Fig. 8). A ROS accumulation of barley roots stressed with the soil borne fungus *Piriformospora indica* was shown to the fungal-derived PAMP chitin (Hilbert *et al.*, 2013). Only OsRAC1 was shown to regulate ROS accumulation by interacting with RBOH-type NADPH oxidases and with the help of a scavenging protein (Wong *et al.*, 2007; Wong *et al.*, 2004). In rice RAC/ROP protein functions and early plant immune responses such as MAPK activation and ROS accumulation are linked to each other (Akamatsu *et al.*, 2013; Kawasaki *et al.*, 1999; Ono *et al.*, 2001). OsRAC1 plays a key role in these immune responses. For the barley susceptibility factor RACB no differences between the two *RACB*-transgenic and WT barley plants were observed in MAPK activation even though MAPK activation in WT barley was successful (Fig.6) as seen for rice or arabidopsis (Bethke *et al.*, 2012; Ranf *et al.*, 2015; Singh *et al.*, 2012).

11.1.4 Conclusion I.

The initial idea that one mechanism of the susceptibility factor RACB could be the regulation of canonical PTI in barley was not supported, because PTI is largely unchanged in *RACB*-transgenic barley plants. Nevertheless, my data show typical PTI responses in barley as described earlier for other plant species (Jones and Dangl, 2006). However, a connection between a RAC/ROP GTPase and PTI was most recently shown for the monocot rice (Akamatsu *et al.*, 2013). Although PTI in barley seemed to be independent of *RACB*, the barley MAPKs influenced the interaction outcome with *Bgh*. Silencing of the MAPKs led to either enhanced susceptibility (*MPK3-like* and *MPK6-like*), or reduced susceptibility (*MPK4-like*), respectively. In conclusion, RACB seems to be involved in regulating pathways other than controlling early PTI responses against *Bgh*.

Because RACB did not suppress PTI and rather supported than suppressed defense gene expression, a transcriptomic analysis should shed light on the influence of *RACB* on gene expression and thereby on a possible priming of barley for susceptibility against *Bgh*.

11.2 GLOBAL MICROARRAY ANALYSIS SUGGESTS RLKS TO BE HIGHLY REGULATED BY *RACB* DURING POWDERY MILDEW INFECTION.

To better understand the mechanism of *RACB*-modulated signalling, it is necessary to identify interactors of RACB. For identification of genetically *RACB*-interacting elements, the focus was set on *RACB*-modulated gene expression which possibly contributes to susceptibility to the powdery mildew fungus *Bgh*. Global microarray experiments in barley were conducted to understand the mechanisms within the epidermis of barley leading to susceptibility or resistance. Molitor *et al.* (2011) showed for example up-regulation of receptor-kinases and transcription factors at 12 hpi after *Bgh* challenge. Transcriptome analysis of *RACB*-modulated gene expression in barley had not been addressed before. In the performed microarray study, thousands of genes were found to be highly differentially regulated by *Bgh* and *RACB* (Table 4) with stringent filter settings with a fold change cut-off of 2-fold and a false discovery rate corrected p-value of < 0.05 at both time points. More transcripts were regulated by *Bgh* at 12 hpi whereas more transcripts were regulated by *RACB* at 32 *hpi*. This observation proposed that *RACB* may have a stronger effect in the later infection cycle. Additionally, more transcripts were up-regulated than down-regulated by *RACB* showing the huge impact of *RACB* on transcripts strongly expressed during an infection. Suspicously, *CA RACB*-influenced transcripts were highly regulated compared to *RACB RNAi*-influenced transcripts (Table 4, all regulated genes). The observed strong overlap between *CA RACB*-influenced transcripts and *Bgh*-influenced transcripts (Fig. 15) suggest a pre-activation of the *CA RACB* gene set even without *Bgh*-challenge. This pre-activation of *CA RACB* may explain why fewer transcripts were regulated in *CA RACB* barley by *Bgh* when compared to WT or *RACB RNAi* plants (Table 4, all regulated genes).

To estimate the influence of *Bgh* infection on plants containing different levels of *RACB* transcripts or activity, all gene expression data were clustered by means of principal component analysis (Fig. 11). PCA analysis showed that *Bgh*-treatment had a strong influence on barley gene expression as all mock-treated samples clustered clearly separated from the inoculated samples indicating the strong effect of *Bgh*. Furthermore, the level of *RACB* expression of the distinct plant lines had a strong effect as well. In the cluster of mock-inoculated barley, *CA RACB* lines were clearly divergent from *RACB RNAi* and WT lines in the PCA analysis. In contrast, in the cluster where *Bgh*-treated samples appeared, *RACB RNAi* lines were clearly distinguishable from the other two. This difference could be due to the fact that the fungal influence on gene expression in *RACB RNAi* plants was substantially lower than in WT and in super-susceptible *CA RACB* plants. In the cluster where mock-treated samples appeared, the difference might be explained by the strong *RACB*-modulated gene expression in *CA RACB* plants even when untreated.

Pathway analysis revealed many biological pathways to be significantly regulated. Ten pathways with a number of transcripts above 50 from all transripts at 12 hpi and at 32 hpi were shown in Table 5. With the seven *RACB* and *Bgh* comparisons presented in Table 5 (WT *Bgh* vs. WT mock, *CA RACB* mock vs. WT mock, *RACB RNAi* mock vs. WT mock, *CA RACB Bgh* vs. *CA RACB* mock, *RACB RNAi Bgh* vs. *RACB RNAi* mock, *CA RACB Bgh* vs. WT *Bgh*, *RACB RNAi Bgh* vs. WT *Bgh*) the influence of *RACB*, of *Bgh* and

combination of both was covered. Prominent observations were that all of the 10 pathways were significantly regulated by *RACB* (comparisons: *CA RACB* mock vs. WT mock and *RNAi RACB* mock vs. WT mock) and *Bgh* (WT *Bgh* vs. WT mock) with the exception for cell organisation. This pathway was only significantly regulated in WT *Bgh* vs WT mock, *RACB RNAi* mock vs. WT mock and *RACB RNAi Bgh* vs. WT *Bgh*. The high overlapping up-regulation of the same transcripts by *Bgh* and *CA RACB* and the fact that these transcripts are down-regulated by *RACB RNAi* (Fig. 15) support the idea that these genes are already over-expressed in non-*Bgh*-treated *CA RACB* plants. Those transcripts in the non-infected super-susceptible *CA RACB* line (compare also Table 4) support the susceptibility to *Bgh* during an infection. In the lists of stringently regulated transcripts (Fig. 15, Table S3, Table S4) many transcripts belong to the signalling pathway or to transcripts related to vesicle transport. These biological pathways were the only two out of the presented ten biological pathways which were significantly regulated in all seven comparisons at either 12 hpi or 32 hpi or both (Table 5).

With a focus on the signalling pathways, Fig. 14 showed that receptor kinases were oppositely regulated in the mock-treated comparisons *CA RACB* mock vs. WT mock and *RACB RNAi* mock vs. WT mock. This supports the idea that RLKs have a great impact on the RAC/ROP GTPase RACB. This result is interesting in regard to the observations from Molitor *et al.* (2011). They analysed systemic resistance against *Bgh* induced by mycorrhiza-colonization in barley roots with a transcriptomic approach. As output specific gene sets to be mostly regulated such as LRR-RLKs, WRKY transcription factors or vesicle-localized gene products were found. Though they analysed systemic resistance of barley against *Bgh* induced by *Piriformospora indica* and not susceptibility of barley against *Bgh*, the similar specific gene sets were identified. For example, *PR* gene expression was primed by *Piriformospora indica* mycorrhization for resistance to *Bgh* explaining the important mechanism to reduce susceptibility in mycorrhiza-colonized *Bgh*-challenged barley plants. Other specific gene sets such as the LRR-RLKs support the hypothesis of this work that such gene sets are of particular interest in *RACB*-driven interaction between the barley plant and its pathogen *Bgh*.

Compared to other RAC/ROPs from other species where mainly developmental processes such as cell polarity (Humphries *et al.*, 2011), or regulation of plant growth (Duan *et al.*, 2010; Huang *et al.*, 2014) but also abiotic stress situations (Xu *et al.*, 2010) are RAC/ROP-regulated, RACB seems to play a role in biotic stress induced by *Bgh.* Clustering was used as a tool for grouping similarly expressed genes in regard to treatment or genotype. Similar expressed transcripts within the signalling cascade were presented in three categories (Fig. 13, *RACB*-regulated in yellow, *Bgh*-regulated in green and *RACB*- and *Bgh*-regulated in red). At both time points several clusters showed transcripts to be significantly dependent on *RACB*- and *Bgh*- regulation. Furthermore, these groups contained many receptor-like kinases which were observed to be differentially regulated by *Bgh* (Fig. 15). In regard to known literature this became of most interest during this work. There are examples of other RLKs of other species such as rice or arabidopsis which were found to act upstream of RAC/ROP proteins. The rice LysM containing RLKs OsCEBIP1 and OsCERK1 acts upstream of the RAC/ROP protein OsRAC1 to transduce immune responses upon PAMP challenging (Kawano 2013). The arabidopsis malectin-like

domain containing RLK FERONIA acts as well upstream of AtROP2 and AtROP11 to regulate root hair development (Duan *et al.*, 2010).

In this work, many of the transcripts were annotated to be receptor kinases, but also many transcription factors, pathogenesis-related or hormone-associated transcripts were found (Table S3, S4, S5). These kinds of transcripts support the hypothesis that *RACB* and *Bgh* act in biotic stress situations. Potentially, transcripts observed during pathway analysis may include new regulators of diverse functions within the barley-powdery mildew interaction.

11.2.1 Conclusion II.

From pathway analysis of global gene expression the following conclusions are drawn:

1) *Bgh*-infection and expression of *CA RACB* support the expression of overlapping sets of transcripts.
2) Pathway analysis of gene expression and stringent filtering of differentially expressed genes suggest signalling receptor-like kinases to be expressed in a *RACB*-modulated manner.
3) Data suggest that RACB is involved in modulating expression of genes, which are also expressed in the compatible interaction with *Bgh*. It is therefore speculated that *Bgh* manipulates RACB function for modulating host gene expression to the benefit of the parasite.

11.3 qRT-PCR DATA CONFIRMED IMPACT OF *RACB* AND *BGH* ON RLKS.

I used qRT-PCR for verification of microarray data. qRT-PCR and microarray can vary from each other but data documenting this disagreement are rare. However, biological variations as well as less specificity of the analysed genes because of highly conserved regions (Jambunathan and McNellis, 2003) have to be considered in that regard. In this work I verified differential expression of WRKY transcription factors, wall-associated kinases and domain of unknown function 26 kinases, found during microarray analysis to be modulated by *RACB* and *Bgh* by qRT-PCR (Fig. 16). Genes out of each of the three groups were identified to have a strong expression in barley after pathogen attack and were thereby used as positive markers for expression during *Bgh*-infection. Transcription factors were prominently found in former microarray analysis by Molitor et al. (2011) as highly regulated transcripts at 12 hpi and WRKYs are known to act positively or negatively in plant immunity (Kim *et al.*, 2008; Lai *et al.*, 2008; Zheng *et al.*, 2007; Zheng *et al.*, 2006). For qRT-PCR the already published WRKY2 and WRKY22 were used as positive controls for successful *Bgh* infection. The other analysed WRKYs were strongly induced after pathogen attack and by *CA RACB* and vice versa down-regulated when *RACB* was down-knocked. It was conspicuous that pathway analysis revealed mainly WRKYs which were dedicated to be involved in immunity in other species (Table S6).

The expression data of the analysed barley *DUF26-RLKs* in this work suggested that these type of RLKs is strongly involved during immunity of barley. At both time points expression was induced after *Bgh*-infection. Additionally *CA RACB* induced expression whereas *RACB RNAi* decreased expression. qRT-PCR results were in line with the microarray data except for *DUF26-RLK a*, which nevertheless showed

the same expression tendency. This apparent mis-correlation might be explained by less strongly differentially expression (Fig. 16). All analysed DUF26-RLKs showed an amino acid similarity of 49 % to the already characterized barley DUF26-RLK, HvCRK1 (Fig. S11). In transient barley assays where *HvCRK1* was silenced, a higher resistance to *Bgh* and MLO function was observed (Rayapuram *et al.*, 2012). Showing that HvCRK1 seem to play an important role during *Bgh*-infection and thereby supporting the results obtained in this study. Expression of the analysed barley *HvWAK-RLKs* was strongly induced by *Bgh* and *CA RACB* (Fig. 16) promoting the hypothesis that WAK-RLKs play roles during pathogen interaction (Delteil *et al.*, 2016). In barley no wall-associated kinase was identified for biotic stress situations but HvWAK1 was characterized as a regulator of root growth (Kaur *et al.*, 2013). For example, a WAK-RLK was shown in microarray studies in wheat to be enhanced expressed after *Rhizoctonia cerealis* though follow-up experiments showed that it may not be the key regulator for the defense response. Nevertheless, this supports that WAK-RLKs are important factors during immunity as shown for arabidopsis *WAK1* – an ortholog of *HvWAK-RLK* a studied in this work. In arabidopsis and rice over-expression led to enhanced resistance to *Botrytis cinerea* (Macho and Zipfel, 2014) and to *Magnaporthe oryzae* (Li *et al.*, 2009).

A set of six candidate genes (Table S5) was included in the verification analysis. Those genes were identified by setting a stringent filter on microarray data with a fold-change cut-off > 2 and a FDR-corrected p-value of <0.05 for all differentially regulated *RACB*-dependent genes. This list of 142 genes (Table S2) at 12 hpi was compared to the list at 32 hpi resulting in 15 overlapping genes, of which six were selected for TIGS , namely *LRR-P*, *DUF26-RLK b*, *WAK-RLK a, LRR-RLK,* one *S-RLK* and *COP* (Table S5). The latter two two were chosen because of literature of rice where the LRR-RLK XA21 plays a key role during biotic stress (Song *et al.*, 1995) and of arabidopsis literature showing that S-RLKs are involved in innate immunity (Ranf *et al.*, 2015; Singh and Zimmerli, 2013). These genes were also differentially regulated after pathogen attack at 12 hpi but not significantly with a FC>2 for the *CA RACB* mock vs. WT mock and *RACB RNAi* mock vs. WT mock comparison. *COP*, a member of the copine family of Ca^{2+}-dependent phospholipid-binding proteins contains a C2 domain. Such proteins are suggested to be involved in Ca^{2+} signalling, which itself is very important during pathogen attack (de Silva *et al.*, 2011; Zhang *et al.*, 2014) and was strongly de-regulated at 12 hpi (Table S2).

In sum, qRT-PCR was used as independent method to confirm microarray analysis data. Microarray data were verified and expression data showed that different RLK types are highly modulated by *RACB* with and without powdery mildew infection.

11.4 FUNCTIONAL ANALYSIS DELIVERED NEW SUSCEPTIBILITY FACTORS.

After transient-induced gene silencing assays in detached barley leaves three genes were identified as potential new susceptibilty factors. Knock-down of all *LRR-P*, *LRR-RLK* and *S-RLK* resulted in less *Bgh* infection success (Fig. 17) compared to the empty vector controls. None of these three genes – identified by the microarray studies - has been described before in context of disease susceptibility.

11.4.1 LRR-P is a new susceptibility factor.

In this study, *LRR-P* turned out to be a potential susceptibility factor after TIGS experiments (Fig. 17). Significant more haustoria (+ 35 %) when *LRR-P* was over-expressed and vice versa significant less haustoria (- 33 %) when LRR-P was silenced was observed in the epidermal cells of WT barley. This suggested LRR-P as new identified susceptibility factor (Fig. 18). *LRR-P* was annotated as BRASSINOSTEROID INSENSITIVE 1-associated receptor kinase 1 based on rice and arabidopsis homologies in the microarray analysis (see Table S3, S4, S5). For this work it was subsequently named as *LRR-protein* because it does not contain an intracellular kinase domain (Fig. 22) though it phylogenetically clustered with SERK proteins from arabidopsis and barley (Fig. 21). LRR-P is a protein of 224 aa only (Fig. 22) and is predicted to contain four or five LRRs and a secretory signal peptide dependent on the program which is used. The amount of the LRRs is similar to that of AtBAK1 (Chaparro-Garcia *et al.*, 2011) which is a member of the SERK family. Phylogenetically, the four to five containing LRR containing LRR-P is related to the SERK family (Fig. 21) keeping in mind that SERK proteins possess less than 10 LRRs (Hecht *et al.*, 2001). LRR-P built a single cluster in close relation to the SERK proteins of arabidopsis and rice (Fig. 21). Structurally similar proteins such as ZmPAN1 or LRR-LeSHY are involved in developmental processes. ZmPAN1, which showed an amino acid similarity of 28 % (Table S7, Fig. 22), was identified as kinase-dead RLK involved in asymmetric cell division during stomata development (Cartwright *et al.*, 2009). Further, it could be shown that in this process the maize RAC/ROP proteins ROP2 and ROP9 are involved (Humphries *et al.*, 2011). The tomato LRR-P LeSHY, which showed an amino acid similarity of 22 % to HvLRR-P, was characterized as an interacting ligand of the tomato pollen-specific receptor protein kinase (LePRK2) involved during pollen tube growth (Guyon *et al.*, 2004). LeShy is suggested to be secreted (Guyon *et al.*, 2004; Guyon *et al.*, 2000). The arabidopsis PRK2 interacts with the ROP activating RopGEF12 (Zhang and McCormick, 2007) and is thereby involved in ROP-induced growth of pollen tubes (Zhao *et al.*, 2013a). Interestingly, Wang et al. (2014b) identified the same rice locus during a microarray study where rice was infected with *Magnaporthe oryzae*. The rice homolog of HvLRR-P was not analysed in more detail by that group. Though, this finding supports that HvLRR-P might play a key role during pathogen interaction. HvLRR-P shares some structural similarities with ectodomains of RLKs, kinase-dead RLKs, and with receptor ligands (Fig. 22), involved in plant immunity, polar cell development and ROP signalling, it is tempting to speculate that barley LRR-P could also act as a ligand or co-receptor in a receptor complex.

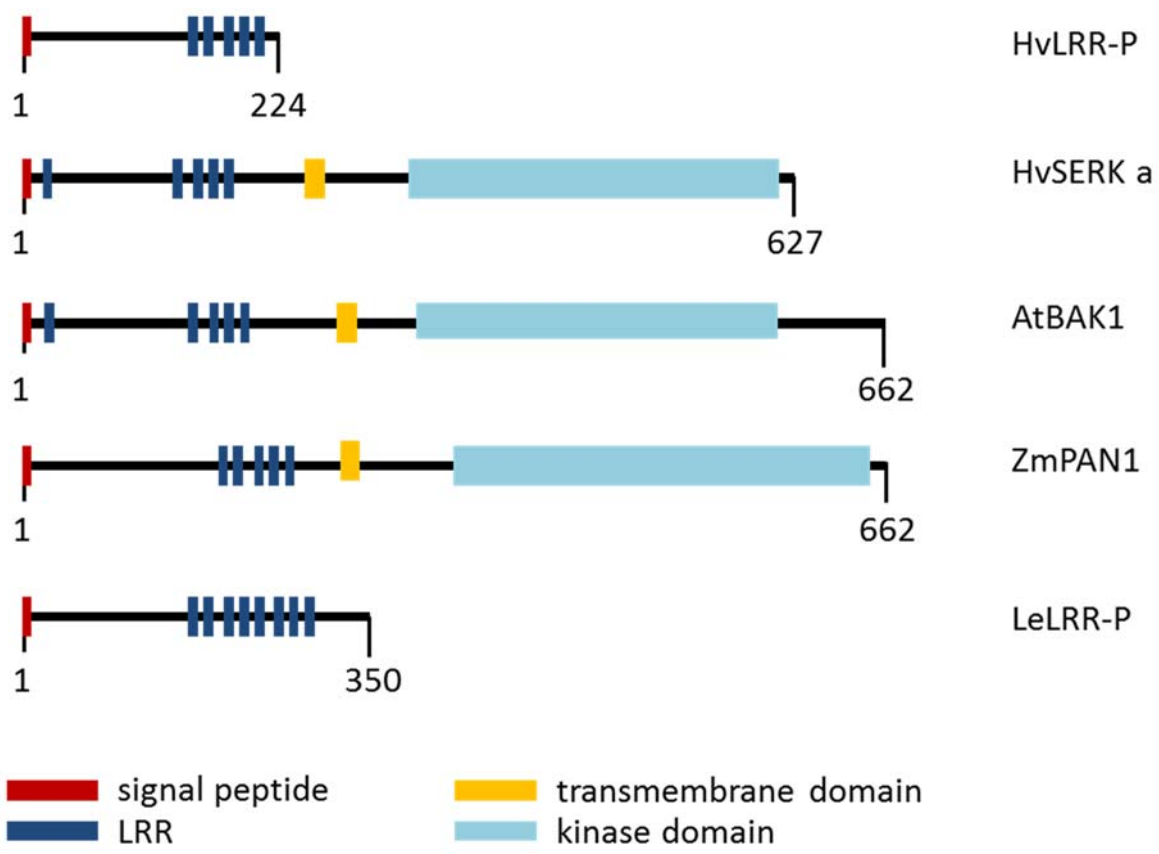

Fig. 22: Protein domains of structurally related LRR-RLKs or LRR-proteins/ligands of barley, arabidopsis, maize and tomato. Proteins are displayed with four different structure domains: brown = signal peptide, dark blue = LRR, yellow = transmembrane domain, blue = kinase domain. All proteins show nearly the same LRR number. HvLRR-P and LeLRR-P are smaller proteins with no clearly predicted transmembrane and kinase domain. The others are typical RLKs. Structure prediction was carried out with LRR-prediction tool LRRfinder (http://www.lrrfinder.com/result.php), with transmembrane domain prediction tool PSORT (http://psort.hgc.jp/form.html) and with NCBI conserved domain prediction (http://www.ncbi.nlm.nih.gov/Structure/cdd/wrpsb.cgi). Used protein sequences were obtained from Genbank: HvLRR-P (acc # BAJ91771), HvSERK a (BAK03316), AtSERK3/AtBAK1 (AEC06260), ZmPAN1 (ACI95776), LeLRR-P/LeSHY(AAR27431).

To clarify the question whether the function of LRR-P in susceptibility to *Bgh* is dependent on *RACB*, further transient transformation assays of barley leaves were performed. With these assays, the effect of different *RACB* variants (*CA RACB, DN RACB, RACB RNAi*) together with the *LRR-P OE* and the *LRR-P RNAi* construct (Fig. 18, Fig. S2) was analysed in regard to *Bgh*-challenge. Single *LRR-P OE* enhanced susceptibility by 35 % as well as *LRR-P-OE-GFP* by 44 % and vice versa *LRR-P RNAi* reduced susceptibility by -33 %. RACB in its constitutively activated version induced susceptibility by 32 % and reduced susceptibility when down-knocked by RNAi by 43 % or showed no change in susceptibility when the dominant-negative version was used (Fig. S2). These results were in line with already obtained data from Schultheiss *et al.* (2003) and Hoefle *et al.* (2011). The strong expression of *LRR-P* in *CA RACB* barley

line (Fig. 16) and *vice versa* less basal expression in *RACB RNAi* line also indicated a possible function of LRR-P as susceptibility factor. To test genetic interaction between *LRR-P* and *RACB*, *LRR-P RNAi* was co-expressed with *CA RACB* resulting in a 30 % enhanced susceptibility. Vice versa co-expression of *LRR-P-OE* and *RACB RNAi* reduced susceptibility by 47 %. This strongly indicated that *LRR-P* is dependent on *RACB*. Though *LRR-P-OE* itself led to enhanced susceptibility by 35 %, *RACB RNAi* reduced this effect. This showed that *LRR-P-OE* is supposed to act upstream of *RACB*. If *LRR-P* would act downstream of *RACB*, susceptibility induced by *LRR-P-OE* would have been not negatively affected by *RACB RNAi* co-expression. These data suggested that *LRR-P* might be a part of a receptor complex with intracellular *RACB* as exemplary described for the rice OsCEBIP with OsRAC1 (Akamatsu *et al.*, 2013) or the tomato LeShy with LePRK1/2 (Huang *et al.*, 2014). Potential barley GEF(s) and RLK(s) are unknown but have to be postulated for a functional module as suggested for other species (Kim *et al.*, 2012) and summarized in Table 8.

Localization studies of LRR-P-GFP in transiently transformed barley cells were difficult. LRR-P-GFP signal was very low even after 24 hpi and decreased up to 48 hpi, which could be due to the fact that it is weakly expressed when compared to free GFP. Further, LRR-P-GFP is largely sectreted and little visible in the apolast, because GFP is pH-sensitive. LRR-P localized diffusely to the cytoplasm, slightly to the membrane (Fig. 19), to ER-like and vesicular structures when co-expressed with *CA RACB* (Fig. 20 C, D) and surrounded the penetration site of *Bgh* (Fig. 19, Fig. 20). This might indicate that possibly LRR-P was imaged at different stages of the secretory pathway. When integrated into the plasma membrane or secreted, LRR-P could function as a co-receptor or ligand of an unknown RLK during barley-powdery mildew interaction as shown for LRR-RLPs of other systems. Some RLPs have a transmembrane domain and can physically interact with related RLKs as e.g. TMM of arabidopsis with the ERECTA RLK triggering stomatal patterning (Nadeau and Sack, 2002). Others such as the arabidopsis CLAVATA3 is a predicted secreted protein is the ligand binding to the CLAVATA1 RLK. This receptor complex is essential for cell proliferation and meristematic development in shoots of arabidopsis (Jeong *et al.*, 1999; Trotochaud *et al.*, 1999; Trotochaud *et al.*, 2000). Furthermore it cannot be excluded that LRR-P has a function in pathogen-unchallenged situations. However, this cannot be concluded from the data of this study. Another point is, that LRR-P is a small protein of only 224 aa which is nearly of the same size as the used GFP tag (240 aa). It could be that the GFP-LRR fusion protein alters the structural formation for other foldings and hinders proper localization of LRR-P. However – as mentioned -, LRR-P-GFP was functional in enhancing susceptibility when over-expressed (Fig. 18) suggesting at least partial functionality of the fusion protein.

11.4.2 S-RLK and LRR-RLK, possible new susceptibility factors.

Beside the characterized LRR-P, two other RLKs, a LRR-RLK and an S-domain RLK, turned out to have possible roles in susceptibility to *Bgh*. Transient assays showed a significant reduced susceptibility of barley to *Bgh* with transient silencing of each of the two genes (Fig. 18). Recently it was shown that a receptor-like kinase containing a S-domain of *A. thaliana* recognizes lipopolysaccharides from gram-negative bacteria (Ranf *et al.*, 2015). Involvement in abiotic stress responses was shown for a S-domain

RLK of rice where overexpression of this kinase improved yield components (Zou *et al.*, 2015). S-domain containing RLKs are typically involved in self-incompatibility of *Brassicaceae* (Singh and Zimmerli, 2013). Up to now, little information is available on S-domain containing RLKs in terms of pathogen infection. The other RLK is similar to the rice gene XA21 coding for a immunity-related LRR-RLK (Song *et al.*, 1995). Thus it seems plausible that the barley LRR-RLK idenfied here also functions in pathogen interaction. Eventually this LRR-RLK is also part of a receptor complex containing LRR-P and RACB. Little is known about receptor complexes in barley. Characterized RLKs from *A. thaliana*, *O. sativa* or *Z. mays,* which can be linked to RAC/ROP proteins (Table 6), have close homologs in barley. This promotes the idea that functions of those are shared over several species and provides a promising field of research where much can be learned from species such as *A. thaliana* or *O. sativa*.

Table 6: Known receptor-ligand complexes with RAC/ROP association in plants.

receptor	Ligand/co-receptor	GEF	ROP	function	literature
AtCLAVATA1 (LRR)	AtCLAVATA2 (LRR)		AtROP	Meristem development	(Trotochaud *et al.*, 1999)
OsCERK1 (LysM)	OsCEBIP (LysM)	OsRACGEF1	OsRAC1	Immunity	(Kawano and Shimamoto, 2013)
ZmPAN2 (LRR)	ZmPAN1 (LRR)		ZmROP2/9	Cell polarity, stomata development	(Humphries *et al.*, 2011)
LePRK1/2 (LRR)	Shy/STIG (LRR)	ROPGEF12/kinase partner protein (KPP)	LeROP	Pollen tube growth	(Guyon *et al.*, 2004; Huang *et al.*, 2014; Kaothien *et al.*, 2005; Zhang and McCormick, 2007)
AtFERONIA (Malectin-like)	RALF1	AtROPGEF4 AtROPGEF6	AtROP2 AtROP11	Regulation of plant growth	(Duan *et al.*, 2010; Haruta *et al.*, 2014; Huang *et al.*, 2013; Li *et al.*, 2012)
TMK1 (LRR)	AtABP1		AtROP2/AtROP4	Polar auxin transport	(Xu *et al.*, 2014; Xu *et al.*, 2010)

11.4.3 Conclusion III.

TIGS analysis of six candidate genes selected from microarray data that were "*RACB-*" and "*Bgh*-regulated" resulted in identification of three promising new susceptibility factors:

- LRR-P, a LRR-containing protein with ≤ five LRR domains, which is structurally similar to SERKs from different plant species,
- S-RLK, an S-domain carrying RLK, and
- LRR-RLK, an LRR-containing receptor kinase with similarities to OsXA21

This work further characterized HvLRR-P as a potential susceptibility factor, which is *RACB*- and *Bgh*-regulated on a gene expression level with differential expression in the *RACB* transgenic lines. Functionally, it induces susceptibility when transiently over-expressed and resistance when transiently knocked-down. Besides that, I suggest that LRR-P might act in a receptor complex together with RACB as it cannot induce susceptibility any more when *RACB* is knocked-down. It is unlikely that RACB and LRR-P interact physically, but LRR-P could act as ligand or co-receptor and RACB as a downstream signalling switch of an unknown receptor. This receptor could mediate a signal via ROPGEFs activating RACB (Fig. 23). Activated GTP-bound RACB might again support expression of the receptor complex in a feed-forward loop to stabilise its own function during infection. This could suggest that the RLK itself needs RACB for recognition of the pathogen. However, it is unknown at which point *Bgh* might interact with such a signalling module. Unpublished data of Mathias Nottensteiner (TU München) suggest that the fungus directly addresses RACB by the means of an effector protein. In that sense feed-forward regulation could provide stability of response kinetics. The identified LRR-RLK with homology to OsXA21 RLK could be the potential “unknown” receptor kinase controlling RACB. Together, microarray data produced and analysed in this work identified a hypothetical signalling module (Fig. 23) under control of *RACB* supporting susceptibility against the powdery mildew fungus *Bgh*.

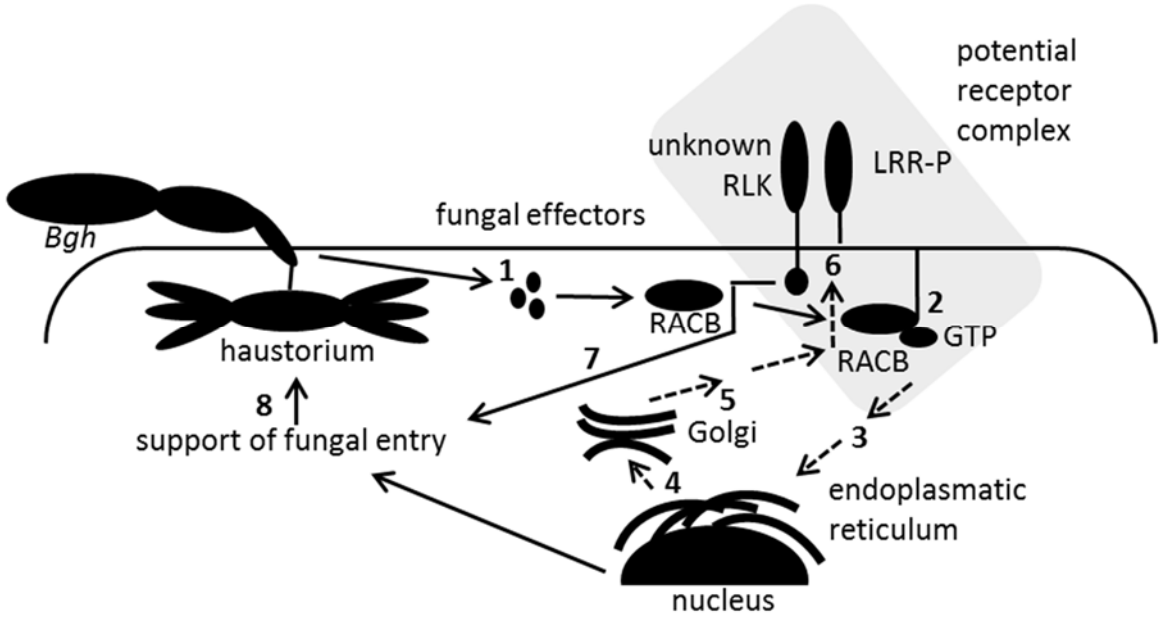

Fig. 23: Possible feed-forward regulation of RLKs mediated by *RACB* in the barley powdery mildew interaction. 1 *Bgh* delivers effectors to activate the inactive GDP-bound form of *RACB* directly. In its active GTP-bound form *RACB* is anchored to the membrane (2). Via several unknown factors (3) signalling components get addressed. After transcription of these components within the nucleus, mRNA is transported out of the nucleus into the cytoplasm where protein synthesis occurs either at free ribosomes or for secreted and plasma membrane-specific proteins at ribosomes bound to the ER (4). Transport of the synthesized proteins in the secretory pathway occurs via the Golgi apparatus (5). Membrane-specific proteins such as RLKs arrive at the membrane and in that situation LRR-P can act as a ligand or cofactor of an unknown RLK. LRR-P could indirectly interact with RACB in a receptor complex or the receptor complex could activate RACB. This RACB signalling module supports fungal entry (7) and hence leads to susceptibility (8).

11.5 OUTLOOK

RLKs have a huge impact on immunity: some RLKs were shown to act upstream of RAC/ROP GTPases such as for example the malectin-like domain containing RLK FERONIA of arabidopsis (Duan *et al.*, 2010) or the LysM domain containing RLK CERK1 of rice (Akamatsu *et al.*, 2013). The high amount of RLKs found in this study suggests that barley bears a set of RLKs potentially involved in susceptibility and/or resistance. It is possible that *RACB* can interact directly with RLK as shown for the corn RLK PAN1 (Humphries *et al.*, 2011) or alternatively is indirectly activated in a receptor complex. As follow-up experiments from this study, the other potential SF S-RLK and LRR-RLK should be analysed. Subcellular co-localisation with RACB and RACB-immuno-precipitation experiments might show protein interaction or identify other RLKs and further interacting partners in a potential RACB-signalling complex. Pathway analysis of differential regulated genes suggests further possibly important factors in the powdery mildew interaction; other RLKs, transcription factors but also components of the vesicle transport could have essential roles. The results of this study indicate a *RACB*-modulated regulatory network during the powdery mildew interaction with barley. As questioned at the beginning of the work, a role of RACB in regulating basal immunity processes was not supported. However, future studies will be necessary to address how basal immunity is regulated in barley. Different from studies of OsRAC1 in rice (Akamatsu *et al.*, 2013) the early plant immune response is not modulated by the RAC/ROP GTPase RACB in barley. Thus, RACB might influence other factors which are not directly connected to immunity. RACB apparently functions mainly via cell polarity-affecting mechanisms rather than immunity-regulating functions (Hoefle *et al.*, 2011; Scheler *et al.*, 2016) In maize, ROPs are needed for positioning the nucleus of the stomata subsidiary mother cell next to the guard mother cell for assymetric cell division (Humphries *et al.*, 2011). The asymmetric cell division of the subsidiary mother cell is triggered via ROP2 and ROP9, resulting in abnormal cell phenotypes when they are knocked-out (Facette and Smith, 2012). Both maize RAC/ROP proteins are homologs of RACB, and in the barley *RACB RNAi* lines used in this study, a corresponding phenotype was observed (Scheler *et al.,* 2016). In terms of interaction with *Bgh,* the fungus seems to profit from polarity during host cell re-programming. Polar events concerning the secretory pathway are needed for penetration resistance but also for susceptibility, in that they lead to the formation of an extrahaustorial membrane (Doermann *et al.*, 2014). Moreover, nucleus movement is discussed to be essential for many processes such as root hair formation, pollen tube growth and in biotic and abiotic stress situations (Griffis *et al.*, 2014) (Scheler *et al*.,2016). Thus, cell polarity including nucleus movement might be a module important for the regulation of resistance. However, the underlying molecular mechanisms have to be elucidated in detail. Studies addressing further signalling components regulating RAC/ROP GTPases up-stream and down-stream are necessary. ROP-GEFs and upstream RLK might have a huge impact in that process as already shown for the Malectin-RLK FERONIA in arabidopsis (Duan *et al.*, 2010) or the OsRAC1GEF in rice (Akamatsu *et al.*, 2013; Kawano *et al.*, 2014). Hence, experiments pointing to interaction between RACB, GEFs and RLKs could help identifying the entire receptor complex. For a possible exploitation of results in plant breeding it has to be kept in mind, that corresponding components of such a complex might have divergent roles in plant immunity and development.

12. REFERENCES

Abass M, Morris PC. 2013. The Hordeum vulgare signalling protein MAP kinase 4 is a regulator of biotic and abiotic stress responses. J Plant Physiol **170**, 1353-1359.

Acevedo-Garcia J, Kusch S, Panstruga R. 2014. Magical mystery tour: MLO proteins in plant immunity and beyond. New Phytologist **204**, 273-281.

Akamatsu A, Wong HL, Fujiwara M, Okuda J, Nishide K, Uno K, Imai K, Umemura K, Kawasaki T, Kawano Y, Shimamoto K. 2013. An OsCEBiP/OsCERK1-OsRacGEF1-OsRac1 module is an essential early component of chitin-induced rice immunity. Cell Host & Microbe **13**, 465-476.

Albrecht C, Russinova E, Kemmerling B, Kwaaitaal M, de Vries SC. 2008. Arabidopsis SOMATIC EMBRYOGENESIS RECEPTOR KINASE proteins serve brassinosteroid-dependent and -independent signaling pathways. Plant Physiol **148**, 611-619.

Ali SS, Kumar GB, Khan M, Doohan FM. 2013. Brassinosteroid enhances resistance to fusarium diseases of barley. Phytopathology **103**, 1260-1267.

An Q, Huckelhoven R, Kogel KH, van Bel AJ. 2006. Multivesicular bodies participate in a cell wall-associated defence response in barley leaves attacked by the pathogenic powdery mildew fungus. Cell Microbiology **8**, 1009-1019.

Andreasson E, Jenkins T, Brodersen P, Thorgrimsen S, Petersen NH, Zhu S, Qiu JL, Micheelsen P, Rocher A, Petersen M, Newman MA, Bjorn Nielsen H, Hirt H, Somssich I, Mattsson O, Mundy J. 2005. The MAP kinase substrate MKS1 is a regulator of plant defense responses. The EMBO Journal **24**, 2579-2589.

Arthur KM, Vejlupkova Z, Meeley RB, Fowler JE. 2003. Maize ROP2 GTPase provides a competitive advantage to the male gametophyte. Genetics **165**, 2137-2151.

Asai T, Tena G, Plotnikova J, Willmann MR, Chiu WL, Gomez-Gomez L, Boller T, Ausubel FM, Sheen J. 2002. MAP kinase signalling cascade in *Arabidopsis* innate immunity. Nature **415**, 977-983.

Ballare CL. 2011. Jasmonate-induced defenses: a tale of intelligence, collaborators and rascals. Trends Plant Sci **16**, 249-257.

Beckers GJ, Jaskiewicz M, Liu Y, Underwood WR, He SY, Zhang S, Conrath U. 2009. Mitogen-activated protein kinases 3 and 6 are required for full priming of stress responses in Arabidopsis thaliana. Plant Cell **21**, 944-953.

Bellin D, Asai S, Delledonne M, Yoshioka H. 2013. Nitric oxide as a mediator for defense responses. Molecular Plant-Microbe Interactions Journal **26**, 271-277.

Benjamini Y, Hochberg Y. 1995. Controlling the false discovery rate: a practical and powerful approach to multiple testing. Journal of the Royal Statistical Society **57**, 289-300.

Berken A. 2006. ROPs in the spotlight of plant signal transduction. Cellular and Molecular Life Sciences **63**, 2446-2459.

Bethke G, Pecher P, Eschen-Lippold L, Tsuda K, Katagiri F, Glazebrook J, Scheel D, Lee J. 2012. Activation of the *Arabidopsis thaliana* mitogen-activated protein kinase MPK11 by the flagellin-derived elicitor peptide, flg22. Molecular Plant-Microbe Interactions Journal **25**, 471-480.

Bethke G, Unthan T, Uhrig JF, Poschl Y, Gust AA, Scheel D, Lee J. 2009. Flg22 regulates the release of an ethylene response factor substrate from MAP kinase 6 in *Arabidopsis thaliana* via ethylene signaling. Proceedings of the National Academy of Sciences **106**, 8067-8072.

Bigeard J, Colcombet J, Hirt H. 2015. Signaling mechanisms in pattern-triggered immunity (PTI). Mol Plant **8**, 521-539.

Bischof M, Eichmann R, Hueckelhoven R. 2011. Pathogenesis-associated transcriptional patterns in *Triticeae*. J Plant Physiol **168**, 9-19.

Bodai L, Marsh JL. 2012. A novel target for Huntington's disease: ERK at the crossroads of signaling. The ERK signaling pathway is implicated in Huntington's disease and its upregulation ameliorates pathology. Bioessays **34**, 142-148.

Bokoch GM, Diebold BA. 2002. Current molecular models for NADPH oxidase regulation by Rac GTPase. Blood **100**, 2692-2696.

Boller T, Felix G. 2009. A renaissance of elicitors: perception of microbe-associated molecular patterns and danger signals by pattern-recognition receptors. Annual Review of Plant Biology **60**, 379-406.
Boller T, He SY. 2009. Innate immunity in plants: an arms race between pattern recognition receptors in plants and effectors in microbial pathogens. Science **324**, 742-744.
Bracha-Drori K, Shichrur K, Lubetzky TC, Yalovsky S. 2008. Functional analysis of arabidopsis postprenylation CaaX processing enzymes and their function in subcellular protein targeting. Plant Physiol **148**, 119-131.
Bradford MM. 1976. A rapid and sensitive method for the quantitation of microgram quantities of protein utilizing the principle of protein-dye binding. Analytical Biochemistry **72**, 248-254.
Bruggmann R, Abderhalden O, Reymond P, Dudler R. 2005. Analysis of epidermis- and mesophyll-specific transcript accumulation in powdery mildew-inoculated wheat leaves. Plant Molecular Biology Reporter **58**, 247-267.
Bueschges R, Hollricher K, Panstruga R, Simons G, Wolter M, Frijters A, van Daelen R, van der Lee T, Diergaarde P, Groenendijk J, Topsch S, Vos P, Salamini F, Schulze-Lefert P. 1997. The barley Mlo gene: a novel control element of plant pathogen resistance. Cell **88**, 695-705.
Caldelari D, Sternberg H, Rodriguez-Concepcion M, Gruissem W, Yalovsky S. 2001. Efficient prenylation by a plant geranylgeranyltransferase-I requires a functional CaaL box motif and a proximal polybasic domain. Plant Physiol **126**, 1416-1429.
Caldo RA, Nettleton D, Wise RP. 2004. Interaction-dependent gene expression in *Mla*-specified response to barley powdery mildew. Plant Cell **16**, 2514-2528.
Cartwright HN, Humphries JA, Smith LG. 2009. PAN1: a receptor-like protein that promotes polarization of an asymmetric cell division in maize. Science **323**, 649-651.
Cernadas RA, Doyle EL, Nino-Liu DO, Wilkins KE, Bancroft T, Wang L, Schmidt CL, Caldo R, Yang B, White FF, Nettleton D, Wise RP, Bogdanove AJ. 2014. Code-assisted discovery of TAL effector targets in bacterial leaf streak of rice reveals contrast with bacterial blight and a novel susceptibility gene. PLoS Pathog **10**, e1003972.
Chaparro-Garcia A, Wilkinson RC, Gimenez-Ibanez S, Findlay K, Coffey MD, Zipfel C, Rathjen JP, Kamoun S, Schornack S. 2011. The receptor-like kinase SERK3/BAK1 is required for basal resistance against the late blight pathogen *phytophthora infestans* in *Nicotiana benthamiana*. PLoS One **6**, e16608.
Chen H, Lai Z, Shi J, Xiao Y, Chen Z, Xu X. 2010a. Roles of arabidopsis WRKY18, WRKY40 and WRKY60 transcription factors in plant responses to abscisic acid and abiotic stress. BMC Plant Biology **10**, 1-15.
Chen L, Shiotani K, Togashi T, Miki D, Aoyama M, Wong HL, Kawasaki T, Shimamoto K. 2010b. Analysis of the RAC/ROP small GTPase family in rice: expression, subcellular localization and role in disease resistance. Plant and Cell Physiology **51**, 585-595.
Chen LY, Wuriyanghan H, Zhang YQ, Duan KX, Chen HW, Li QT, Lu X, He SJ, Ma B, Zhang WK, Lin Q, Chen SY, Zhang JS. 2013. An S-domain receptor-like kinase, OsSIK2, confers abiotic stress tolerance and delays dark-induced leaf senescence in rice. Plant Physiol **163**, 1752-1765.
Chen X, Hedley PE, Morris J, Liu H, Niks RE, Waugh R. 2011. Combining genetical genomics and bulked segregant analysis-based differential expression: an approach to gene localization. Theoretical and Applied Genetics **122**, 1375-1383.
Chen X, Naramoto S, Robert S, Tejos R, Lofke C, Lin D, Yang Z, Friml J. 2012. ABP1 and ROP6 GTPase signaling regulate clathrin-mediated endocytosis in arabidopsis roots. Current Biology **22**, 1326-1332.
Chen X, Zuo S, Schwessinger B, Chern M, Canlas PE, Ruan D, Zhou X, Wang J, Daudi A, Petzold CJ, Heazlewood JL, Ronald PC. 2014. An XA21-associated kinase (OsSERK2) regulates immunity mediated by the XA21 and XA3 immune receptors. Mol Plant **7**, 874-892.
Chi Y, Yang Y, Zhou Y, Zhou J, Fan B, Yu JQ, Chen Z. 2013. Protein-protein interactions in the regulation of WRKY transcription factors. Mol Plant **6**, 287-300.
Chinchilla D, Zipfel C, Robatzek S, Kemmerling B, Nurnberger T, Jones JD, Felix G, Boller T. 2007. A flagellin-induced complex of the receptor FLS2 and BAK1 initiates plant defence. Nature **448**, 497-500.

Chisholm ST, Coaker G, Day B, Staskawicz BJ. 2006. Host-microbe interactions: shaping the evolution of the plant immune response. Cell **124**, 803-814.
Chomczynski P, Sacchi N. 1987. Single-step method of RNA isolation by acid guanidinium thiocyanate-phenol-chloroform extraction. Analytical Biochemistry **162**, 156-159.
Christensen TM, Vejlupkova Z, Sharma YK, Arthur KM, Spatafora JW, Albright CA, Meeley RB, Duvick JP, Quatrano RS, Fowler JE. 2003. Conserved subgroups and developmental regulation in the monocot rop gene family. Plant Physiol **133**, 1791-1808.
Christiansen MW, Gregersen PL. 2014. Members of the barley NAC transcription factor gene family show differential co-regulation with senescence-associated genes during senescence of flag leaves. Journal of Experimental Botany **65**, 4009-4022.
Chujo T, Miyamoto K, Shimogawa T, Shimizu T, Otake Y, Yokotani N, Nishizawa Y, Shibuya N, Nojiri H, Yamane H, Minami E, Okada K. 2013. OsWRKY28, a PAMP-responsive transrepressor, negatively regulates innate immune responses in rice against rice blast fungus. Plant Mol Biol **82**, 23-37.
Clark SE, Williams RW, Meyerowitz EM. 1997. The CLAVATA1 gene encodes a putative receptor kinase that controls shoot and floral meristem size in Arabidopsis. Cell **89**, g575-585.
Craddock C, Lavagi I, Yang Z. 2012. New insights into Rho signaling from plant ROP/Rac GTPases. Trends in Cell Biology **22**, 492-501.
Dai X, Wang Y, Zhang WH. 2015. OsWRKY74, a WRKY transcription factor, modulates tolerance to phosphate starvation in rice. J Exp Bot, 1-14.
de Jonge R, van Esse HP, Maruthachalam K, Bolton MD, Santhanam P, Saber MK, Zhang Z, Usami T, Lievens B, Subbarao KV, Thomma BP. 2012. Tomato immune receptor Ve1 recognizes effector of multiple fungal pathogens uncovered by genome and RNA sequencing. Proceedings of the National Academy of Sciences **109**, 5110-5115.
de Silva K, Laska B, Brown C, Sederoff HW, Khodakovskaya M. 2011. *Arabidopsis thaliana* calcium-dependent lipid-binding protein (AtCLB): a novel repressor of abiotic stress response. Journal of Experimental Botany **62**, 2679-2689.
Delteil A, Gobbato E, Cayrol B, Estevan J, Michel-Romiti C, Dievart A, Kroj T, Morel J-B. 2016. Several wall-associated kinases participate positively and negatively in basal defense against rice blast fungus. BMC Plant Biology **16**, 1-10.
Dey S, Wenig M, Langen G, Sharma S, Kugler KG, Knappe C, Hause B, Bichlmeier M, Babaeizad V, Imani J, Janzik I, Stempfl T, Hueckelhoven R, Kogel KH, Mayer KF, Vlot AC. 2014. Bacteria-triggered systemic immunity in barley is associated with WRKY and ETHYLENE RESPONSIVE FACTORs but not with salicylic acid. Plant Physiol **166**, 2133-2151.
Dievart A, Clark SE. 2004. LRR-containing receptors regulating plant development and defense. Development **131**, 251-261.
Dobon A, Canet JV, Garcia-Andrade J, Angulo C, Neumetzler L, Persson S, Vera P. 2015. Novel disease susceptibility factors for fungal necrotrophic pathogens in Arabidopsis. PLoS Pathog **11**, 1-30.
Doczi R, Brader G, Pettko-Szandtner A, Rajh I, Djamei A, Pitzschke A, Teige M, Hirt H. 2007. The Arabidopsis mitogen-activated protein kinase kinase MKK3 is upstream of group C mitogen-activated protein kinases and participates in pathogen signaling. Plant Cell **19**, 3266-3279.
Doermann P, Kim H, Ott T, Schulze-Lefert P, Trujillo M, Wewer V, Hueckelhoven R. 2014. Cell-autonomous defense, re-organization and trafficking of membranes in plant-microbe interactions. New Phytologist **204**, 815-822.
Dong W, Nowara D, Schweizer P. 2006. Protein polyubiquitination plays a role in basal host resistance of barley. Plant Cell **18**, 3321-3331.
Douchkov D, Luck S, Johrde A, Nowara D, Himmelbach A, Rajaraman J, Stein N, Sharma R, Kilian B, Schweizer P. 2014. Discovery of genes affecting resistance of barley to adapted and non-adapted powdery mildew fungi. Genome Biology **15**, 1-18.
Douchkov D, Nowara D, Zierold U, Schweizer P. 2005. A high-throughput gene-silencing system for the functional assessment of defense-related genes in barley epidermal cells. Molecular Plant-Microbe Interactions Journal **18**, 755-761.

Druka A, Muehlbauer G, Druka I, Caldo R, Baumann U, Rostoks N, Schreiber A, Wise R, Close T, Kleinhofs A, Graner A, Schulman A, Langridge P, Sato K, Hayes P, McNicol J, Marshall D, Waugh R. 2006. An atlas of gene expression from seed to seed through barley development. Functional and Integrative Genomics **6**, 202-211.
Duan Q, Kita D, Li C, Cheung AY, Wu HM. 2010. FERONIA receptor-like kinase regulates RHO GTPase signaling of root hair development. Proceedings of the National Academy of Sciences **107**, 17821-17826.
Eckey C, Korell M, Leib K, Biedenkopf D, Jansen C, Langen G, Kogel KH. 2004. Identification of powdery mildew-induced barley genes by cDNA-AFLP: functional assessment of an early expressed MAP kinase. Plant Mol Biol **55**, 1-15.
Efron B. 1979. Bootstrap methods: another look at the jackknife. The Annals of Statistics **7**, 1-26.
Eichmann R, Bischof M, Weis C, Shaw J, Lacomme C, Schweizer P, Duchkov D, Hensel G, Kumlehn J, Huckelhoven R. 2010. BAX INHIBITOR-1 is required for full susceptibility of barley to powdery mildew. Molecular Plant Microbe Interactions Journal **23**, 1217-1227.
Eichmann R, Hueckelhoven R. 2008. Accommodation of powdery mildew fungi in intact plant cells. J Plant Physiol **165**, 5-18.
Engler C, Kandzia R, Marillonnet S. 2008. A one pot, one step, precision cloning method with high throughput capability. PLoS One **3**, e3647.
Eulgem T, Somssich IE. 2007. Networks of WRKY transcription factors in defense signaling. Curr Opin Plant Biol **10**, 366-371.
Facette MR, Park Y, Sutimantanapi D, Luo A, Cartwright DW, Yang B, Bennett EJ, Sylvester AW, Smith LG. 2015. The SCAR/WAVE complex polarizes PAN receptors and promotes division asymmetry in maize. nature plants **1**, 1-15.
Facette MR, Smith LG. 2012. Division polarity in developing stomata. Curr Opin Plant Biol **15**, 585-592.
Feher A, Lajko DB. 2015. Signals fly when kinases meet RHO-OF-PLANTS (ROP) small G-proteins. Plant Science.
Felix G, Duran JD, Volko S, Boller T. 1999. Plants have a sensitive perception system for the most conserved domain of bacterial flagellin. Plant Journal **18**, 265-276.
Ferrell JE, Jr., Bhatt RR. 1997. Mechanistic studies of the dual phosphorylation of mitogen-activated protein kinase. Journal of Biological Chemistry **272**, 19008-19016.
Fontes EP, Santos AA, Luz DF, Waclawovsky AJ, Chory J. 2004. The geminivirus nuclear shuttle protein is a virulence factor that suppresses transmembrane receptor kinase activity. Genes Dev **18**, 2545-2556.
Fradin EF, Zhang Z, Juarez Ayala JC, Castroverde CD, Nazar RN, Robb J, Liu CM, Thomma BP. 2009. Genetic dissection of *Verticillium* wilt resistance mediated by tomato Ve1. Plant Physiol **150**, 320-332.
Francis SA, Dewey FM, Gurr SJ. 1996. The role of cutinase in germline development and infection by *Erysiphe graminis* f. sp. *hordei*. Physiological and Molecular Plant Pathology **49**, 201-211.
Galletti R, Ferrari S, De Lorenzo G. 2011. *Arabidopsis* MPK3 and MPK6 play different roles in basal and oligogalacturonide- or flagellin-induced resistance against *Botrytis cinerea*. Plant Physiol **157**, 804-814.
Gao QM, Venugopal S, Navarre D, Kachroo A. 2011. Low oleic acid-derived repression of jasmonic acid-inducible defense responses requires the WRKY50 and WRKY51 proteins. Plant Physiol **155**, 464-476.
Gil F, Gay JL. 1977. Ultrastructural and physiological properties of the host interfacial components of the haustoria of *Erysiphe pisi in vivo* and *in vitro*. Physiological Plant Pathology **10**, 1-12.
Gish LA, Clark SE. 2011. The RLK/Pelle family of kinases. The Plant Journal **66**, 117-127.
Glawe DA. 2008. The powdery mildews: a review of the world's most familiar (yet poorly known) plant pathogens. Annu Rev Phytopathol **46**, 27-51.
Goehre V, Jones AM, Sklenar J, Robatzek S, Weber AP. 2012. Molecular crosstalk between PAMP-triggered immunity and photosynthesis. Molecular Plant-Microbe Interactions Journal **25**, 1083-1092.

Gomez-Gomez L, Boller T. 2000. FLS2: an LRR receptor-like kinase involved in the perception of the bacterial elicitor flagellin in *Arabidopsis*. Molecular Cell **5**, 1003-1011.
Goujon M, McWilliam H, Li W, Valentin F, Squizzato S, Paern J, Lopez R. 2010. A new bioinformatics analysis tools framework at EMBL-EBI. Nucleic Acids Res **38**, W695-699.
Green JR, Carver TL, Gurr SJ. 2002. The formation and function of infection and feeding structures. In: Bélanger RR, Bushnell WR, Dik AJ, Carver TL, eds. *The powdery mildews: A comprehensive treatise.* St. Paul, Minnesota, 66-82.
Griffis AH, Groves NR, Zhou X, Meier I. 2014. Nuclei in motion: movement and positioning of plant nuclei in development, signaling, symbiosis, and disease. Frontiers in Plant Science **5**, 129.
Gu Y, Wang Z, Yang Z. 2004. ROP/RAC GTPase: an old new master regulator for plant signaling. Curr Opin Plant Biol **7**, 527-536.
Gudesblat GE, Iusem ND, Morris PC. 2007. Guard cell-specific inhibition of Arabidopsis MPK3 expression causes abnormal stomatal responses to abscisic acid and hydrogen peroxide. New Phytologist **173**, 713-721.
Gui CP, Dong X, Liu HK, Huang WJ, Zhang D, Wang SJ, Barberini ML, Gao XY, Muschietti J, McCormick S, Tang WH. 2014. Overexpression of the tomato pollen receptor kinase LePRK1 rewires pollen tube growth to a blebbing mode. Plant Cell **26**, 3538-3555.
Guo H, Li L, Ye H, Yu X, Algreen A, Yin Y. 2009. Three related receptor-like kinases are required for optimal cell elongation in *Arabidopsis thaliana*. Proceedings of the National Academy of Sciences **106**, 7648-7653.
Guyon V, Tang WH, Monti MM, Raiola A, De Lorenzo G, McCormick S, Taylor LP. 2004. Antisense phenotypes reveal a role for SHY, a pollen-specific leucine-rich repeat protein, in pollen tube growth. The Plant Journal **39**, 643-654.
Guyon VN, Astwood JD, Garner EC, Dunker AK, Taylor LP. 2000. Isolation and characterization of cDNAs expressed in the early stages of flavonol-induced pollen germination in petunia. Plant Physiol **123**, 699-710.
Hafez YM, Mourad RY, Mansour M, Abdelaal KAA. 2014. Impact of non-traditional compounds and fungicides on physiological and biochemical characters of barley infected with *Blumeria graminis* f. sp. *hordei* under field conditions. Egyptian Journal of Biological Pest Control **24**, 445-453.
Hansen M, Friis C, Bowra S, Holm PB, Vincze E. 2009. A pathway-specific microarray analysis highlights the complex and co-ordinated transcriptional networks of the developing grain of field-grown barley. J Exp Bot **60**, 153-167.
Haruta M, Sabat G, Stecker K, Minkoff BB, Sussman MR. 2014. A peptide hormone and its receptor protein kinase regulate plant cell expansion. Science **343**, 408-411.
Hause B, Demus U, Teichmann C, Parthier B, Wasternack C. 1996. Developmental and tissue-specific expression of JIP-23, a jasmonate-inducible protein of barley. Plant Cell Physiology **37**, 641-649.
Hause B, Maier W, Miersch O, Kramell R, Strack D. 2002. Induction of jasmonate biosynthesis in arbuscular mycorrhizal barley roots. Plant Physiol **130**, 1213-1220.
He ZH, Fujiki M, Kohorn BD. 1996. A cell wall-associated, receptor-like protein kinase. The Journal of Biological Chemistry **271**, 19789-19793.
Hecht V, Vielle-Calzada JP, Hartog MV, Schmidt ED, Boutilier K, Grossniklaus U, de Vries SC. 2001. The *Arabidopsis* SOMATIC EMBRYOGENESIS RECEPTOR KINASE 1 gene is expressed in developing ovules and embryos and enhances embryogenic competence in culture. Plant Physiol **127**, 803-816.
Hewezi T, Baum TJ. 2013. Manipulation of plant cells by cyst and root-knot nematode effectors. Molecular Plant-Microbe Interactions Journal **26**, 9-16.
Higashi K, Ishiga Y, Inagaki Y, Toyoda K, Shiraishi T, Ichinose Y. 2008. Modulation of defense signal transduction by flagellin-induced WRKY41 transcription factor in *Arabidopsis thaliana*. Molecular Genetics and Genomics **279**, 303-312.
Hilbert M, Nostadt R, Zuccaro A. 2013. Exogenous auxin affects the oxidative burst in barley roots colonized by *Piriformospora indica*. Plant Signaling and Behaviour **8**, 1-5.

Hoefle C, Huesmann C, Schultheiss H, Bornke F, Hensel G, Kumlehn J, Hueckelhoven R. 2011. A barley ROP GTPase ACTIVATING PROTEIN associates with microtubules and regulates entry of the barley powdery mildew fungus into leaf epidermal cells. Plant Cell **23**, 2422-2439.
Hollmann J, Gregersen PL, Krupinska K. 2014. Identification of predominant genes involved in regulation and execution of senescence-associated nitrogen remobilization in flag leaves of field grown barley. J Exp Bot **65**, 3963-3973.
Hu H, Wang J, Shi C, Yuan C, Peng C, Yin J, Li W, He M, Wang J, Ma B, Wang Y, Li S, Chen X. 2015. A receptor like kinase gene with expressional responsiveness on *Xanthomonas oryzae pv. oryzae* is essential for Xa21-mediated disease resistance. Rice **8**, 1-9.
Huang GQ, Li E, Ge FR, Li S, Wang Q, Zhang CQ, Zhang Y. 2013. *Arabidopsis* RopGEF4 and RopGEF10 are important for FERONIA-mediated developmental but not environmental regulation of root hair growth. New Phytologist **200**, 1089-1101.
Huang WJ, Liu HK, McCormick S, Tang WH. 2014. Tomato pistil factor STIG1 promotes in vivo pollen tube growth by binding to phosphatidylinositol 3-phosphate and the extracellular domain of the pollen receptor kinase LePRK2. Plant Cell **26**, 2505-2523.
Hueckelhoven R. 2005. Powdery mildew susceptibility and biotrophic infection strategies. FEMS Microbiol Lett **245**, 9-17.
Hueckelhoven R. 2007. Cell wall-associated mechanisms of disease resistance and susceptibility. Annu Rev Phytopathol **45**, 101-127.
Hueckelhoven R, Dechert C, Kogel KH. 2003. Overexpression of barley BAX inhibitor 1 induces breakdown of mlo-mediated penetration resistance to Blumeria graminis. Proceedings of the National Academy of Sciences **100**, 5555-5560.
Hueckelhoven R, Eichmann R, Weis C, Hoefle C, Proels RK. 2013. Genetic loss of susceptibility: a costly route to disease resistance? Plant Pathology **62**, 56-62.
Hueckelhoven R, Fodor J, Preis C, Kogel KH. 1999. Hypersensitive cell death and papilla formation in barley attacked by the powdery mildew fungus are associated with hydrogen peroxide but not with salicylic acid accumulation. Plant Physiol **119**, 1251-1260.
Huesmann C, Reiner T, Hoefle C, Preuss J, Jurca ME, Domoki K, Feher A, Hueckelhoven R. 2012. Barley ROP binding kinase1 is involved in microtubule organization and in basal penetration resistance to the barley powdery mildew. fungus. Plant Physiol **159**, 311-320.
Humphries JA, Vejlupkova Z, Luo A, Meeley RB, Sylvester AW, Fowler JE, Smith LG. 2011. ROP GTPases act with the receptor-like protein PAN1 to polarize asymmetric cell division in maize. Plant Cell **23**, 2273-2284.
Ichimura K, Shinozaki K, Tena G, Sheen J, Henry Y, Champion A, Kreis M, Zhang S, Hirt H, Wilson C, Heberel-Bors E, Ellis BE, Morris PC, Innes RW, Ecker JR, Scheel D, Klessig DF, Machida Y, Mundy J, Ohashi Y, Walker JC. 2002. Mitogen-activated protein kinase cascades in plants: a new nomenclature. Trends Plant Sci **7**, 301-308.
Ishihama N, Yoshioka H. 2012. Post-translational regulation of WRKY transcription factors in plant immunity. Curr Opin Plant Biol **15**, 431-437.
Jambunathan N, McNellis TW. 2003. Regulation of *Arabidopsis* COPINE 1 gene expression in response to pathogens and abiotic stimuli. Plant Physiol **132**, 1370-1381.
Janda M, Matouskova J, Burketova L, Valentova O. 2014. Interconnection between actin cytoskeleton and plant defense signaling. Plant Signalling & Behaviour **9**, 1-4.
Jeong S, Trotochaud AE, Clark SE. 1999. The *Arabidopsis* CLAVATA2 gene encodes a receptor-like protein required for the stability of the CLAVATA1 receptor-like kinase. Plant Cell **11**, 1925-1934.
Jones JD, Dangl JL. 2006. The plant immune system. Nature **444**, 323-329.
Jones MA, Raymond MJ, Yang Z, Smirnoff N. 2007. NADPH oxidase-dependent reactive oxygen species formation required for root hair growth depends on ROP GTPase. J Exp Bot **58**, 1261-1270.
Jung YH, Agrawal GK, Rakwal R, Kim JA, Lee MO, Choi PG, Kim YJ, Kim MJ, Shibato J, Kim SH, Iwahashi H, Jwa NS. 2006. Functional characterization of OsRacB GTPase--a potentially negative regulator of basal disease resistance in rice. Plant Physiology and Biochemistry **44**, 68-77.

Kaku H, Nishizawa Y, Ishii-Minami N, Akimoto-Tomiyama C, Dohmae N, Takio K, Minami E, Shibuya N. 2006. Plant cells recognize chitin fragments for defense signaling through a plasma membrane receptor. Proceedings of the National Academy of Sciences **103**, 11086-11091.
Kaothien P, Ok SH, Shuai B, Wengier D, Cotter R, Kelley D, Kiriakopolos S, Muschietti J, McCormick S. 2005. Kinase partner protein interacts with the LePRK1 and LePRK2 receptor kinases and plays a role in polarized pollen tube growth. Plant Journal **42**, 492-503.
Kaur R, Singh K, Singh J. 2013. A root-specific wall-associated kinase gene, HvWAK1, regulates root growth and is highly divergent in barley and other cereals. Functional and Integrative Genomics **13**, 167-177.
Kawano Y, Kaneko-Kawano T, Shimamoto K. 2014. Rho family GTPase-dependent immunity in plants and animals. Frontiers in Plant Science **5**, 1-12.
Kawano Y, Shimamoto K. 2013. Early signaling network in rice PRR-mediated and R-mediated immunity. Curr Opin Plant Biol **16**, 496-504.
Kawasaki T, Henmi K, Ono E, Hatakeyama S, Iwano M, Satoh H, Shimamoto K. 1999. The small GTP-binding protein rac is a regulator of cell death in plants. Proceedings of the National Academy of Sciences **96**, 10922-10926.
Kawasaki T, Koita H, Nakatsubo T, Hasegawa K, Wakabayashi K, Takahashi H, Umemura K, Umezawa T, Shimamoto K. 2006. Cinnamoyl-CoA reductase, a key enzyme in lignin biosynthesis, is an effector of small GTPase Rac in defense signaling in rice. Proceedings of the National Academy of Sciences **103**, 230-235.
Kayes JM, Clark SE. 1998. CLAVATA2, a regulator of meristem and organ development in *Arabidopsis*. Development **125**, 3843-3851.
Kersey PJ, Allen JE, Christensen M, Davis P, Falin LJ, Grabmueller C, Hughes DS, Humphrey J, Kerhornou A, Khobova J, Langridge N, McDowall MD, Maheswari U, Maslen G, Nuhn M, Ong CK, Paulini M, Pedro H, Toneva I, Tuli MA, Walts B, Williams G, Wilson D, Youens-Clark K, Monaco MK, Stein J, Wei X, Ware D, Bolser DM, Howe KL, Kulesha E, Lawson D, Staines DM. 2014. Ensembl Genomes 2013: scaling up access to genome-wide data. Nucleic Acids Res **42**, D546-552.
Kessler SA, Lindner H, Jones DS, Grossniklaus U. 2015. Functional analysis of related CrRLK1L receptor-like kinases in pollen tube reception. EMBO Reports **16**, 107-115.
Kibbe WA. 2007. OligoCalc: an online oligonucleotide properties calculator. Nucleic Acids Res **35**, 43-46.
Kim EK, Choi EJ. 2010. Pathological roles of MAPK signaling pathways in human diseases. Biochimica et Biophysica Acta **1802**, 396-405.
Kim KC, Lai Z, Fan B, Chen Z. 2008. *Arabidopsis* WRKY38 and WRKY62 transcription factors interact with histone deacetylase 19 in basal defense. Plant Cell **20**, 2357-2371.
Kim S-H, Oikawa T, Kyozuka J, Wong HL, Umemura K, Kishi-Kaboshi M, Takahashi A, Kawano Y, Kawasaki T, Shimamoto K. 2012. The bHLH Rac Immunity1 (RAI1) is activated by OsRac1 via OsMAPK3 and OsMAPK6 in rice immunity. Plant and Cell Physiology **53**, 740-754.
Kinane J, Oliver RP. 2003. Evidence that the appressorial development in barley powdery mildew is controlled by MAP kinase activity in conjunction with the cAMP pathway. Fungal Genetics and Biology **39**, 94-102.
Kishi-Kaboshi M, Okada K, Kurimoto L, Murakami S, Umezawa T, Shibuya N, Yamane H, Miyao A, Takatsuji H, Takahashi A, Hirochika H. 2010. A rice fungal MAMP-responsive MAPK cascade regulates metabolic flow to antimicrobial metabolite synthesis. Plant Journal **63**, 599-612.
Kogel KH, Ortel B, Jarosch R, Atzorn R, Schiffer R, Wasternack C. 1995. Resistance in barley against the powdery mildew fungus (*Erysiphe graminis f.sp.hordei*) is not associated with enhanced levels of endogenous jasmonates. European Journal of Plant Pathology **101**, 319-332.
Kolade OO, Bamford VA, Ancillo Anton G, Jones JD, Vera P, Hemmings AM. 2006. In vitro characterization of the cysteine-rich capping domains in a plant leucine rich repeat protein. Biochimica et Biophysica Acta **1764**, 1043-1053.
Kruger NJ. 1994. The Bradford method for protein quantitation. Methods in Molecular Biology **32**, 9-15.

Kruijt M, MJ DEK, de Wit PJ. 2005. Receptor-like proteins involved in plant disease resistance. Mol Plant Pathol **6**, 85-97.
Kunoh H, Itoh T, Kohno M, Ishizaki H. 1979. Are primary germ tubes of conidia unique to *Erysiphe graminis*? Annals of the Phytopathological Society of Japan **45**, 675-682.
Kyriakis JM, Avruch J. 2012. Mammalian MAPK signal transduction pathways activated by stress and inflammation: a 10-year update. Physiological Reviews **92**, 689-737.
Laemmli UK. 1970. Cleavage of structural proteins during the assembly of the head of bacteriophage T4. Nature **227**, 680-685.
Lai Z, Vinod K, Zheng Z, Fan B, Chen Z. 2008. Roles of *Arabidopsis* WRKY3 and WRKY4 transcription factors in plant responses to pathogens. BMC Plant Biology **8**, 68.
Lannoo N, Van Damme EJ. 2014. Lectin domains at the frontiers of plant defense. Frontiers in Plant Science **5**, 1-16.
Lapin D, Van den Ackerveken G. 2013. Susceptibility to plant disease: more than a failure of host immunity. Trends in Plant Science **18**, 546-554.
Larkin MA, Blackshields G, Brown NP, Chenna R, McGettigan PA, McWilliam H, Valentin F, Wallace IM, Wilm A, Lopez R, Thompson JD, Gibson TJ, Higgins DG. 2007. Clustal W and Clustal X version 2.0. Bioinformatics **23**, 2947-2948.
Lavy M, Bracha-Drori K, Sternberg H, Yalovsky S. 2002. A cell-specific, prenylation-independent mechanism regulates targeting of type II RACs. Plant Cell **14**, 2431-2450.
Lavy M, Yalovsky S. 2006. Association of arabidopsis type-II ROPs with the plasma membrane requires a conserved C-terminal sequence motif and a proximal polybasic domain. Plant Journal **46**, 934-947.
Lee JS, Kuroha T, Hnilova M, Khatayevich D, Kanaoka MM, McAbee JM, Sarikaya M, Tamerler C, Torii KU. 2012. Direct interaction of ligand-receptor pairs specifying stomatal patterning. Genes & Develpment **26**, 126-136.
Li H, Zhou SY, Zhao WS, Su SC, Peng YL. 2009. A novel wall-associated receptor-like protein kinase gene, OsWAK1, plays important roles in rice blast disease resistance. Plant Mol Biol **69**, 337-346.
Li J, Chory J. 1997. A putative leucine-rich repeat receptor kinase involved in brassinosteroid signal transduction. Cell **90**, 929-938.
Li J, Wen J, Lease KA, Doke JT, Tax FE, Walker JC. 2002. BAK1, an Arabidopsis LRR receptor-like protein kinase, interacts with BRI1 and modulates brassinosteroid signaling. Cell **110**, sun213-222.
Li Z, Kang J, Sui N, Liu D. 2012. ROP11 GTPase is a negative regulator of multiple ABA responses in *Arabidopsis*. Journal of Integrative Plant Biology **54**, 169-179.
Lieberherr D, Thao NP, Nakashima A, Umemura K, Kawasaki T, Shimamoto K. 2005. A sphingolipid elicitor-inducible mitogen-activated protein kinase is regulated by the small GTPase OsRac1 and heterotrimeric G-protein in rice. Plant Physiol **138**, 1644-1652.
Liebrand TW, van den Berg GC, Zhang Z, Smit P, Cordewener JH, America AH, Sklenar J, Jones AM, Tameling WI, Robatzek S, Thomma BP, Joosten MH. 2013. Receptor-like kinase SOBIR1/EVR interacts with receptor-like proteins in plant immunity against fungal infection. Proceedings of the National Academy of Sciences **110**, 10010-10015.
Lindner H, Muller LM, Boisson-Dernier A, Grossniklaus U. 2012. CrRLK1L receptor-like kinases: not just another brick in the wall. Curr Opin Plant Biol **15**, 659-669.
Liu W LJ, Triplett L, Leach JE, Wang GL. 2014. Novel insights into rice innate immunity against bacterial and fungal pathogens. Annu Rev Phytopathol **52**, 213-241.
Livak KJ, Schmittgen TD. 2001. Analysis of relative gene expression data using real-time quantitative PCR and the 2(-Delta Delta C(T)) Method. Methods **25**, 402-408.
Lodha TD, Basak J. 2012. Plant-pathogen interactions: what microarray tells about it? Molecular Biotechnology **50**, 87-97.
Lopez-Bucio JS, Dubrovsky JG, Raya-Gonzalez J, Ugartechea-Chirino Y, Lopez-Bucio J, de Luna-Valdez LA, Ramos-Vega M, Leon P, Guevara-Garcia AA. 2014. *Arabidopsis thaliana* mitogen-activated protein kinase 6 is involved in seed formation and modulation of primary and lateral root development. J Exp Bot **65**, 169-183.

Lorang J, Kidarsa T, Bradford CS, Gilbert B, Curtis M, Tzeng SC, Maier CS, Wolpert TJ. 2012. Tricking the guard: exploiting plant defense for disease susceptibility. Science **338**, 659-662.
Lozano-Duran R, Bourdais G, He SY, Robatzek S. 2014. The bacterial effector HopM1 suppresses PAMP-triggered oxidative burst and stomatal immunity. New Phytologist **202**, 259-269.
Macho AP, Zipfel C. 2014. Plant PRRs and the activation of innate immune signaling. Molecular Cell **54**, 263-272.
Mare C, Mazzucotelli E, Crosatti C, Francia E, Stanca AM, Cattivelli L. 2004. Hv-WRKY38: a new transcription factor involved in cold- and drought-response in barley. Plant Mol Biol **55**, 399-416.
Mariano AC, Andrade MO, Santos AA, Carolino SM, Oliveira ML, Baracat-Pereira MC, Brommonshenkel SH, Fontes EP. 2004. Identification of a novel receptor-like protein kinase that interacts with a geminivirus nuclear shuttle protein. Virology **318**, 24-31.
Marinissen MJ, Chiariello M, Gutkind JS. 2001. Regulation of gene expression by the small GTPase Rho through the ERK6 (p38 gamma) MAP kinase pathway. Genes Dev **15**, 535-553.
Martin GB, Brommonschenkel SH, Chunwongse J, Frary A, Ganal MW, Spivey R, Wu T, Earle ED, Tanksley SD. 1993. Map-based cloning of a protein kinase gene conferring disease resistance in tomato. Science **262**, 1432-1436.
Mayer KFXM, M.; Hedley, P.E.; Simkova, H.; Liu, H.; Morris, J.A.;, Steuernagel, B.; Taudien, S.; Roessner, S.; Gundlach, H.; Kubalakova M.; Suchankova, P.; Murat, F.; Felder, M.; Nussbaumer, T.; Graner, A.; Salse, J.; Endo, T.; Sakai, H.; Tanaka, T.; Itoh, T.; Sato, K.; Platzer, M.; Matsumoto, T.; Scholz, U.; Dolez, J.; Waugh,R. and Stein, N. 2011. Unlocking the barley genome by chromosomal and comparative genomics. The Plant Cell **23**, 1249-1263.
Meng X, Zhang S. 2013. MAPK cascades in plant disease resistance signaling. Annual Review in Phytopathology **51**, 245-266.
Meng Y, Wise RP. 2012. HvWRKY10, HvWRKY19, and HvWRKY28 regulate Mla-triggered immunity and basal defense to barley powdery mildew. Molecular Plant-Microbe Interactions Journal **25**, 1492-1505.
Miki D, Itoh R, Shimamoto K. 2005. RNA silencing of single and multiple members in a gene family of rice. Plant Physiol **138**, 1903-1913.
Miya A, Albert P, Shinya T, Desaki Y, Ichimura K, Shirasu K, Narusaka Y, Kawakami N, Kaku H, Shibuya N. 2007. CERK1, a LysM receptor kinase, is essential for chitin elicitor signaling in *Arabidopsis*. Proceedings of the National Academy of Sciences **104**, 19613-19618.
Miyawaki KN, Yang Z. 2014. Extracellular signals and receptor-like kinases regulating ROP GTPases in plants. Frontiers in Plant Science **5**, 449.
Mochida K, Yoshida T, Sakurai T, Ogihara Y, Shinozaki K. 2009. TriFLDB: a database of clustered full-length coding sequences from *Triticeae* with applications to comparative grass genomics. Plant Physiol **150**, 1135-1146.
Molendijk AJ, Ruperti B, Palme K. 2004. Small GTPases in vesicle trafficking. Curr Opin Plant Biol **7**, 694-700.
Molitor A, Zajic D, Voll LM, Pons KHJ, Samans B, Kogel KH, Waller F. 2011. Barley leaf transcriptome and metabolite analysis reveals new aspects of compatibility and *Piriformospora indica*-mediated systemic induced resistance to powdery mildew. Molecular Plant Microbe Interactions **24**, 1427-1439.
Morrison DK. 2012. MAP kinase pathways. Cold Spring Harbor Perspectives in Biology **4**, 1-6.
Motion GB, Amaro TM, Kulagina N, Huitema E. 2015. Nuclear processes associated with plant immunity and pathogen susceptibility. Brief Funct Genomics **14**, 243-252.
Muschietti J, Eyal Y, McCormick S. 1998. Pollen tube localization implies a role in pollen–pistil interactions for the tomato receptor-like protein kinases LePRK1 and LePRK2. Plant Cell **10**, 319-330.
Nadeau JA, Sack FD. 2002. Control of stomatal distribution on the *Arabidopsis* leaf surface. Science **296**, 1697-1700.
Nam KH, Li J. 2002. BRI1/BAK1, a receptor kinase pair mediating brassinosteroid signaling. Cell **110**, 203-212.

Newman MA, Sundelin T, Nielsen JT, Erbs G. 2013. MAMP (microbe-associated molecular pattern) triggered immunity in plants. Frontiers in Plant Science **4**, 1-14.
Nibau C, Wu HM, Cheung AY. 2006. RAC/ROP GTPases: 'hubs' for signal integration and diversification in plants. Trends Plant Sci **11**, 309-315.
Nicaise V, Roux M, Zipfel C. 2009. Recent advances in PAMP-triggered immunity against bacteria: pattern recognition receptors watch over and raise the alarm. Plant Physiol **150**, 1638-1647.
Nie M, Balda MS, Matter K. 2012. Stress- and Rho-activated ZO-1-associated nucleic acid binding protein binding to p21 mRNA mediates stabilization, translation, and cell survival. Proceedings of the National Academy of Sciences **109**, 10897-10902.
Nottensteiner M. 2015. Molecular characterization of retroelement encoded ROPIP1 as virulence effector of *Blumeria graminis* f.sp. *hordei*, TU München, Freising.
Nuehse TS, Peck SC, Hirt H, Boller T. 2000. Microbial elicitors induce activation and dual phosphorylation of the *Arabidopsis thaliana* MAPK6. Journal of Biological Chemistry **275**, 7521-7526.
Ogawa M, Shinohara H, Sakagami Y, Matsubayashi Y. 2008. *Arabidopsis* CLV3 peptide directly binds CLV1 ectodomain. Science **319**, 294.
Ono E, Wong HL, Kawasaki T, Hasegawa M, Kodama O, Shimamoto K. 2001. Essential role of the small GTPase Rac in disease resistance of rice. Proceedings of the National Academy of Sciences **98**, 759-764.
Opalski KS, Schultheiss H, Kogel KH, Hueckelhoven R. 2005. The receptor-like MLO protein and the RAC/ROP family G-protein RACB modulate actin reorganization in barley attacked by the biotrophic powdery mildew fungus *Blumeria graminis f.sp. hordei.* The Plant Journal **41**, 291-303.
Oparka KJ. 1994. Plasmolysis: new insights into an old process. New Phytologist **126**, 571-591.
Ostertag M, Stammler J, Douchkov D, Eichmann R, Huckelhoven R. 2013. The conserved oligomeric Golgi complex is involved in penetration resistance of barley to the barley powdery mildew fungus. Mol Plant Pathol **14**, 230-240.
Pandey DK, Chaudhary B. 2014. Role of plant somatic embryogenesis receptor kinases (SERKs) in cell-to-embryo transitional activity: key at novel assorted structural subunits. American Journal of Plant Sciences **5**, 1-16.
Pandey GK, Sharma M, Pandey A, Shanmugam T. 2015. *GTPases: versatile regulators of signal transduction in plants*: Springer.
Park HS, Ryu HY, Kim BH, Kim SY, Yoon IS, Nam KH. 2011. A subset of OsSERK genes, including OsBAK1, affects normal growth and leaf development of rice. Molecules and Cells **32**, 561-569.
Pathuri IP, Eichmann R, Hueckelhoven R. 2009. Plant small monomeric G-proteins (RAC/ROPs) of barley are common elements of susceptibility to fungal leaf pathogens, cell expansion and stomata development. Plant Signalling & Behaviour **4**, 109-110.
Pathuri IP, Zellerhoff N, Schaffrath U, Hensel G, Kumlehn J, Kogel K, Eichmann R, Hueckelhoven R. 2008. Constitutively activated barley ROPs modulate epidermal cell size, defense reactions and interactions with fungal leaf pathogens. Plant Cell Rep **27**, 1877-1887.
Pattengale ND, Alipour M, Bininda-Emonds OR, Moret BM, Stamatakis A. 2010. How many bootstrap replicates are necessary? Journal of Computational Biology **17**, 337-354.
Pavan S, Jacobsen E, Visser RG, Bai Y. 2010. Loss of susceptibility as a novel breeding strategy for durable and broad-spectrum resistance. Molecular Breeding **25**, 1-12.
Pearson K. 1901. On lines and planes of closest fit to a system of points in space. The London, Edinburgh, and Dublin Philosophical Magazine and Journal of Science **6**, 559-572.
Pedley KF, Martin GB. 2005. Role of mitogen-activated protein kinases in plant immunity. Curr Opin Plant Biol **8**, 541-547.
Peng Y, Bartley LE, Chen X, Dardick C, Chern M, Ruan R, Canlas PE, Ronald PC. 2008. OsWRKY62 is a negative regulator of basal and Xa21-mediated defense against *Xanthomonas oryzae pv. oryzae* in rice. Mol Plant **1**, 446-458.
Pennington HG, Li L, Spanu PD. 2015. Identification and selection of normalization controls forquantitative transcript analysis in *Blumeria graminis.* Mol Plant Pathol, 1-9.

Perez P, Cansado J. 2010. Cell integrity signaling and response to stress in fission yeast. Current Protein and Peptide Science **11**, 680-692.
Peterhaensel C, Freialdenhoven A, Kurth J, Kolsch R, Schulze-Lefert P. 1997. Interaction analyses of genes required for resistance responses to powdery mildew in barley reveal distinct pathwayslLeading to leaf cell death. Plant Cell **9**, 1397-1409.
Petersen M, Brodersen P, Naested H, Andreasson E, Lindhart U, Johansen B, Nielsen HB, Lacy M, Austin MJ, Parker JE, Sharma SB, Klessig DF, Martienssen R, Mattsson O, Jensen AB, Mundy J. 2000. *Arabidopsis* map kinase 4 negatively regulates systemic acquired resistance. Cell **103**, 1111-1120.
Pitzschke A, Schikora A, Hirt H. 2009. MAPK cascade signalling networks in plant defence. Curr Opin Plant Biol **12**, 421-426.
Poraty-Gavra L, Zimmermann P, Haigis S, Bednarek P, Hazak O, Stelmakh OR, Sadot E, Schulze-Lefert P, Gruissem W, Yalovsky S. 2013. The *Arabidopsis* Rho of plants GTPase AtROP6 functions in developmental and pathogen response pathways. Plant Physiol **161**, 1172-1188.
Proels RK, Oberhollenzer K, Pathuri IP, Hensel G, Kumlehn J, Hueckelhoven R. 2010. RBOHF2 of barley is required for normal development of penetration resistance to the parasitic fungus *Blumeria graminis f. sp. hordei*. Molecular Plant-Microbe Interactions Journal **23**, 1143-1150.
Qi M, Elion EA. 2005. MAP kinase pathways. Journal of Cell Science **118**, 3569-3572.
Qin Y, Dong J. 2015. Focusing on the focus: What else beyond the master switches for polar cell growth? Mol Plant **8**, 582-594.
Qiu JL, Fiil BK, Petersen K, Nielsen HB, Botanga CJ, Thorgrimsen S, Palma K, Suarez-Rodriguez MC, Sandbech-Clausen S, Lichota J, Brodersen P, Grasser KD, Mattsson O, Glazebrook J, Mundy J, Petersen M. 2008a. *Arabidopsis* MAP kinase 4 regulates gene expression through transcription factor release in the nucleus. The EMBO Journal **27**, 2214-2221.
Qiu JL, Zhou L, Yun BW, Nielsen HB, Fiil BK, Petersen K, Mackinlay J, Loake GJ, Mundy J, Morris PC. 2008b. Arabidopsis mitogen-activated protein kinase kinases MKK1 and MKK2 have overlapping functions in defense signaling mediated by MEKK1, MPK4, and MKS1. Plant Physiol **148**, 212-222.
Radchuk VV, Sreenivasulu N, Radchuk RI, Wobus U, Weschke W. 2005. The methylation cycle and its possible functions in barley endosperm development. Plant Mol Biol **59**, 289-307.
Ramamoorthy R, Jiang SY, Kumar N, Venkatesh PN, Ramachandran S. 2008. A comprehensive transcriptional profiling of the WRKY gene family in rice under various abiotic and phytohormone treatments. Plant Cell Physiology **49**, 865-879.
Ramonell K, Berrocal-Lobo M, Koh S, Wan J, Edwards H, Stacey G, Somerville S. 2005. Loss-of-function mutations in chitin responsive genes show increased susceptibility to the powdery mildew pathogen *Erysiphe cichoracearum*. Plant Physiol **138**, 1027-1036.
Ranf S, Eschen-Lippold L, Pecher P, Lee J, Scheel D. 2011. Interplay between calcium signalling and early signalling elements during defence responses to microbe- or damage-associated molecular patterns. The Plant Journal **68**, 100-113.
Ranf S, Gisch N, Schaffer M, Illig T, Westphal L, Knirel YA, Sanchez-Carballo PM, Zahringer U, Huckelhoven R, Lee J, Scheel D. 2015. A lectin S-domain receptor kinase mediates lipopolysaccharide sensing in *Arabidopsis thaliana.* Nature Immunology **16**, 426-433.
Rayapuram C, Jensen MK, Maiser F, Shanir JV, Hornshoj H, Rung JH, Gregersen PL, Schweizer P, Collinge DB, Lyngkjaer MF. 2012. Regulation of basal resistance by a powdery mildew-induced cysteine-rich receptor-like protein kinase in barley. Mol Plant Pathol **13**, 135-147.
Reinbothe S, Reinbothe C, Lehmann J, Becker W, Apel K, Parthier B. 1994. JIP60, a methyl jasmonate-induced ribosome-inactivating protein involved in plant stress reactions. Proceedings of the National Academy of Sciences **91**, 7012-7016.
Reiner T, Hoefle C, Hueckelhoven R. 2015. A barley SKP1-like protein controls abundance of the susceptibility factor RACB and influences the interaction of barley with the barley powdery mildew fungus. Mol Plant Pathol, 1-12.
Replogle A, Wang J, Paolillo V, Smeda J, Kinoshita A, Durbak A, Tax FE, Wang X, Sawa S, Mitchum MG. 2013. Synergistic interaction of CLAVATA1, CLAVATA2, and RECEPTOR-LIKE PROTEIN KINASE 2 in cyst nematode parasitism of *Arabidopsis*. Molecular Plant-Microbe Interactions Journal **26**, 87-96.

Reyna NS, Yang Y. 2006. Molecular analysis of the rice MAP kinase gene family in relation to *Magnaporthe grisea* infection. Molecular Plant Microbe Interactions **19**, 530-540.
Ron M, Avni A. 2004. The receptor for the fungal elicitor ethylene-inducing xylanase is a member of a resistance-like gene family in tomato. Plant Cell **16**, l1604-1615.
Roux M, Schwessinger B, Albrecht C, Chinchilla D, Jones A, Holton N, Malinovsky FG, Tor M, de Vries S, Zipfel C. 2011. The Arabidopsis leucine-rich repeat receptor-like kinases BAK1/SERK3 and BKK1/SERK4 are required for innate immunity to hemibiotrophic and biotrophic pathogens. Plant Cell **23**, l2440-2455.
Rustgi S, Pollmann S, Buhr F, Springer A, Reinbothe C, von Wettstein D, Reinbothe S. 2014. JIP60-mediated, jasmonate- and senescence-induced molecular switch in translation toward stress and defense protein synthesis. Proceedings of the National Academy of Sciences **111**, 14181-14186.
Saijo YT, N.; Lu, X.; Rauf, P.; Pajerowska-Mukhtar, K.; Haeweker, H.; Dong, X.; Robatzek, S.; Schulze-Lefert, P. 2009. Receptor quality control in the endoplasmic reticulum for plant innate immunity. The EMBO Journal **28**, 3439-3449.
Santos AA, Lopes KV, Apfata JA, Fontes EP. 2010. NSP-interacting kinase, NIK: a transducer of plant defence signalling. J Exp Bot **61**, 3839-3845.
Scheer JM, Ryan CA, Jr. 2002. The systemin receptor SR160 from *Lycopersicon peruvianum* is a member of the LRR receptor kinase family. Proceedings of the National Academy of Sciences **99**, 9585-9590.
Scheler B, Schnepf V, Galgenmueller C, Ranf S, Hueckelhoven R. 2016. Barley disease susceptibility factor RACB acts in epidermal cell polarity and nucleus positioning. Journal of Experimental Botany **67**, 3263-3275.
Scheler C, Durner J, Astier J. 2013. Nitric oxide and reactive oxygen species in plant biotic interactions. Curr Opin Plant Biol **16**, 534-539.
Schulte D, Close TJ, Graner A, Langridge P, Matsumoto T, Muehlbauer G, Sato K, Schulman AH, Waugh R, Wise RP, Stein N. 2009. The international barley sequencing consortium--at the threshold of efficient access to the barley genome. Plant Physiol **149**, 142-147.
Schultheiss H, Dechert C, Kiraly L, Fodor J, Michel K, Kogel KH, Hueckelhoven R. 2003. Functional assessment of the pathogenesis-related protein PR1b in barley. Plant Science **165**, 1275-1280.
Schultheiss H, Dechert C, Kogel KH, Hueckelhoven R. 2002. A small GTP-binding host protein is required for entry of powdery mildew fungus into epidermal cells of barley. Plant Physiol **128**, 1447-1454.
Schultheiss H, Hensel G, Imani J, Broeders S, Sonnewald U, Kogel K, Kumlehn J, Hueckelhoven R. 2005. Ectopic expression of constitutively activated RACB in barley enhances susceptibility to powdery mildew and abiotic stress. Plant Physiol **139**, 353-362.
Schultheiss H, Preuss J, Pircher T, Eichmann R, Hueckelhoven R. 2008. Barley RIC171 interacts with RACB in planta and supports entry of the powdery mildew fungus. Cell Microbiol **10**, 1815-1826.
Schulze-Lefert P. 2004. Knocking on the heaven's wall: pathogenesis of and resistance to biotrophic fungi at the cell wall. Curr Opin Plant Biol **7**, 377-383.
Schweizer P, Pokorny J, Abderhalden O, Dudler R. 1999. A transient assay system for the functional assessment of defense-related genes in wheat. Molecular Plant Microbe Interactions Journal **12**, 647-654.
Sheikh AH, Raghuram B, Jalmi SK, Wankhede DP, Singh P, Sinha AK. 2013. Interaction between two rice mitogen activated protein kinases and its possible role in plant defense. BMC Plant Biol **13**, 1-11.
Shen QH, Saijo Y, Mauch S, Biskup C, Bieri S, Keller B, Seki H, Ulker B, Somssich IE, Schulze-Lefert P. 2007. Nuclear activity of MLA immune receptors links isolate-specific and basal disease-resistance responses. Science **315**, 1098-1103.
Shen X, Yuan B, Liu H, Li X, Xu C, Wang S. 2010. Opposite functions of a rice mitogen-activated protein kinase during the process of resistance against *Xanthomonas oryzae*. Plant Journal **64**, 86-99.
Shiu SH, Karlowski WM, Pan R, Tzeng YH, Mayer KFX, Li WH. 2004. Comparative analysis of the receptor-like kinase family in Arabidopsis and Rice. Plant Cell **16**, 1220-1234.

Shpak ED, McAbee JM, Pillitteri LJ, Torii KU. 2005. Stomatal patterning and differentiation by synergistic interactions of receptor kinases. Science **309**, 290-293.
Singh P, Zimmerli L. 2013. Lectin receptor kinases in plant innate immunity. Frontiers in Plant Science **4**, 1-4.
Singh R, Jwa NS. 2013. The rice MAPKK-MAPK interactome: the biological significance of MAPK components in hormone signal transduction. Plant Cell Report **32**, 923-931.
Singh R, Lee MO, Lee JE, Choi J, Park JH, Kim EH, Yoo RH, Cho JI, Jeon JS, Rakwal R, Agrawal GK, Moon JS, Jwa NS. 2012. Rice mitogen-activated protein kinase interactome analysis using the yeast two-hybrid system. Plant Physiol **160**, 477-487.
Singla B, Khurana JP, Khurana P. 2009. Structural characterization and expression analysis of the SERK/SERL gene family in rice (*Oryza sativa*). International Journal of Plant Genomics **2009**, 1-8.
Smith JM, Heese A. 2014. Rapid bioassay to measure early reactive oxygen species production in *Arabidopsis* leave tissue in response to living *Pseudomonas syringae*. Plant Methods **10**, 1-9.
Song WY, Wang GL, Chen LL, Kim HS, Pi LY, Holsten T, Gardner J, Wang B, Zhai WX, Zhu LH, Fauquet C, Ronald P. 1995. A receptor kinase-like protein encoded by the rice disease resistance gene, Xa21. Science **270**, 1804-1806.
Sorek N, Gutman O, Bar E, Abu-Abied M, Feng X, Running MP, Lewinsohn E, Ori N, Sadot E, Henis YI, Yalovsky S. 2011. Differential effects of prenylation and s-acylation on type I and II ROPS membrane interaction and function. Plant Physiol **155**, 706-720.
Sorek N, Poraty L, Sternberg H, Bar E, Lewinsohn E, Yalovsky S. 2007. Activation status-coupled transient S acylation determines membrane partitioning of a plant Rho-related GTPase. Molecular and Cellular Biology **27**, 2144-2154.
Stoughton RB. 2005. Applications of DNA microarrays in biology. Annual Review in Biochemistry **74**, 53-82.
Sun X, Cao Y, Yang Z, Xu C, Li X, Wang S, Zhang Q. 2004. Xa26, a gene conferring resistance to *Xanthomonas oryzae pv. oryzae* in rice, encodes an LRR receptor kinase-like protein. The Plant Journal **37**, 517-527.
Sun Y, Li L, Macho AP, Han Z, Hu Z, Zipfel C, Zhou JM, Chai J. 2013. Structural basis for flg22-induced activation of the Arabidopsis FLS2-BAK1 immune complex. Science **342**, 624-628.
Swiderski MR, Innes RW. 2001. The Arabidopsis PBS1 resistance gene encodes a member of a novel protein kinase subfamily. The Plant Journal **26**, 101-112.
Taj G, Giri P, Tasleem M, Kumar A. 2014. MAPK signaling cascades and transcriptional reprogramming in plant–pathogen interactions. In: Gaur R, Sharma, P, ed. *Approaches to plant stress and their management.* India: Springer, 297-316.
Tamura K, Nei M. 1993. Estimation of the number of nucleotide substitutions in the control region of mitochondrial DNA in humans and chimpanzees. Molecular Biology and Evolution **10**, 512-526.
Tamura K, Stecher G, Peterson D, Filipski A, Kumar S. 2013. MEGA6: Molecular Evolutionary Genetics Analysis version 6.0. Molecular Biology and Evolution **30**, 2725-2729.
Tan KC, Ipcho SV, Trengove RD, Oliver RP, Solomon PS. 2009. Assessing the impact of transcriptomics, proteomics and metabolomics on fungal phytopathology. Mol Plant Pathol **10**, 703-715.
Thimm O, Blasing O, Gibon Y, Nagel A, Meyer S, Kruger P, Selbig J, Muller LA, Rhee SY, Stitt M. 2004. MAPMAN: a user-driven tool to display genomics data sets onto diagrams of metabolic pathways and other biological processes. Plant Journal **37**, 914-939.
Torii KU, Mitsukawa N, Oosumi T, Matsuura Y, Yokoyama R, Whittier RF, Komeda Y. 1996. The Arabidopsis ERECTA gene encodes a putative receptor protein kinase with extracellular leucine-rich repeats. Plant Cell **8**, 735-746.
Torres MA. 2010. ROS in biotic interactions. Physiologia Plantarum **138**, 414-429.
Trotochaud AE, Hao T, Wu G, Yang Z, Clark SE. 1999. The CLAVATA1 receptor-like kinase requires CLAVATA3 for its assembly into a signaling complex that includes KAPP and a Rho-related protein. Plant Cell **11**, 393-406.

Trotochaud AE, Jeong S, Clark SE. 2000. CLAVATA3, a multimeric ligand for the CLAVATA1 receptor-kinase. Science **289**, 613-617.
Trujillo M, Kogel KH, Hueckelhoven R. 2004. Superoxide and hydrogen peroxide play different roles in the nonhost interaction of barley and wheat with inappropriate formae speciales of *Blumeria graminis*. Molecular Plant Microbe Interactions **17**, 304-312.
Untergasser A, Cutcutache I, Koressaar T, Ye J, Faircloth BC, Remm M, Rozen SG. 2012. Primer3--new capabilities and interfaces. Nucleic Acids Res **40**, e115.
Usadel B, Nagel A, Thimm O, Redestig H, Blaesing OE, Palacios-Rojas N, Selbig J, Hannemann J, Piques MC, Steinhauser D, Scheible WR, Gibon Y, Morcuende R, Weicht D, Meyer S, Stitt M. 2005. Extension of the visualization tool MapMan to allow statistical analysis of arrays, display of corresponding genes, and comparison with known responses. Plant Physiol **138**, 1195-1204.
Usadel B, Poree F, Nagel A, Lohse M, Czedik-Eysenberg A, Stitt M. 2009. A guide to using MapMan to visualize and compare Omics data in plants: a case study in the crop species, Maize. Plant Cell & Environment **32**, 1211-1229.
Vaid N, Macovei A, Tuteja N. 2013. Knights in action: lectin receptor-like kinases in plant development and stress responses. Mol Plant **6**, 1405-1418.
van der Linde K, Hemetsberger C, Kastner C, Kaschani F, van der Hoorn RA, Kumlehn J, Doehlemann G. 2012. A maize cystatin suppresses host immunity by inhibiting apoplastic cysteine proteases. Plant Cell **24**, 1285-1300.
van Loon LC, Pierpoint WS, Boller T, Conejero V. 1994. Recommendations for naming plant pathogenesis-related proteins. Plant Molecular Biology Reporter **12**, 245-264.
van Schie CC, Takken FL. 2014. Susceptibility genes 101: how to be a good host. Annual Review of Phytopatholgy **52**, 551-581.
Vogel JP, Raab TK, Schiff C, Somerville SC. 2002. PMR6, a pectate lyase-like gene required for powdery mildew susceptibility in arabidopsis. Plant Cell **14**, 2095-2106.
Waites R, Simon R. 2000. Signaling cell fate in plant meristems. Three clubs on one tousle. Cell **103**, 835-838.
Walia A, Lee JS, Wasteneys G, Ellis B. 2009. *Arabidopsis* mitogen-activated protein kinase MPK18 mediates cortical microtubule functions in plant cells. Plant Journal **59**, 565-575.
Wang F, Jing W, Zhang W. 2014a. The mitogen-activated protein kinase cascade MKK1-MPK4 mediates salt signaling in rice. Plant Science **227**, 181-189.
Wang H, Liu Y, Bruffett K, Lee J, Hause G, Walker JC, Zhang S. 2008. Haplo-insufficiency of MPK3 in MPK6 mutant background uncovers a novel function of these two MAPKs in *Arabidopsis* ovule development. Plant Cell **20**, 602-613.
Wang Y, Kwon SJ, Wu J, Choi J, Lee YH, Agrawal GK, Tamogami S, Rakwal R, Park SR, Kim BG, Jung KH, Kang KY, Kim SG, Kim ST. 2014b. Transcriptome analysis of early responsive genes in rice during *Magnaporthe oryzae* infection. The Plant Pathology Journal **30**, 343-354.
Wang YK, S.G.; Wu, J.; Huh, H.H.; Lee, S.J.; Rakwal, R.; Agrawal, G.K.; Park, Z.Y.; Young Kang, K.; Kim, S.T. 2013. Secretome analysis of the rice bacterium *Xanthomonas oryzae (Xoo)* using in vitro and in planta systems. Proteomics **13**, 1901-1912.
Wang Z, Gerstein M, Snyder M. 2009. RNA-Seq: a revolutionary tool for transcriptomics. Nature Reviews Genetics **10**, 57-63.
Waterhouse AM, Procter JB, Martin DM, Clamp M, Barton GJ. 2009. Jalview Version 2--a multiple sequence alignment editor and analysis workbench. Bioinformatics **25**, 1189-1191.
Weber E, Engler C, Gruetzner R, Werner S, Marillonnet S. 2011. A modular cloning system for standardized assembly of multigene constructs. PLoS One **6**, e16765.
Wei Y, Zhang Z, Andersen CH, Schmelzer E, Gregersen PL, Collinge DB, Smedegaard-Petersen V, Thordal-Christensen H. 1998. An epidermis/papilla-specific oxalate oxidase-like protein in the defence response of barley attacked by the powdery mildew fungus. Plant Mol Biol **36**, 101-112.
Winge P, Brembu T, Kristensen R, Bones AM. 2000. Genetic structure and evolution of RAC-GTPases in *Arabidopsis thaliana*. Genetics **156**, 1959-1971.

Wise RP, Moscou MJ, Bogdanove AJ, Whitham SA. 2007. Transcript profiling in host-pathogen interactions. Annual Review in Phytopathology **45**, 329-369.
Wong HL, Pinontoan R, Hayashi K, Tabata R, Yaeno T, Hasegawa K, Kojima C, Yoshioka H, Iba K, Kawasaki T, Shimamoto K. 2007. Regulation of rice NADPH oxidase by binding of Rac GTPase to its N-terminal extension. Plant Cell **19**, 4022-4034.
Wong HL, Sakamoto T, Kawasaki T, Umemura K, Shimamoto K. 2004. Down-regulation of metallothionein, a reactive oxygen scavenger, by the small GTPase OsRAC1 in rice. Plant Physiol **135**, 1447-1456.
Wu L, Du C, Zeng Z, Zhang M, Han H. 2014. Study on the signal transduction pathway of plant defense to pathogens. Agriculture Science &Technology **15**, 517-519.
Xiong L, Yang Y. 2003. Disease resistance and abiotic stress tolerance in rice are inversely modulated by an abscisic acid-inducible mitogen-activated protein kinase. Plant Cell **15**, 745-759.
Xu J, Audenaert K, Hofte M, De Vleesschauwer D. 2013. Abscisic acid promotes susceptibility to the rice leaf blight pathogen pv by suppressing salicylic acid-mediated defenses. PLoS One **8**, e67413.
Xu T, Dai N, Chen J, Nagawa S, Cao M, Li H, Zhou Z, Chen X, De Rycke R, Rakusova H, Wang W, Jones AM, Friml J, Patterson SE, Bleecker AB, Yang Z. 2014. Cell surface ABP1-TMK auxin-sensing complex activates ROP GTPase signaling. Science **343**, 1025-1028.
Xu T, Wen M, Nagawa S, Fu Y, Chen JG, Wu MJ, Perrot-Rechenmann C, Friml J, Jones AM, Yang Z. 2010. Controls cellular interdigitation in *Arabidopsis*. Cell **143**, 99-110.
Yang K, Qi L, Zhang Z. 2014. Isolation and characterization of a novel wall-associated kinase gene TaWAK5 in wheat (*Triticum aestivum*). The Crop Journal **2**, 255-266.
Yang Z. 2002. Small GTPases: versatile signaling switches in plants. Plant Cell **14 Suppl**, S375-388.
Yang Z, Fu Y. 2007. ROP/RAC GTPase signaling. Curr Opin Plant Biol **10**, 490-494.
Yokotani N, Sato Y, Tanabe S, Chujo T, Shimizu T, Okada K, Yamane H, Shimono M, Sugano S, Takatsuji H, Kaku H, Minami E, Nishizawa Y. 2013. WRKY76 is a rice transcriptional repressor playing opposite roles in blast disease resistance and cold stress tolerance. J Exp Bot **64**, 5085-5097.
Yoshioka H, Mase K, Yoshioka M, Kobayashi M, Asai S. 2011. Regulatory mechanisms of nitric oxide and reactive oxygen species generation and their role in plant immunity. Nitric Oxide **25**, 216-221.
Zhang CQ, Xu Y, Lu Y, Yu HX, Gu MH, Liu QQ. 2011. The WRKY transcription factor OsWRKY78 regulates stem elongation and seed development in rice. Planta **234**, 541-554.
Zhang J, Nei M. 1997. Accuracies of ancestral amino acid sequences inferred by the parsimony, likelihood, and distance methods. Journal of Molecular Evolution **44 Suppl 1**, S139-146.
Zhang L, Du L, Poovaiah BW. 2014. Calcium signaling and biotic defense responses in plants. Plant Signalling and Behaviour **9**, e973818-973811 - e973818-973814.
Zhang W, Fraiture M, Kolb D, Loffelhardt B, Desaki Y, Boutrot FF, Tor M, Zipfel C, Gust AA, Brunner F. 2013. *Arabidopsis* receptor-like protein30 and receptor-like kinase suppressor of BIR1-1/EVERSHED mediate innate immunity to necrotrophic fungi. Plant Cell **25**, 4227-4241.
Zhang Y, McCormick S. 2007. A distinct mechanism regulating a pollen-specific guanine nucleotide exchange factor for the small GTPase ROP in *Arabidopsis thaliana.* Proceedings of the National Academy of Sciences **104**, 18830-18835.
Zhang Z, Gurr SJ. 2001. Expression and sequence analysis of the *Blumeria graminis* mitogen-activated protein kinase genes, mpk1 and mpk2. Gene **266**, 57-65.
Zhang ZL, Shin M, Zou X, Huang J, Ho TH, Shen QJ. 2009. A negative regulator encoded by a rice WRKY gene represses both abscisic acid and gibberellins signaling in aleurone cells. Plant Mol Biol **70**, 139-151.
Zhao XY, Wang Q, Li S, Ge FR, Zhou LZ, McCormick S, Zhang Y. 2013a. The juxtamembrane and carboxy-terminal domains of *Arabidopsis* PRK2 are critical for ROP-induced growth in pollen tubes. J Exp Bot **64**, 5599-5610.
Zhao Z, Liu H, Wang C, Xu JR. 2013b. Comparative analysis of fungal genomes reveals different plant cell wall degrading capacity in fungi. BMC Genomics **15**, 1-15.
Zheng Z, Mosher SL, Fan B, Klessig DF, Chen Z. 2007. Functional analysis of Arabidopsis WRKY25 transcription factor in plant defense against *Pseudomonas syringae*. BMC Plant Biology **7**, 2.

Zheng Z, Qamar SA, Chen Z, Mengiste T. 2006. *Arabidopsis* WRKY33 transcription factor is required for resistance to necrotrophic fungal pathogens. The Plant Journal **48**, 592-605.
Zhou J, Loh YT, Bressan RA, Martin GB. 1995. The tomato gene *Pti1* encodes a serine/threonine kinase that is phosphorylated by *Pto* and is involved in the hypersensitive response. Cell **83**, b925-935.
Zierold U, Scholz U, Schweizer P. 2005. Transcriptome analysis of *mlo*-mediated resistance in the epidermis of barley. Mol Plant Pathol **6**, 139-151.
Zipfel C. 2014. Plant pattern-recognition receptors. Trends in Immunology **35**, 345-351.
Zipfel C, Kunze G, Chinchilla D, Caniard A, Jones JD, Boller T, Felix G. 2006. Perception of the bacterial PAMP EF-Tu by the receptor EFR restricts Agrobacterium-mediated transformation. Cell **125**, 749-760.
Zou X, Qin Z, Zhang C, Liu B, Liu J, Zhang C, Lin C, Li H, Zhao T. 2015. Over-expression of an S-domain receptor-like kinase extracellular domain improves panicle architecture and grain yield in rice. J Exp Bot.
Zuckerkandl E, Pauling L. 1965. Evolutionary divergence and convergence in proteins. In: Bryson V, Vogel HJ, eds. *Evolving Genes and Proteins*. New York: Academic Press, 97-166.
Zuo S, Zhou X, Chen M, Zhang S, Schwessinger B, Ruan D, Yuan C, Wang J, Chen X, Ronald PC. 2014. OsSERK1 regulates rice development but not immunity to *Xanthomonas oryzae* pv. *oryzae* or *Magnaporthe oryzae*. Journal of Integrative Plant Biology **56**, 1179-1192.

13. SUPPLEMENTARY MATERIAL

Table S1: **Transcript numbers included in each 15 clusters at both time points**. Additionally, the transcripts of the signalling pathways are added. Cluster analysis was performed with MapMan with Euclidean distance.

time point	cluster #	all transcripts	signalling transcripts	time point	cluster #	all transcripts	signalling transcripts
12	1	84	1	32	1	157	44
12	2	1243	105	32	2	196	4
12	3	593	70	32	3	639	11
12	4	464	31	32	4	392	30
12	5	593	14	32	5	607	22
12	6	311	12	32	6	697	50
12	7	359	24	32	7	217	6
12	8	420	13	32	8	322	50
12	9	459	2	32	9	217	8
12	10	1349	41	32	10	453	10
12	11	476	40	32	11	928	70
12	12	173	48	32	12	371	5
12	13	937	111	32	13	217	5
12	14	302	12	32	14	832	51
12	15	1342	57	32	15	404	15
	sum	**9105**	**527**			**6649**	**381**

Table S2: List of 142 genes significantly regulated by *RACB* at 12 hpi. *RACB* expression sets *CA RACB* mock vs. WT mock and *RNAi RACB* mock vs. WT mock were filtered for opposite regulation. *Bgh*-dependent regulation was analysed in the WT *Bgh* vs WT mock expression set for all the oppositely regulated transcripts. Non-*Bgh*-regulated transcripts were excluded from further analysis. P_35_ numbers correspond to array numbers and annotation was followed by the rice annotation out of MIPS annotation file constructed by Karl Kugler, HelmhotzZentrum München). NA = not applicable, not significantly regulated in the appropriate single comparison.

		Log2-fold change cut-off 1; FDR corr. p-value < 0.05		
P_35_	**RICE annotation of the appropriate barley homolog**	***CA RACB* mock vs. WT mock**	***RACB RNAi* mock vs. WT mock**	**WT *Bgh* vs WT mock**
P_35_15510	LOC_Os11g31540.1 2e-66 BRASSINOSTEROID INSENSITIVE 1-associated receptor kinase 1 precursor putative expressed	4.191	-1.523	4.923
P_35_1762	LOC_Os08g41290.1 1e-72 AIR12 putative expressed	3.865	-1.358	2.369
P_35_5757	LOC_Os09g20090.1 2e-92 L-ascorbate oxidase precursor putative expressed	3.748	-1.137	2.223
P_35_35513	No hits found	3.703	-1.155	3.741
P_35_9462	LOC_Os04g09900.3 2e-61 ent-kaurene synthase A chloroplast precursor putative expressed	3.649	-1.047	1.208
P_35_10720	LOC_Os10g04730.1 2e-63 protein kinase putative expressed	3.619	-1.578	2.191
P_35_9635	LOC_Os12g41540.1 9e-12 protein kinase putative expressed	3.552	-1.493	4.502
P_35_15828	LOC_Os12g36830.1 3e-30 pathogenesis-related protein 10 putative expressed	3.405	-1.290	4.408
P_35_6982	LOC_Os02g50460.1 6e-50 immediate-early fungal elicitor protein CMPG1 putative expressed	3.377	-1.188	3.302
P_35_33	LOC_Os01g03380.1 2e-29 Bowman-Birk type bran trypsin inhibitor precursor putative expressed	3.349	-2.155	NA
P_35_2025	LOC_Os03g61470.1 2e-42 PGPS/D12 putative expressed	3.322	-1.267	2.132
P_35_9455	LOC_Os06g13320.1 1e-75 S-domain receptor-like protein kinase putative expressed	3.308	-1.009	5.764
P_35_11525	LOC_Os01g01302.1 1e-08 shikimate kinase family protein expressed	3.163	-1.004	2.416
P_35_11081	LOC_Os01g20910.1 3e-11 RING-H2 finger protein ATL2L putative expressed	3.057	-1.502	NA
P_35_24518	LOC_Os07g03710.1 2e-53 pathogenesis-related protein PRB1-3 precursor putative expressed	3.005	-1.929	NA
P_35_43536	LOC_Os01g53040.1 4e-19 OsWRKY14 - Superfamily of rice TFs having WRKY and zinc finger domains expressed	2.985	-1.273	1.578
P_35_25908	LOC_Os11g38780.1 1e-36 calcium ion binding protein putative	2.956	-1.971	4.747
P_35_19740	LOC_Os09g04339.1 2e-54 expressed protein	2.953	-1.086	2.854
P_35_18411	LOC_Os01g66510.1 2e-72 MLO-like protein 1 putative expressed	2.941	-1.705	3.489
P_35_22055	LOC_Os04g10160.1 2e-72 cytochrome P450 CYP99A1 putative expressed	2.935	-1.574	3.222
P_35_22419	LOC_Os03g09880.1 6e-59 AIR12 putative expressed	2.916	-1.371	NA

		Log2-fold change cut-off 1; FDR corr. p-value < 0.05		
P_35_	**RICE annotation of the appropriate barley homolog**	***CA RACB* mock vs. WT mock**	***RACB RNAi* mock vs. WT mock**	**WT *Bgh* vs WT mock**
P_35_41141	LOC_Os08g42580.1 4e-22 LysM receptor-like kinase putative expressed	2.909	-1.041	4.189
P_35_27106	LOC_Os09g38910.1 7e-19 OsWAK92 - OsWAK receptor-like protein kinase expressed	2.845	-1.762	4.476
P_35_21465	No hits found	2.831	-1.091	1.636
P_35_40359	LOC_Os07g13800.1 7e-05 cytokinin-N-glucosyltransferase 1 putative expressed	2.827	-1.288	2.473
P_35_24248	LOC_Os07g31884.1 3e-30 transparent testa 12 protein putative expressed	2.798	-1.233	3.005
P_35_18944	LOC_Os03g58980.1 2e-81 germin-like protein subfamily T member 2 precursor putative expressed	2.797	-1.569	3.241
P_35_14625	LOC_Os01g42870.1 6e-49 10-deacetylbaccatin III 10-O-acetyltransferase putative expressed	2.772	-1.377	3.338
P_35_15826	LOC_Os12g36830.1 7e-31 pathogenesis-related protein 10 putative expressed	2.758	-1.150	2.928
P_35_25548	LOC_Os08g04560.1 9e-16 aromatic-L-amino-acid decarboxylase putative expressed	2.752	-1.065	2.004
P_35_48104	LOC_Os09g36290.1 1e-11 phosphatase DCR2 putative expressed	2.707	-1.173	1.208
P_35_15190	LOC_Os09g33680.1 0.0 cyanogenic beta-glucosidase precursor putative expressed	2.706	-1.455	NA
P_35_10624	LOC_Os01g62190.1 1e-39 PEThy putative expressed	2.699	-1.225	NA
P_35_43411	LOC_Os06g12090.1 3e-16 GTP-binding protein SAR2 putative expressed	2.634	-1.014	2.771
P_35_15829	LOC_Os12g36830.1 1e-37 pathogenesis-related protein 10 putative expressed	2.609	-1.278	2.939
P_35_20630	LOC_Os03g15080.1 1e-65 expressed protein	2.607	-1.424	2.741
P_35_5050	LOC_Os04g29960.1 2e-34 OsWAK43 - OsWAK receptor-like protein kinase expressed	2.601	-1.484	2.775
P_35_8212	LOC_Os01g50100.1 4e-90 multidrug resistance protein 4 putative expressed	2.597	-1.246	3.968
P_35_26745	LOC_Os03g13740.1 2e-12 immediate-early fungal elicitor protein CMPG1 putative expressed	2.567	-1.341	2.067
P_35_22418	LOC_Os12g08700.1 9e-16 expressed protein	2.544	-1.392	NA
P_35_50221	LOC_Os07g44499.1 4e-16 peroxidase 56 precursor putative expressed	2.538	-1.027	3.364
P_35_11038	LOC_Os03g29410.1 1e-98 protein kinase APK1B chloroplast precursor putative expressed	2.518	-1.158	6.028
P_35_16819	No hits found	2.456	-1.418	NA
P_35_15780	LOC_Os04g32920.5 0.0 potassium transporter 1 putative expressed	2.440	-1.186	NA
P_35_710	LOC_Os05g33130.1 1e-129 basic endochitinase A precursor putative expressed	2.433	-1.381	NA
P_35_24054	LOC_Os12g19030.1 2e-73 copine family protein expressed	2.407	-2.396	1.890
P_35_11893	LOC_Os12g42200.1 6e-33 ATCHX19 putative expressed	2.367	-1.508	1.989
P_35_6104	LOC_Os06g22330.1 3e-49 expressed protein	2.357	-1.104	4.921
P_35_24669	LOC_Os06g06350.1 0.0 ACS-like protein putative expressed	2.354	-1.286	3.173

		Log2-fold change cut-off 1; FDR corr. p-value < 0.05		
P_35_	**RICE annotation of the appropriate barley homolog**	***CA RACB* mock vs. WT mock**	***RACB RNAi* mock vs. WT mock**	**WT *Bgh* vs WT mock**
P_35_14552	No hits found	2.313	-1.283	NA
P_35_15508	LOC_Os11g31540.1 1e-68 BRASSINOSTEROID INSENSITIVE 1-associated receptor kinase 1 precursor putative expressed	2.308	-1.387	2.988
P_35_34422	LOC_Os03g17470.1 7e-25 IN2-1 protein putative expressed	2.301	-1.002	2.871
P_35_15620	LOC_Os04g41680.1 9e-97 endochitinase A precursor putative expressed	2.290	-1.138	1.564
P_35_19716	No hits found	2.288	-1.271	2.418
P_35_25247	LOC_Os01g11650.1 1e-40 esterase precursor putative expressed	2.287	-1.461	2.689
P_35_25828	No hits found	2.222	-1.388	2.208
P_35_26695	LOC_Os03g01150.2 1e-77 palmitoyl-protein thioesterase 1 precursor putative expressed	2.216	-1.088	1.527
P_35_21949	LOC_Os08g35310.1 1e-103 isoflavone-7-O-methytransferase 9 putative	2.197	-2.093	NA
P_35_13330	LOC_Os06g13180.1 1e-79 metalloendoproteinase 1 precursor putative expressed	2.197	-1.315	4.260
P_35_21250	LOC_Os09g29540.1 5e-91 OsWAK82 - OsWAK receptor-like cytoplasmic kinase (OsWAK-RLCK) expressed	2.171	-1.743	2.245
P_35_9588	LOC_Os12g24320.1 2e-20 cell Division Protein AAA ATPase family putative expressed	2.146	-1.006	3.742
P_35_12191	LOC_Os09g30454.1 1e-55 OsWAK87 - OsWAK receptor-like protein kinase expressed	2.129	-2.106	2.077
P_35_42427	LOC_Os02g11870.1 3e-24 expressed protein	2.125	-1.026	4.972
P_35_1700	LOC_Os04g24290.1 1e-149 protein kinase putative	2.093	-1.127	1.643
P_35_14345	LOC_Os07g48050.1 1e-115 peroxidase precursor putative expressed	2.067	-1.851	4.423
P_35_3901	LOC_Os01g48620.1 1e-102 expressed protein	2.049	-1.138	2.945
P_35_23723	LOC_Os12g28177.1 6e-67 cell Division Protein AAA ATPase family putative expressed	2.048	-1.894	3.927
P_35_15464	LOC_Os08g28240.1 1e-54 crocetin dialdehyde putative expressed	2.036	-1.435	NA
P_35_40297	LOC_Os03g20949.1 3e-87 phospholipid-transporting ATPase 1 putative expressed	2.002	-1.042	4.728
P_35_9620	LOC_Os05g45410.1 4e-27 heat shock factor putative expressed	1.999	-1.287	3.556
P_35_5202	No hits found	1.994	-1.714	4.446
P_35_5521	No hits found	1.982	-1.249	NA
P_35_14518	LOC_Os02g36940.1 1e-68 expressed protein	1.965	-1.280	2.684
P_35_48059	LOC_Os01g22352.1 3e-17 peroxidase 2 precursor putative expressed	1.943	-1.185	NA
P_35_20698	LOC_Os03g60560.1 4e-37 ZFP16-2 putative expressed	1.943	-1.416	NA
P_35_43396	No hits found	1.936	-1.460	NA

		Log2-fold change cut-off 1; FDR corr. p-value < 0.05		
P_35_	**RICE annotation of the appropriate barley homolog**	***CA RACB* mock vs. WT mock**	***RACB RNAi* mock vs. WT mock**	**WT *Bgh* vs WT mock**
P_35_1120	No hits found	1.917	-1.029	3.787
P_35_14350	LOC_Os01g22352.1 1e-137 peroxidase 2 precursor putative expressed	1.904	-1.117	NA
P_35_30433	LOC_Os05g48210.1 8e-10 expressed protein	1.903	-1.065	1.823
P_35_9814	LOC_Os09g37834.1 2e-94 serine/threonine-protein kinase receptor precursor putative expressed	1.893	-1.415	1.582
P_35_603	LOC_Os06g29730.1 7e-06 expressed protein	1.881	-1.031	1.452
P_35_1119	LOC_Os05g04700.1 8e-10 hydrophobic protein LTI6B putative expressed	1.877	-1.203	3.602
P_35_20068	LOC_Os03g37840.1 0.0 potassium transporter 16 putative expressed	1.865	-1.002	1.395
P_35_42222	LOC_Os01g50100.1 2e-88 multidrug resistance protein 4 putative expressed	1.857	-1.219	4.182
P_35_13705	LOC_Os07g23570.1 1e-156 cytochrome P450 72A1 putative expressed	1.854	-1.922	NA
P_35_19948	LOC_Os04g48850.1 6e-63 1-aminocyclopropane-1-carboxylate synthase putative expressed	1.849	-1.674	3.759
P_35_16564	LOC_Os01g04330.1 9e-65 calmodulin-related protein 2 touch-induced putative expressed	1.845	-1.494	1.875
P_35_249	LOC_Os10g34910.1 1e-76 secretory protein putative	1.827	-1.414	2.872
P_35_150	LOC_Os06g29730.1 6e-06 expressed protein	1.816	-1.028	2.623
P_35_5259	LOC_Os07g20610.1 5e-34 serine/threonine-protein kinase receptor precursor putative	1.810	-1.237	2.716
P_35_40770	No hits found	1.807	-1.085	4.340
P_35_774	LOC_Os11g37950.1 4e-64 win2 precursor putative expressed	1.805	-1.142	1.877
P_35_27010	No hits found	1.771	-1.456	1.675
P_35_5257	LOC_Os05g42210.1 2e-86 serine/threonine-protein kinase receptor precursor putative expressed	1.740	-1.286	2.615
P_35_29940	LOC_Os12g29950.2 3e-23 nitrate and chloride transporter putative expressed	1.730	-1.273	4.268
P_35_2397	No hits found	1.724	-1.162	2.096
P_35_8169	LOC_Os04g37700.1 1e-33 expressed protein	1.722	-1.242	NA
P_35_48052	LOC_Os01g43774.1 5e-23 cytochrome P450 72A1 putative expressed	1.680	-1.498	1.803
P_35_26211	LOC_Os05g41370.1 2e-25 receptor-like protein kinase homolog RK20-1 putative expressed	1.674	-1.478	3.740
P_35_1698	LOC_Os04g24220.3 6e-60 OsWAK32 - OsWAK receptor-like protein kinase expressed	1.672	-1.271	NA
P_35_23760	LOC_Os03g52380.1 4e-21 expressed protein	1.654	-1.425	2.232
P_35_41435	LOC_Os07g38800.1 8e-37 lectin-like receptor kinase 7 putative expressed	1.652	-1.769	1.974
P_35_606	LOC_Os12g22030.2 1e-09 serine hydroxymethyltransferase mitochondrial precursor putative expressed	1.638	-1.256	NA

		Log2-fold change cut-off 1; FDR corr. p-value < 0.05		
P_35_	**RICE annotation of the appropriate barley homolog**	***CA RACB* mock vs. WT mock**	***RACB RNAi* mock vs. WT mock**	**WT *Bgh* vs WT mock**
P_35_16231	LOC_Os02g17090.1 0.0 cucumisin precursor putative expressed	1.635	-2.150	4.262
P_35_6100	LOC_Os07g35660.1 1e-56 receptor-like serine-threonine protein kinase putative expressed	1.627	-1.041	3.860
P_35_949	LOC_Os09g04310.1 3e-27 expressed protein	1.613	-1.278	1.609
P_35_20965	LOC_Os02g39330.1 1e-127 endochitinase PR4 precursor putative expressed	1.609	-1.495	4.866
P_35_23361	LOC_Os07g38800.1 9e-21 lectin-like receptor kinase 7 putative expressed	1.604	-1.074	1.684
P_35_5423	LOC_Os04g58710.1 2e-78 peroxisomal-coenzyme A synthetase putative expressed	1.603	-1.181	3.981
P_35_10619	LOC_Os03g62200.1 1e-109 ammonium transporter 2 putative expressed	1.600	-1.340	1.776
P_35_10046	LOC_Os01g61460.1 1e-127 expressed protein	1.597	-1.248	3.697
P_35_6585	LOC_Os06g04900.1 3e-80 hexose carrier protein HEX6 putative expressed	1.592	-1.301	3.157
P_35_5444	LOC_Os05g31020.1 1e-113 eukaryotic peptide chain release factor subunit 1-1 putative expressed	1.561	-1.686	NA
P_35_41681	LOC_Os03g13300.1 2e-23 glutamate decarboxylase putative expressed	1.539	-1.268	1.629
P_35_15131	LOC_Os07g47700.1 0.0 UDP-glucuronic acid decarboxylase 1 putative expressed	1.538	-1.246	4.584
P_35_14951	LOC_Os08g08990.1 1e-105 germin-like protein subfamily 1 member 11 precursor putative expressed	1.497	-1.695	7.026
P_35_13049	LOC_Os11g42200.1 5e-36 laccase LAC2-1 putative expressed	1.472	-1.958	NA
P_35_27978	LOC_Os11g10310.1 3e-56 receptor-like protein kinase precursor putative expressed	1.454	-1.337	1.418
P_35_8642	LOC_Os10g10360.4 2e-66 NBS-LRR disease resistance protein putative expressed	1.442	-1.162	1.997
P_35_3466	LOC_Os03g03350.1 0.0 glycoside hydrolase family 28 putative expressed	1.437	-1.049	1.553
P_35_14142	LOC_Os03g13300.1 0.0 glutamate decarboxylase putative expressed	1.410	-1.101	1.641
P_35_9926	LOC_Os09g26144.1 1e-05 glutamate receptor 2.8 precursor putative expressed	1.333	-1.139	2.018
P_35_34887	LOC_Os07g45480.1 3e-26 conserved hypothetical protein	1.310	-1.308	2.189
P_35_47932	No hits found	1.293	-1.162	NA
P_35_1476	LOC_Os07g39740.1 1e-150 esterase precursor putative expressed	1.278	-1.200	NA
P_35_40027	LOC_Os10g38360.1 7e-07 glutathione S-transferase GSTU6 putative expressed	1.275	-1.004	2.508
P_35_5546	LOC_Os03g53200.1 1e-72 calmodulin putative expressed	1.253	-1.036	1.535
P_35_16041	LOC_Os03g55410.1 1e-130 peroxidase 51 precursor putative expressed	1.235	-1.067	1.125
P_35_48525	No hits found	1.220	-1.163	4.436
P_35_18546	LOC_Os01g62430.3 8e-59 elicitor-responsive protein 1 putative expressed	1.216	-1.024	5.285
P_35_6082	LOC_Os04g51150.1 6e-32 transposon protein putative unclassified expressed	1.207	-1.196	NA

		Log2-fold change cut-off 1; FDR corr. p-value < 0.05		
P_35_	**RICE annotation of the appropriate barley homolog**	***CA RACB* mock vs. WT mock**	***RACB RNAi* mock vs. WT mock**	**WT *Bgh* vs WT mock**
P_35_41226	LOC_Os01g04470.1 3e-07 hypothetical protein	1.206	-1.158	2.423
P_35_17226	LOC_Os12g02960.1 9e-68 glutathione S-transferase putative expressed	1.186	-1.115	2.522
P_35_48528	LOC_Os04g23700.1 2e-40 ATP binding protein putative expressed	1.181	-1.071	1.014
P_35_30393	No hits found	1.144	-1.189	NA
P_35_23415	LOC_Os05g25390.1 1e-158 protein kinase putative expressed	1.141	-1.271	3.479
P_35_20192	LOC_Os05g05620.1 3e-62 glutathione S-transferase GSTF1 putative expressed	1.122	-1.076	2.848
P_35_44375	No hits found	1.074	-1.111	2.490
P_35_4958	LOC_Os05g35960.1 2e-13 conserved hypothetical protein	1.001	-1.156	1.191
P_35_1073	LOC_Os01g60770.1 1e-112 alpha-expansin 10 precursor putative expressed	-1.096	1.736	-1.347
P_35_47978	LOC_Os04g48200.1 3e-88 cytochrome P450 87A3 putative expressed	-1.178	1.104	NA
P_35_19157	LOC_Os05g34320.2 0.0 beta-hexosaminidase beta chain precursor putative expressed	-2.319	3.693	-2.525

Table S3: List of 113 genes significantly regulated by both *RACB* and *Bgh* at 12 hpi. Expression values are given in LOG2 and listed after *RACB*-dependent comparisons and WT *Bgh* vs WT mock for the analysis of *Bgh*-dependent regulation. Non-*Bgh*-regulated transcripts were excluded from further analysis. The four clusters from Fig.15 are presented from a to d. P_35 numbers and their corresponding rice annotations are given.

			Log 2-fold change cut-off 1, FDR corr. p-value < 0.05		
P_35	**cluster**	**rice**	***CA RACB* mock vs. WT mock**	***RNAi RACB* mock vs. WT mock**	**WT *Bgh* vs. WT mock**
P_35_1762	d	LOC_Os08g41290.1 1e-72 AIR12 putative expressed	3.865	-1.358	2.369
P_35_5757	d	LOC_Os09g20090.1 2e-92 L-ascorbate oxidase precursor putative expressed	3.748	-1.137	2.223
P_35_9462	d	LOC_Os04g09900.3 2e-61 ent-kaurene synthase A chloroplast precursor putative expressed	3.649	-1.047	1.208
P_35_10720	d	LOC_Os10g04730.1 2e-63 protein kinase putative expressed	3.619	-1.578	2.191
P_35_2025	d	LOC_Os03g61470.1 2e-42 PGPS/D12 putative expressed	3.322	-1.267	2.132
P_35_11525	d	LOC_Os01g01302.1 1e-08 shikimate kinase family protein expressed	3.163	-1.004	2.416
P_35_43536	d	LOC_Os01g53040.1 4e-19 OsWRKY14 - Superfamily of rice TFs having WRKY and zinc finger domains expressed	2.985	-1.273	1.578
P_35_21465	d	No hits found	2.831	-1.091	1.636
P_35_40359	d	LOC_Os07g13800.1 7e-05 cytokinin-N-glucosyltransferase 1 putative expressed	2.827	-1.288	2.473
P_35_25548	d	LOC_Os08g04560.1 9e-16 aromatic-L-amino-acid decarboxylase putative expressed	2.752	-1.065	2.004
P_35_48104	d	LOC_Os09g36290.1 1e-11 phosphatase DCR2 putative expressed	2.707	-1.173	1.208
P_35_26745	d	LOC_Os03g13740.1 2e-12 immediate-early fungal elicitor protein CMPG1 putative expressed	2.567	-1.416	2.067
P_35_603	d	LOC_Os06g29730.1 7e-06 expressed protein	1.881	-1.031	1.452
P_35_20068	d	LOC_Os03g37840.1 0.0 potassium transporter 16 putative expressed	1.865	-1.002	1.395
P_35_15510	c	LOC_Os11g31540.1 2e-66 BRASSINOSTEROID INSENSITIVE 1-associated receptor kinase 1 precursor putative expressed	4.191	-1.523	4.923
P_35_9455	c	LOC_Os06g13320.1 1e-75 S-domain receptor-like protein kinase putative expressed	3.308	-1.009	5.764
P_35_11038	c	LOC_Os03g29410.1 1e-98 protein kinase APK1B chloroplast precursor putative expressed	2.518	-1.158	6.028
P_35_6104	c	LOC_Os06g22330.1 3e-49 expressed protein	2.357	-1.104	4.921
P_35_13330	c	LOC_Os06g13180.1 1e-79 metalloendoproteinase 1 precursor putative expressed	2.197	-1.315	4.260
P_35_9588	c	LOC_Os12g24320.1 2e-20 cell Division Protein AAA ATPase family putative expressed	2.146	-1.006	3.742
P_35_42427	c	LOC_Os02g11870.1 3e-24 expressed protein	2.125	-1.026	4.972
P_35_40297	c	LOC_Os03g20949.1 3e-87 phospholipid-transporting ATPase 1 putative expressed	2.002	-1.042	4.728
P_35_9620	c	LOC_Os05g45410.1 4e-27 heat shock factor putative expressed	1.999	-1.287	3.556
P_35_1120	c	No hits found	1.917	-1.029	3.787

			Log 2-fold change cut-off 1, FDR corr. p-value < 0.05		
P_35	**cluster**	**rice**	***CA RACB* mock vs. WT mock**	***RNAi RACB* mock vs. WT mock**	**WT *Bgh* vs. WT mock**
P_35_1119	c	LOC_Os05g04700.1 8e-10 hydrophobic protein LTI6B putative expressed	1.877	-1.203	3.602
P_35_42222	c	LOC_Os01g50100.1 2e-88 multidrug resistance protein 4 putative expressed	1.857	-1.219	4.182
P_35_40770	c	No hits found	1.807	-1.085	4.340
P_35_29940	c	LOC_Os12g29950.2 3e-23 nitrate and chloride transporter putative expressed	1.730	-1.273	4.268
P_35_26211	c	LOC_Os05g41370.1 2e-25 receptor-like protein kinase homolog RK20-1 putative expressed	1.674	-1.478	3.740
P_35_6100	c	LOC_Os07g35660.1 1e-56 receptor-like serine-threonine protein kinase putative expressed	1.627	-1.041	3.860
P_35_5423	c	LOC_Os04g58710.1 2e-78 peroxisomal-coenzyme A synthetase putative expressed	1.603	-1.181	3.981
P_35_10046	c	LOC_Os01g61460.1 1e-127 expressed protein	1.597	-1.248	3.697
P_35_15131	c	LOC_Os07g47700.1 0.0 UDP-glucuronic acid decarboxylase 1 putative expressed	1.538	-1.246	4.584
P_35_14951	c	LOC_Os08g08990.1 1e-105 germin-like protein subfamily 1 member 11 precursor putative expressed	1.497	-1.695	7.026
P_35_40027	c	LOC_Os10g38360.1 7e-07 glutathione S-transferase GSTU6 putative expressed	1.275	-1.004	2.508
P_35_48525	c	No hits found	1.220	-1.163	4.436
P_35_17226	c	LOC_Os12g02960.1 9e-68 glutathione S-transferase putative expressed	1.186	-1.115	2.522
P_35_23415	c	LOC_Os05g25390.1 1e-158 protein kinase putative expressed	1.141	-1.271	3.479
P_35_20192	c	LOC_Os05g05620.1 3e-62 glutathione S-transferase GSTF1 putative expressed	1.122	-1.076	2.848
P_35_35513	b	No hits found	3.703	-1.155	3.741
P_35_9635	b	LOC_Os12g41540.1 9e-12 protein kinase putative expressed	3.552	-1.493	4.502
P_35_15828	b	LOC_Os12g36830.1 3e-30 pathogenesis-related protein 10 putative expressed	3.405	-1.290	4.408
P_35_6982	b	LOC_Os02g50460.1 6e-50 immediate-early fungal elicitor protein CMPG1 putative expressed	3.377	-1.188	3.302
P_35_25908	b	LOC_Os11g38780.1 1e-36 calcium ion binding protein putative	2.956	-1.971	4.747
P_35_19740	b	LOC_Os09g04339.1 2e-54 expressed protein	2.953	-1.086	2.854
P_35_18411	b	LOC_Os01g66510.1 2e-72 MLO-like protein 1 putative expressed	2.941	-1.705	3.489
P_35_22055	b	LOC_Os04g10160.1 2e-72 cytochrome P450 CYP99A1 putative expressed	2.935	-1.574	3.222
P_35_41141	b	LOC_Os08g42580.1 4e-22 LysM receptor-like kinase putative expressed	2.909	-1.041	4.189
P_35_27106	b	LOC_Os09g38910.1 7e-19 OsWAK92 - OsWAK receptor-like protein kinase expressed	2.845	-1.762	4.476
P_35_24248	b	LOC_Os07g31884.1 3e-30 transparent testa 12 protein putative expressed	2.798	-1.233	3.005
P_35_18944	b	LOC_Os03g58980.1 2e-81 germin-like protein subfamily T member 2 precursor putative expressed	2.797	-1.569	3.241
P_35_14625	b	LOC_Os01g42870.1 6e-49 10-deacetylbaccatin III 10-O-acetyltransferase putative expressed	2.772	-1.377	3.338

			Log 2-fold change cut-off 1, FDR corr. p-value < 0.05		
P_35	**cluster**	**rice**	***CA RACB* mock vs. WT mock**	***RNAi RACB* mock vs. WT mock**	**WT *Bgh* vs. WT mock**
P_35_15826	b	LOC_Os12g36830.1 7e-31 pathogenesis-related protein 10 putative expressed	2.758	-1.150	2.928
P_35_43411	b	LOC_Os06g12090.1 3e-16 GTP-binding protein SAR2 putative expressed	2.634	-1.014	2.771
P_35_15829	b	LOC_Os12g36830.1 1e-37 pathogenesis-related protein 10 putative expressed	2.609	-1.278	2.939
P_35_20630	b	LOC_Os03g15080.1 1e-65 expressed protein	2.607	-1.424	2.741
P_35_5050	b	LOC_Os04g29960.1 2e-34 OsWAK43 - OsWAK receptor-like protein kinase expressed	2.601	-1.484	2.775
P_35_8212	b	LOC_Os01g50100.1 4e-90 multidrug resistance protein 4 putative expressed	2.597	-1.246	3.968
P_35_50221	b	LOC_Os07g44499.1 4e-16 peroxidase 56 precursor putative expressed	2.538	-1.027	3.364
P_35_24054	b	LOC_Os12g19030.1 2e-73 copine family protein expressed	2.407	-2.396	1.890
P_35_11893	b	LOC_Os12g42200.1 6e-33 ATCHX19 putative expressed	2.367	-1.508	1.989
P_35_24669	b	LOC_Os06g06350.1 0.0 ACS-like protein putative expressed	2.354	-1.286	3.173
P_35_15508	b	LOC_Os11g31540.1 1e-68 BRASSINOSTEROID INSENSITIVE 1-associated receptor kinase 1 precursor putative expressed	2.308	-1.387	2.988
P_35_34422	b	LOC_Os03g17470.1 7e-25 IN2-1 protein putative expressed	2.301	-1.002	2.871
P_35_15620	b	LOC_Os04g41680.1 9e-97 endochitinase A precursor putative expressed	2.290	-1.138	1.564
P_35_19716	b	No hits found	2.288	-1.271	2.418
P_35_25247	b	LOC_Os01g11650.1 1e-40 esterase precursor putative expressed	2.287	-1.461	2.689
P_35_25828	b	No hits found	2.222	-1.388	2.208
P_35_26695	b	LOC_Os03g01150.2 1e-77 palmitoyl-protein thioesterase 1 precursor putative expressed	2.164	-1.088	1.527
P_35_21250	b	LOC_Os09g29540.1 5e-91 OsWAK82 - OsWAK receptor-like cytoplasmic kinase (OsWAK-RLCK) expressed	2.171	-1.743	2.245
P_35_12191	b	LOC_Os09g30454.1 1e-55 OsWAK87 - OsWAK receptor-like protein kinase expressed	2.129	-2.106	2.077
P_35_1700	b	LOC_Os04g24290.1 1e-149 protein kinase putative	2.093	-1.127	1.643
P_35_14345	b	LOC_Os07g48050.1 1e-115 peroxidase precursor putative expressed	2.067	-1.851	4.423
P_35_3901	b	LOC_Os01g48620.1 1e-102 expressed protein	2.049	-1.138	2.945
P_35_23723	b	LOC_Os12g28177.1 6e-67 cell Division Protein AAA ATPase family putative expressed	2.048	-1.894	3.927
P_35_5202	b	No hits found	1.994	-1.714	4.446
P_35_14518	b	LOC_Os02g36940.1 1e-68 expressed protein	1.965	-1.280	2.684
P_35_30433	b	LOC_Os05g48210.1 8e-10 expressed protein	1.903	-1.065	1.823
P_35_9814	b	LOC_Os09g37834.1 2e-94 serine/threonine-protein kinase receptor precursor putative expressed	1.893	-1.415	1.582

			Log 2-fold change cut-off 1, FDR corr. p-value < 0.05		
P_35	**cluster**	**rice**	***CA RACB* mock vs. WT mock**	***RNAi RACB* mock vs. WT mock**	**WT *Bgh* vs. WT mock**
P_35_19948	b	LOC_Os04g48850.1 6e-63 1-aminocyclopropane-1-carboxylate synthase putative expressed	1.849	-1.674	3.759
P_35_16564	b	LOC_Os01g04330.1 9e-65 calmodulin-related protein 2 touch-induced putative expressed	1.845	-1.494	1.875
P_35_249	b	LOC_Os10g34910.1 1e-76 secretory protein putative	1.827	-1.414	2.872
P_35_150	b	LOC_Os06g29730.1 6e-06 expressed protein	1.816	-1.028	2.623
P_35_5259	b	LOC_Os07g20610.1 5e-34 serine/threonine-protein kinase receptor precursor putative	1.810	-1.237	2.716
P_35_774	b	LOC_Os11g37950.1 4e-64 win2 precursor putative expressed	1.805	-1.142	1.877
P_35_27010	b	No hits found	1.771	-1.456	1.675
P_35_5257	b	LOC_Os05g42210.1 2e-86 serine/threonine-protein kinase receptor precursor putative expressed	1.740	-1.286	2.615
P_35_2397	b	No hits found	1.724	-1.162	2.096
P_35_48052	b	LOC_Os01g43774.1 5e-23 cytochrome P450 72A1 putative expressed	1.680	-1.498	1.803
P_35_23760	b	LOC_Os03g52380.1 4e-21 expressed protein	1.654	-1.425	2.232
P_35_41435	b	LOC_Os07g38800.1 8e-37 lectin-like receptor kinase 7 putative expressed	1.652	-1.769	1.974
P_35_16231	b	LOC_Os02g17090.1 0.0 cucumisin precursor putative expressed	1.635	-2.150	4.262
P_35_949	b	LOC_Os09g04310.1 3e-27 expressed protein	1.613	-1.278	1.609
P_35_20965	b	LOC_Os02g39330.1 1e-127 endochitinase PR4 precursor putative expressed	1.609	-1.495	4.866
P_35_23361	b	LOC_Os07g38800.1 9e-21 lectin-like receptor kinase 7 putative expressed	1.604	-1.074	1.684
P_35_10619	b	LOC_Os03g62200.1 1e-109 ammonium transporter 2 putative expressed	1.600	-1.340	1.776
P_35_6585	b	LOC_Os06g04900.1 3e-80 hexose carrier protein HEX6 putative expressed	1.592	-1.301	3.157
P_35_41681	b	LOC_Os03g13300.1 2e-23 glutamate decarboxylase putative expressed	1.539	-1.268	1.629
P_35_27978	b	LOC_Os11g10310.1 3e-56 receptor-like protein kinase precursor putative expressed	1.454	-1.337	1.418
P_35_8642	b	LOC_Os10g10360.4 2e-66 NBS-LRR disease resistance protein putative expressed	1.442	-1.162	1.997
P_35_3466	b	LOC_Os03g03350.1 0.0 glycoside hydrolase family 28 putative expressed	1.437	-1.049	1.553
P_35_14142	b	LOC_Os03g13300.1 0.0 glutamate decarboxylase putative expressed	1.410	-1.101	1.641
P_35_9926	b	LOC_Os09g26144.1 1e-05 glutamate receptor 2.8 precursor putative expressed	1.333	-1.139	2.018
P_35_34887	b	LOC_Os07g45480.1 3e-26 conserved hypothetical protein	1.310	-1.308	2.189
P_35_5546	b	LOC_Os03g53200.1 1e-72 calmodulin putative expressed	1.253	-1.036	1.535
P_35_16041	b	LOC_Os03g55410.1 1e-130 peroxidase 51 precursor putative expressed	1.235	-1.067	1.125
P_35_18546	b	LOC_Os01g62430.3 8e-59 elicitor-responsive protein 1 putative expressed	1.216	-1.024	5.285

			Log 2-fold change cut-off 1, FDR corr. p-value < 0.05		
P_35	**cluster**	**rice**	***CA RACB* mock vs. WT mock**	***RNAi RACB* mock vs. WT mock**	**WT *Bgh* vs. WT mock**
P_35_41226	b	LOC_Os01g04470.1 3e-07 hypothetical protein	1.206	-1.158	2.423
P_35_48528	b	LOC_Os04g23700.1 2e-40 ATP binding protein putative expressed	1.181	-1.071	1.014
P_35_44375	b	No hits found	1.074	-1.111	2.490
P_35_4958	b	LOC_Os05g35960.1 2e-13 conserved hypothetical protein	1.001	-1.156	1.191
P_35_1073	a	LOC_Os01g60770.1 1e-112 alpha-expansin 10 precursor putative expressed	-1.096	1.736	-1.347
P_35_19157	a	LOC_Os05g34320.2 0.0 beta-hexosaminidase beta chain precursor putative expressed	-2.319	3.693	-2.525

Table S4: List of 10 genes significantly and differentially regulated by *RACB* and *Bgh* at 32 hpi. Mock comparisons *CA RACB* mock vs. WT mock and *RACB RNAi* mock vs. WT mock were reviewed for opposite regulation. *Bgh*-dependent regulation was analysed in the WT *Bgh* vs WT mock expression set for Cathe oppositely regulated transcripts. Non-*Bgh*-regulated transcripts were excluded from further analysis before. Expression values are displayed as LOG FC2. P_35_ numbers correspond to array annotation with rice annotation based on the annotation file from Klaus Mayer.

			fold change cut-off 2, p-value < 0.05		
P_35_	**cluster**	**RICE annotation to the appropriate barley homolog**	***CA RACB* mock vs. WT mock**	***RACB RNAi* mock vs. WT mock**	**WT *Bgh* vs. WT mock**
P_35_26520	b	LOC_Os06g45630.1 4e-70 ATP binding protein putative expressed	3.201	-1.664	3.996
P_35_5202	a	No hits found	3.000	-1.378	4.984
P_35_21250	b	LOC_Os09g29540.1 5e-91 OsWAK82 - OsWAK receptor-like cytoplasmic kinase (OsWAK-RLCK) expressed	2.881	-1.635	3.817
P_35_23033	b	LOC_Os02g56370.1 7e-83 OsWAK20 - OsWAK receptor-like protein kinase expressed	2.810	-1.399	3.344
P_35_15510	b	LOC_Os11g31540.1 2e-66 BRASSINOSTEROID INSENSITIVE 1-associated receptor kinase 1 precursor putative expressed	2.559	-1.991	4.046
P_35_5394	a	LOC_Os04g39010.1 3e-20 ATFP4 putative expressed	1.918	-1.154	4.233
P_35_6100	b	LOC_Os07g35660.1 1e-56 receptor-like serine-threonine protein kinase putative expressed	1.679	-1.487	2.351
P_35_18749	a	LOC_Os06g28124.1 1e-108 glycosyltransferase putative expressed	1.468	-1.366	2.096
P_35_39767	a	LOC_Os01g49820.2 3e-71 lipid phosphate phosphatase 3 chloroplast precursor putative expressed	1.412	-1.044	1.581
P_35_7436	a	LOC_Os04g54140.1 5e-60 receptor-like kinase putative expressed	1.094	-1.149	2.193

Table S5: List of six candidate genes de-regulated by *RACB* for functional analysis by TIGS.

				Log2-fold change (cut-off 1, FDR corr. p-value < 0.05)					
				32 h			12 h		
P_35_	**re-annotation**	**cluster**	**RICE annotation to the appropiate barley homolog**	***CA RACB* mock vs. WT mock**	***RNAi RACB* mock vs. WT mock**	**WT *Bgh* vs. WT mock**	***CA RACB* mock vs. WT mock**	***RNAi RACB* mock vs. WT mock**	**WT *Bgh* vs. WT mock**
P_35_26520	*LRR-RLK*	*b*	*LOC_Os06g45630.1 4e-70 ATP binding protein putative expressed*	*3.202*	*-1.664*	*3.996*	*NA*	*NA*	*4.795*
P_35_21250	**WAK-RLK a**	**b**	**LOC_Os09g29540.1 5e-91 OsWAK82 - OsWAK receptor-like cytoplasmic kinase (OsWAK-RLCK) expressed**	**2.881**	**-1.635**	**3.817**	**2.171**	**-1.743**	**2.245**
P_35_15510	**LRR-P**	**b**	**LOC_Os11g31540.1 2e-66 BRASSINOSTEROID INSENSITIVE 1-associated receptor kinase 1 precursor putative expressed**	**2.559**	**-1.991**	**4.046**	**4.192**	**-1.523**	**4.924**
P_35_24054	*COP*	*b*	*LOC_Os12g19030.1 2e-73 copine family protein expressed*	*1.707*	*-2.073*	*NA*	*2.407*	*-2.397*	*1.890*
P_35_6100	**DUF26-RLK b**	**b**	**LOC_Os07g35660.1 1e-56 receptor-like serine-threonine protein kinase putative expressed**	**1.679**	**-1.488**	**2.352**	**1.628**	**-1.042**	**3.861**
P_35_7436	*S-RLK*	*a*	*LOC_Os04g54140.1 5e-60 receptor-like kinase putative expressed*	*1.095*	*-1.150*	*2.194*	*NA*	*NA*	*NA*

Table S6: Barley WRKY transcription factors analysed in this study. Significantly regulated WRKYs have already characterized orthologs in rice and arabidopsis.

	putative ortholog			
barley	rice	arabidopsis	function	literature
HvWRKY2	OsWRKY28	AtWRKY40	negative regulators of resistance to *Bgh,* rice blast fungus, *P. syringae* and *G. orontii*	barley: (Eckey *et al.*, 2004; Shen *et al.*, 2007) rice: (Chujo *et al.*, 2013) arabidopsis: (Chen *et al.*, 2010a)
HvWRKY3	OsWRKY76	AtWRKY40	negative repressor of resistance to *M. oryzae, P. syringae* and *G. orontii*	barley : uncharacterized rice: (Yokotani *et al.*, 2013) arabidopsis: (Chen *et al.*, 2010a)
HvWRKY18	OsWRKY26	AtWRKY51	repressor of JA signalling by mis-expression of WRKY51	barley: uncharacterized rice: uncharacterized arabidopsis: (Gao *et al.*, 2011)
HvWRKY20	OsWRKY7	AtWRKY40	negative regulator of defence against *P.syringae, G.orontii, Pseudomonas*	barley: uncharacterized rice: uncharacterized arabidopsis: (Chen *et al.*, 2010a; Higashi *et al.*, 2008)
HvWRKY22	OsWRKY74	AtWRKY41	potential positive regulator of systemic immunity regulator of abiotic stress in rice	barley: (Dey *et al.*, 2014) rice: (Dai *et al.*, 2015) arabidopsis: (Higashi *et al.*, 2008)

Table S7: Expression correlation analysis of selected receptor classes and WRKY transcription factors. Based on the percentage gene expression per comparison (Fig.14) was created. Correlation analysis was carried out with R and therein with the Spearman`s rank sum test based on all available qRT-PCR (3 biological replicates).

	percentage [%]		
gene	**12h**	**32h**	**12h+32h**
DUF26-RLK a	29	89	52
DUF26-RLK b	71	71	74
DUF26-RLK c	93	75	83
WAK-RLK a	82	89	90
WAK-RLK b	79	86	83
WAK-RLK c	68	79	81
LRR-P	75	85	80
LRR-RLK	96	93	90
COP	79	71	71
S-RLK	64	18	35
WRKY2	79	93	77
WRKY3	96	NA	NA
WRKY18	82	75	70
WRKY20	57	38	43
WRKY22	93	46	54

Table S8: Based on amino acid similarity is HvLRR-P most similar to HvSERK a. Based on an alignment of the protein sequences of HvLRR-P (BAJ91771), HvSERK a (BAK03316), AtBAK1 (AEE86223), ZmPAN1 (ACI95776) and LeLRR-P (AAR27431) performed with ClustalW (http://www.genome.jp/tools-bin/clustalw), similarity of amino acids is given in percent [%]. Amino acid similarity corresponds to HvLRR-P.

	HvSERK a	**AtBAK1**	**ZmPAN1**	**LeLRR-P**
HvLRR-P	56 %	38 %	28 %	22 %

Table S9: Amino acid similarity between HvMPK4 and HvMPK4-like. Based on an alignment of the protein sequences of the barley MAPKs carried out with ClustalW (http://www.genome.jp/tools-bin/clustalw), the amino acid similarity was calculated in percent [%]. Protein sequences were obtained from Genbank: HvMPK4 (AK252980; was transcribed intor protein sequence with the *Triticeas* full-length CDS database (Mochida *et al.*, 2009)), HvMPK3-like (MLOC_17814), HvMPK4-like (MLOC_5653), HvMPK6-like (AK376245), AtMPK3 (At3g45640), AtMPK4 (At4g01370), AtMPK6 (At2g43790), OsMPK4 (CAB61889). Bold labelled numbers show the highest similarity.

	AtMPK3	**AtMPK4**	**OsMPK4**	**HvMPK4**	**AtMPK6**
HvMPK3-like	**73 %**	63 %	54 %	53 %	72 %
HvMPK4-like	65 %	**79 %**	54 %	52 %	68 %
HvMPK4	53 %	53 %	**93 %**	100 %	53 %
HvMPK6-like	74 %	68 %	55 %	53 %	**85 %**

Table S10: Amino acid similarity between HvCRK1 and HvDUF26-RLK a, b, and c. Based on an alignment of the protein sequences of the barley MAPKs carried out with ClustalW (http://www.genome.jp/tools-bin/clustalw), the amino acid similarity was calculated in percent [%]. Accession numbers used: HvCRK1 (FR717136), HvDUF26-RLK a (AK368110), HvDUF26-RLK b (AK368111), HvDUF26-RLK c (AK253014).

	HvCRK1
HvDUF26-RLK a	49
HvDUF26-RLK b	49
HvDUF26-RLK c	49

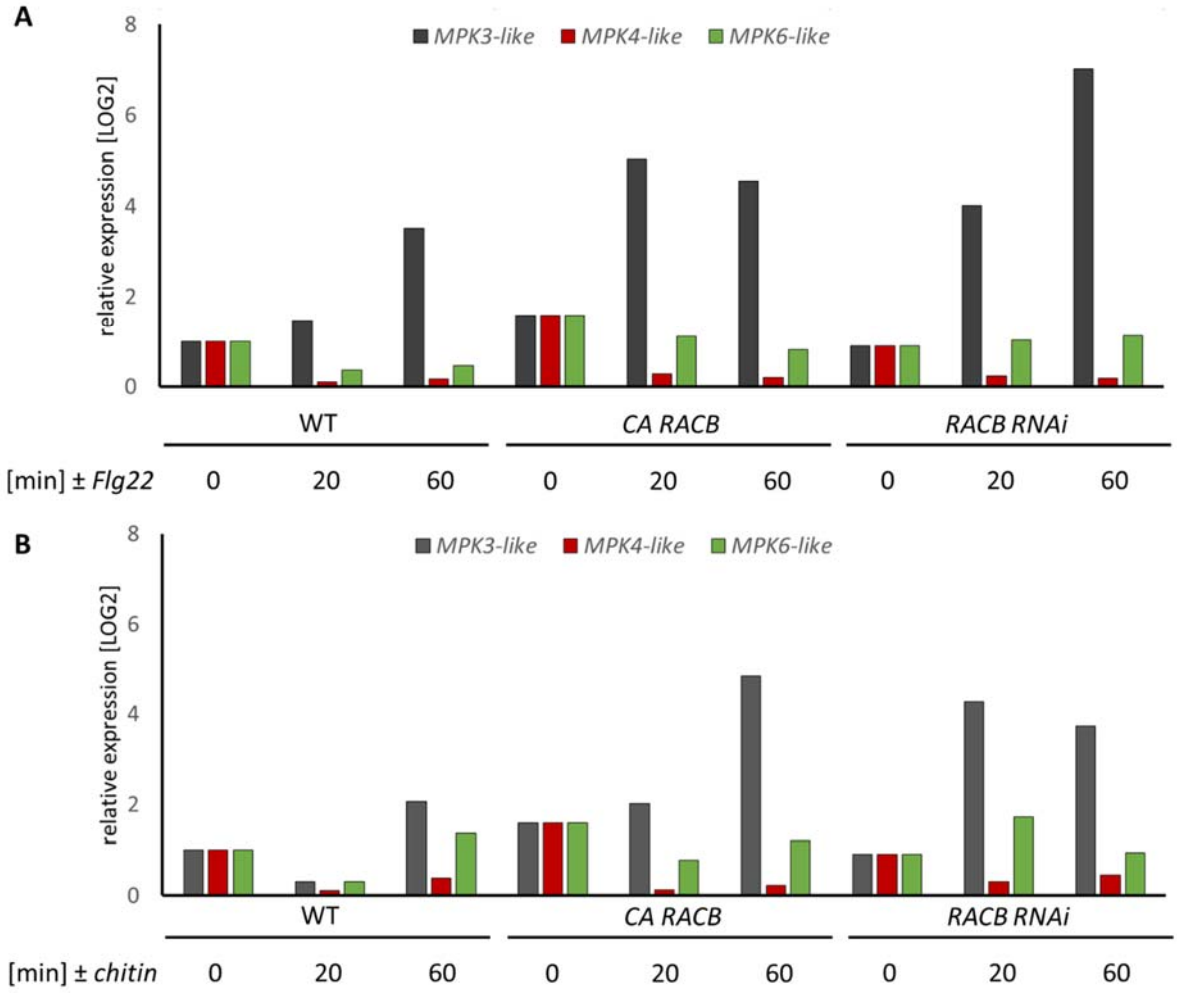

Fig. S1: Gene expression of barley MAPKs after *flg22* and *chitin* treatment revealed no clear effect of *RACB*-transgenic barley plants. WT, CA *RACB* over-expressing and *RACB RNAi* plants were either mock-treated (-) or treated with different PAMPs after several time points and collected for gene expression analysis. **A** All three barley MAPKs show no differences within their expression in the *RACB* transgenes when challenged with *flg22* (100 nM). **B** All three barley MAPKs show no differences within their expression in the *RACB* transgenes when challenged with *chitin* (10 µg/mL-1). 24 LD of three plants per genotype were used for PAMP elicitation. PAMPs were added at 0 min and harvested in liquid N_2 after 0, 20, 60 min. From all collected leaf material RNA was extracted using Trizol and cDNA synthesis performed with QuantiTect Reverse Transcription Kit (Quiagen, Mannheim, Germany). qRT-PCR was carried out with SYBR® Green PCR Master Mic in a MxPro3005P cycler with 10 ng cDNA. Calculation was performed according to the ΔΔ Ct method (Pennington *et al.*, 2015) and normalized to untreated WT at 0 min. Data displayed are out of one biological replicate. Accession numbers of analysed genes: *UBC2* (M60175), *MPK3-like* (MLOC_17814), *MPK4-like* (AK357723), *MPK6-like* (AK376245).

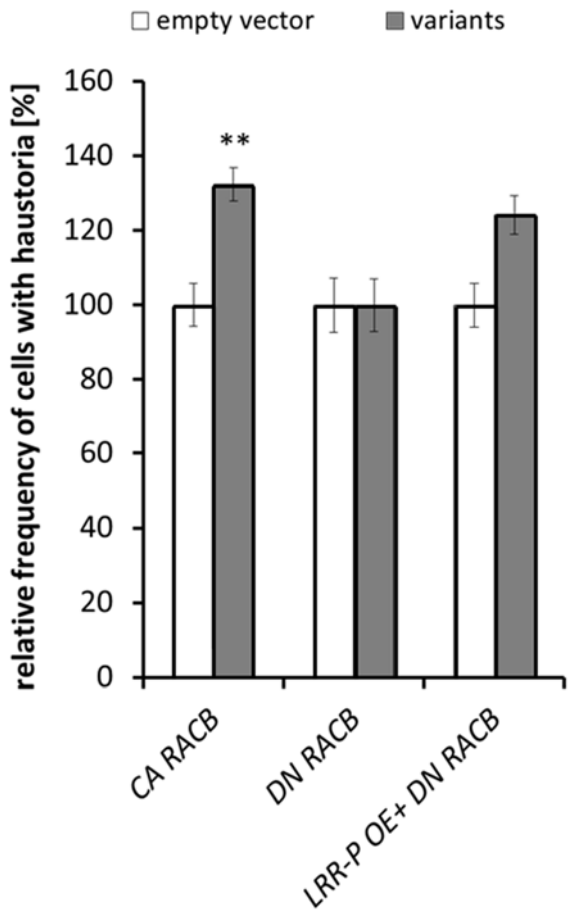

Fig. S2: Impact on susceptibility after transient-induced over-expression with different RACB versions. Ballistic transformation of leaf segments of 7 days old WT Golden Promise plants with *Bgh* inoculation after 1 day and microscopically evaluation 2 days after inoculation resulted in a significantly enhanced single cell susceptibility phenotype for expression of CA RACB and LRR-P OE + DN RACB but not DN RACB alone. Haustoria frequency of the control was set to 100 % and error bars derive from the variance of individual repetitions to the mean. Bars represent standard errors. ** represent significance at p –value < 0.01 according to a two-sided unpaired Student`s t-test performed on the non-transformed raw data.

14. ACKNOWLEDGEMENT

Hereby, I would like to thank all the people who made my thesis possible:

Great thanks go to Prof. Dr. Ralph Hückelhoven for giving me the opportunity to perform my PhD thesis at his chair, for all his great supervision during my theoretical and practical work and for delivering this interesting topic.

I also thank PD Dr. Erika Isono for taking over as my second reviewer and Prof. Dr. Erwin Grill for taking over the chair of the examination committee.

I am very grateful to Corina Vlot-Schuster and Melanie Knappe from the Helmholtz Zentrum München for their help and the opportunity to perform my microarrays at their chair. Also, many thanks go to Klaus Mayer and Karl Kugler from the Helmholtz Zentrum München for providing the annotation files for the barley array. For the custom-made array design, I would further like to thank Dr. Pete Hedley from the James Hutton Institute in Scotland. Thanks to Stefanie Ranf for all her helpful ideas, technical guidance and discussions. Thanks to Reinhard Pröls for his helpful ideas during writing.

Many thanks go to Tina Reiner for her great and helpful input during the writing procedure.

Our secretaries Traudl and Claudia, I am thankful for all your help and the nice atmosphere we always had.

Thanks to all my nice lab members for nice conversations and for becoming good friends during that time.

Greatest thanks go to Prof. Dr. Christina Wege for her strong belief in me, her help and support in every situation and at every time through the last years. Thank you very much.

Many thanks go to all my dearest friends, who always believed in me, helped me whenever I needed a “time-out” and supported me in every situation.

Finally, I want to dedicate this thesis to my parents: without you nothing would be possible and greatest thank for your endless discussions, your help in every situation and your impressive support and love. Thank you.

15. CURRICULUM VITAE

Persönliche Angaben:

Name:	Vera Schnepf
Geburtsdatum:	31.12.1984
Geburtsort:	Waiblingen
Familienstand:	ledig
Staatsangehörigkeit:	deutsch

Ausbildung:

1995 – 2004	Wirtemberggymnasium Stuttgart-Untertürkheim, Abitur
2005 – 2011	Studium der Technischen Biologie an der Universität Stuttgart, Diplom
10/2009 – 02/2010	Auslandsaufenthalt & Studienarbeit bei Dr. Stuart MacFarlane, James Hutton Institute (ehemals Scottish Crop Research Institute), finanziert durch Bayer Crop Science Thema: „Molecular interactions of economically relevant raspberry viruses and their hosts“
07/2010 – 07/2011	Diplomarbeit in der Abteilung Molekularbiologie und Virologie der Pflanzen in der Gruppe von Prof. Dr. Christina Wege, Universität Stuttgart Thema: „Effect of inactivated RDR6 on begomoviruses of different pathogenicity”
11/2011 – 07/2015	Wissenschaftliche Mitarbeiterin/Promotionsarbeit am Lehrstuhl für Phytopathologie unter Leitung von Prof. Dr. Ralph Hückelhoven, Technische Universität München Thema: „Functions of the barley RAC/ROP GTPase RACB in the early plant immune response and in transcriptional reprogramming”